CZECH TECHNICAL UNIVERSITY IN PRAGUE

FACULTY OF MECHANICAL ENGINEERING

Department of production machines and equipment

Master thesis

Single-purpose grinder spindle quality control and assurance within small series production

2021   **Maria Kamenskaya**

I. OSOBNÍ A STUDIJNÍ ÚDAJE

Příjmení: **Kamenskaya**   Jméno: **Maria**   Osobní číslo: **466404**

Fakulta/ústav: **Fakulta strojní**

Zadávající katedra/ústav: **Ústav výrobních strojů a zařízení**

Studijní program: **Strojní inženýrství**

Studijní obor: **Výrobní stroje a zařízení**

II. ÚDAJE K DIPLOMOVÉ PRÁCI

Název diplomové práce:

Kontrola a zajištění vysoké kvality vřetena jednoúčelové brusky v rámci malosériové výroby

Název diplomové práce anglicky:

Single-purpose grinder spindle quality control and assurance within small series production

Pokyny pro vypracování:

Popis tématu: Finální kontrolu jakosti výroby a montáže brousicích vřeten je možno provádět pomocí metod vibrodiagnostiky. Cílem práce je provést úvodní měření vybraných parametrů na reálných vřetenech a pomocí analýzy naměřených hodnot stanovit postup kontroly kvality vřetenových jednotek. Osnova práce: Přehled metod měření vibrací vřeten, rozměrových a geometrických tolerancí souvisejících částí a dalších parametrů vhodných pro určování kvality výroby a montáže vřetenových jednotek obráběcích strojů. Vybrat vhodnou měřicí aparaturu a provést měření definovaných parametrů na několika vřetenových jednotkách. Stanovit postup kontroly kvality vřeten. Rozsah grafické části: 0 stran. Rozsah textové části: 60-80 stran;

Seznam doporučené literatury:

KREIDL, Marcel; ŠMÍD, Radislav. Technická diagnostika. Praha: BEN - technická literatura, 2006. ISBN 80-7300-158-6; BILOŠ, Jan; BILOŠOVÁ, Alena. Vibrační diagnostika. Ostrava: Vysoká škola báňská - Technická univerzita Ostrava, 2012. ISBN 978-80-248-2755-1; JANOUŠEK, I, KOZÁK, J., TARABA, O. Technická diagnostika. Praha: SNTL, 1988; Firemní literatura: SKF, Bruel Kjaer, Adash, SPM, Shenck, FAG

Jméno a pracoviště vedoucí(ho) diplomové práce:

Ing. David Burian, Ph.D.,   ústav výrobních strojů a zařízení   FS

Jméno a pracoviště druhé(ho) vedoucí(ho) nebo konzultanta(ky) diplomové práce:

Datum zadání diplomové práce: **29.04.2021**   Termín odevzdání diplomové práce: **25.07.2021**

Platnost zadání diplomové práce: **30.09.2021**

_____   _____   _____
Ing. David Burian, Ph.D.   Ing. Matěj Sulitka, Ph.D.   prof. Ing. Michael Valášek, DrSc.
podpis vedoucí(ho) práce   podpis vedoucí(ho) ústavu/katedry   podpis děkana(ky)

III. PŘEVZETÍ ZADÁNÍ

Diplomantka bere na vědomí, že je povinna vypracovat diplomovou práci samostatně, bez cizí pomoci, s výjimkou poskytnutých konzultací.
Seznam použité literatury, jiných pramenů a jmen konzultantů je třeba uvést v diplomové práci.

.
_____   _____
Datum převzetí zadání   Podpis studentky

MASTER'S THESIS ASSIGNMENT

CTU CZECH TECHNICAL UNIVERSITY IN PRAGUE

I. Personal and study details

Student's name:	**Kamenskaya Maria**	Personal ID number:	**466404**
Faculty / Institute:	**Faculty of Mechanical Engineering**		
Department / Institute:	**Department of Production Machines and Equipment**		
Study program:	**Mechanical Engineering**		
Branch of study:	**Production Machines and Equipment**		

II. Master's thesis details

Master's thesis title in English:

Single-purpose grinder spindle quality control and assurance within small series production

Master's thesis title in Czech:

Kontrola a zajištění vysoké kvality vřetena jednoúčelové brusky v rámci malosériové výroby

Guidelines:

Topic description: Final quality control of production and assembly of grinding spindles can be performed using vibrodiagnostic methods. The aim of the work is to perform an initial measurement of selected parameters on real spindles and to analyze the measured values to determine the procedure of quality control of spindle units. Work description: Overview of methods for measuring spindle vibrations, dimensional and geometric tolerances of related parts and other parameters suitable for determining the quality of production and assembly of spindle units of machine tools. Select a suitable measuring apparatus and measure the defined parameters on several spindle units. Establish a spindle quality control procedure. Graphic part range: 0 pages. Text part range: 60-80 pages.

Bibliography / sources:

KREIDL, Marcel; ŠMÍD, Radislav. Technická diagnostika. Praha: BEN - technická literatura, 2006. ISBN 80-7300-158-6; BILOŠ, Jan; BILOŠOVÁ, Alena. Vibrační diagnostika. Ostrava: Vysoká škola báňská - Technická univerzita Ostrava, 2012. ISBN 978-80-248-2755-1; JANOUŠEK, I, KOZÁK, J., TARABA, O. Technická diagnostika. Praha: SNTL, 1988; Firemní literatura: SKF, Bruel Kjaer, Adash, SPM, Shenck, FAG

Name and workplace of master's thesis supervisor:

Ing. David Burian, Ph.D.,   Department of Production Machines and Equipment,   FME

Name and workplace of second master's thesis supervisor or consultant:

Date of master's thesis assignment: **29.04.2021**   Deadline for master's thesis submission: **25.07.2021**

Assignment valid until: **30.09.2021**

_____   _____   _____
Ing. David Burian, Ph.D.   Ing. Matěj Sulitka, Ph.D.   prof. Ing. Michael Valášek, DrSc.
Supervisor's signature   Head of department's signature   Dean's signature

III. Assignment receipt

The student acknowledges that the master's thesis is an individual work. The student must produce her thesis without the assistance of others, with the exception of provided consultations. Within the master's thesis, the author must state the names of consultants and include a list of references.

_____   _____
Date of assignment receipt   Student's signature

DECLARATION OF AUTHORSHIP

I hereby declare that this master thesis is my own work and all referenced sources have been appropriately quoted in the References section in accordance with Methodical guideline No. 1/2009 for adhering to ethical principles when elaborating an academic final thesis issued by CTU in Prague 1.7.2009.

I declare no potential conflict of interest with respect to usage of this work within the meaning of the Act No. 121/2000 Coll. of April 7, 2000, on Copyright and Related Rights and on Amendments to Certain Acts (Copyright Act).

In Prague   23. 07. 2021   Maria Kamenskaya

ACKNOWLEDGEMENTS

Annotation

Annotation: The effects of dimensional tolerances and bearing fits is studied experimentally to define the role of dimensional tolerances and other quality-affecting factors in spindle vibrations under different speeds. A stand for vibration measurement and spindle testing purposes is proposed. Vibration measurement is applied to the spindle series. Final quality control procedure is proposed.

Anotace

Autor:	Bc. Maria Kamenskaya
Název DP:	Kontrola a zajištění vysoké kvality vřetena jednoúčelové brusky v rámci malosériové výroby
Rozsah práce:	120 str., 73 obr., 28 tab.
Školní rok vyhotovení:	2021
Škola:	ČVUT v Praze, Fakulta strojní
Ústav:	Ú12135 – Ústav výrobních strojů a zařízení
Vedoucí DP:	Ing. David Burian, Ph.D.
Konzultant:	Ing. Martin Tiefenbach – Viking CNC Prague
Zadavatel:	ČVUT – Fakulta strojní
Využití:	Vytvoření podkladů pro proces zajištění kvality vřeten brusky
Klíčová slova:	vibrační diagnostika, detekce ložiskových poruch, zajištění kvality

Anotace:	Práce se zabývá analýzou vlivu rozměrových tolerancí a uložení ložisek a jiných parametrů ovlivňujících kvalitu na vibrace vřetene za různých otáček. Je navžená stanice pro účely testování a měření vřeten. Je provedeno měření vibrací na roční sérii vřeten brusky. Je stanoven postup kontroly kvality vřeten.

Contents

List of abbreviations

Description	Contradiction
CNC	Computer Numeric Control
FFT	Fast Forier Transform
RMS	Root Maen Square
RPM	Rotations Per Minute
BPFO	Ball Passing Frequency Outer
BPFI	Ball Passing Frequency Outer
BCSOR	Ball Cage Stationary Outer Race
BCSIR	Ball Cage Stationary Inner Race
BSF	Ball Speed Frequency
BFF	Ball Fault Frequency
PTP	Peak-To-Peak
SE	Spike Energy
SP	Shock Pulse
ISO	International Organization for Standardization
FM	Failure Mode
RE	Rolling Element
RFID	Radio Frequency Identification
IIoT	Industrial Internet of Things

NBR	Nitrile Butadiene Rubber
HMI	Human Machine Interface
IEPE	Integrated Electronics Piezo-Electric
ID	Inner Diameter
OD	Outer Diameter

List of symbols

Symbol	Units	Parameter
a	$[m.s^{-2}]$	acceleration
b_c	$[m]$	coupling distance
b_m	$[m]$	motor axis distance
b_s	$[m]$	distance between motor bracket and spindle pipe
C_{fs}	$[m]$	front bearing ID seat circularity
C_{rs}	$[m]$	rear bearing ID seat circularity
d	$[m]$	bearing ball diameter
D	$[m]$	bearing pitch diameter
d_c	$[m]$	coupling diameter
D_s	$[m]$	spindle pipe actual outer diameter
f	$[s^{-1}]$	frequency
h_c	$[m]$	coupling height
h_i	$[m]$	inner space ring height
h_m	$[m]$	motor height
h_o	$[m]$	outer space ring height
h_s	$[m]$	spindle pipe height
id_{fs}	$[m]$	Front bearing ID seat
id_{rs}	$[m]$	Inner diameter

ID_{fb}	[m]	Front bearing Inner Diameter
ID_{rb}	[m]	Rear bearing ID
N	[1]	number of balls
od_{fb}	[m]	Front bearing Outer Diameter
od_{rb}	[m]	Rear bearing OD
OD_{fp}	[m]	Front bearing OD seat
OD_{rp}	[m]	Rear bearing OD seat
r	[m]	radius
t	[s]	time
T	[s]	time period
v	[m.s^{-1}]	velocity
β	[rad]	bearing contact angle
δ	[m]	Spacer rings height difference

1. Introduction

A machine tool spindle has to meet certain quality requirements. Its performance has to be carefully monitored, because in case of a problem with spindle performance, there is a large probability that the quality of the final product is affected. This work is mainly focused on indicating the causes of problems, which can be detected directly during the spindle's first pre-assembly run – excessive vibrations and untypical noise. By revealing the problems of this type, faulty spindles can be prevented from use until the cause of the problem is determined and eliminated. Spindle assembly is a complex unit, and the resultant unsatisfactory performance could be, in turn, a complex issue comprised of many causes, each of a different degree of impact. Appropriate ways of vibration data acquisition, treatment and analysis needed to get to its root causes are examined in this paper in order to subsequently define the appropriate process and equipment in context of a quality assurance procedure for spindles of a tap flute CNC grinder FG-15 developed by Viking CNC.

2. Research section

2.1 Vibration diagnostics methods in rotating machinery

Vibration is a motion in a regularly reversing direction, induced by a force impact. In the realm of rotating machinery, the causing force is unwanted and appears to be a side effect of various flaws, which are always present in a real-world mechanical system. A mechanical system (e. g. spindle assembly) is considered to be in a good operating condition when the unwanted force and a caused vibrational motion is negligible and does not require further improvement and inspection. Otherwise, certain measures have to be taken to eliminate the source of an excessive vibration and to draw the vibration down to an acceptable range.

Vibration can be measured in order to interpret its character, which implicitly contains the information about the vibration-causing force. For a proper fault detection procedure, it is critical to understand the basic mechanical principles lying in the basis of every potential vibration source.

2.1.1 Vibration causes and associated force character

In today's machine tools operation reality, the most common causes of the vibration are damaged bearings, misalignment, looseness, and unbalance. Table 1 presents the typical vibration causes with a characteristic causing force type. The presented range of causes is not exhaustive and only covers problems which could be expected to occur in a grinder spindle assembly with roller bearings. More comprehensive list of vibration causes is presented in [1]. Three types of force character – periodic force, discrete force impulse, and a force randomly changing in time magnitude - are considered. Biloš, Bilošová [2] give an extensive definition of the force types and the vibrations associated with them.

Table 1. Vibration causes and associated force character

Vibration cause	Force character
1. Bearing damage	Impulsive in the moment of damage occurrence, then changes to periodic or random
2. Misalignment	Periodic
3. Unbalance	Periodic

4. Looseness	Periodic or random
5. Structural resonances	Periodic
6. Bent shaft	Periodic
7. Cracked shaft	Impulsive in the moment of damage occurrence, then changes to periodic
8. Rubs	Periodic or random

In most cases presented in Table 1, the vibration-inducing force has a periodic character, i. e. it alternates its magnitude with a certain periodicity, which can be described by a frequency of the induced vibration. In case of forced vibration (causes 1, 2, 3, 6, 7, 8), the frequency is the same as the frequency of the acting force. In case of structural resonances, system responds with vibrations on natural frequencies of its objects. Harmonics of these frequencies are also likely to occur in both cases. The aim of vibration diagnostics is mainly to distinguish the unusual frequencies and relate them to certain causes of performance issues.

When some mechanical damage is on its very onset, a change in force abruptly appears as an impulse and results in a sudden raise of vibration level (causes 1, 7). Several advanced diagnostic techniques which allow for impulsive effects detection are available.

It is extremely important to consider that the force is proportional to acceleration, according to Newton's second law, and in case of rotational motion, consider the following relations:

$$a = \frac{v^2}{r}, \tag{1}$$

$$v = \frac{2\pi \cdot n}{60} \cdot r \tag{2}$$

where

That means, the load transmitted by vibration-causing force increases with the squared value of the rotational speed, so handling the problem is becoming progressively more difficult at high speeds.

2.1.2 Vibration signal analysis techniques

The main idea of vibration analysis techniques is following: when a dynamic system of a machine tool, or its structural component, such as, in particular, spindle assembly, is in a good operating condition, its vibration measurement signal has a corresponding characteristic shape. If one of a performance-affecting factors is out of control and affects dynamic performance badly, the signal response is different. The cause of the unacceptable performance may be revealed by means of analyzing the spectrum irregularities and relating them to the possible causes.

Norton, Karczub [1] suggest categorizing the existing techniques into 4 subsections, which are:

- signal magnitude analysis
- time-domain analysis of individual signal
- frequency domain analysis
- dual signal analysis in either time or frequency domain

They claim, that the first two techniques are usually grouped together in condition monitoring. Along with frequency domain analysis, these techniques are commonly used in vibration diagnostics, whereas the dual signal analysis technique is classified as a more advanced one.

Time (and magnitude) domain signal contains information about the overall waveform shape, the peak amplitude and its change in time, as well as about the general character of the response (if it is impulsive, random, or periodic).

Frequency domain signal is obtained by the Fast Fourier Transformation (FFT) applied on a time-domain signal, and, in turn, provides information about different frequencies' degree of contribution to the overall vibration, and, since most of problematic vibrations are caused by a periodically alternating force (v. Table 1), the fault frequencies, indicating the vibration source, can be readily identified from the obtained frequency spectrum.

Figure 1 provides a schematic representation of vibration signal time and frequency components and illustrates, which information can be obtained from a measured signal treated over time or frequency domain.
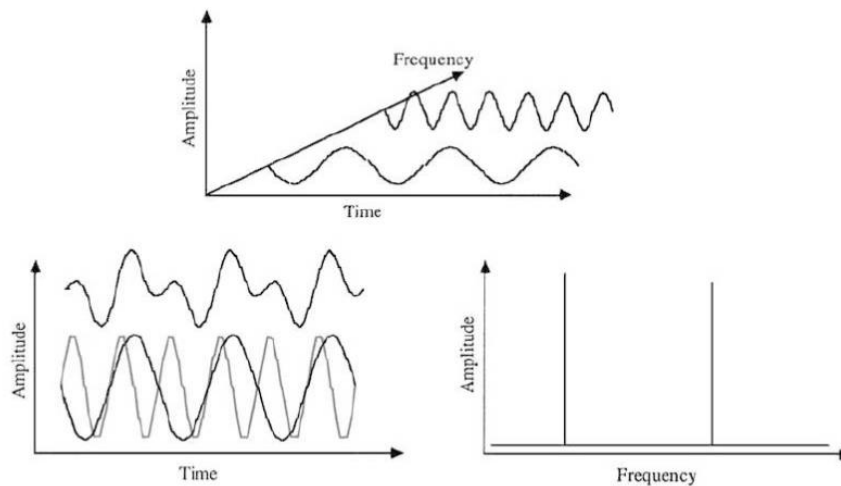
Figure 1. Time and frequency components of a vibration signal. [1]

2.1.2.1 Magnitude and time domain analysis techniques

Time domain vibration measurement is, basically, a record of a vibration signal change over some period of time. It can contain information about, for instance, significant discrete peaks, which appear with a certain periodicity and can be detected i. a. by visual inspection of the vibration plot – as in Figure 2, where peaks and their periodicity are fairly distinct. The other important data that can be obtained is the vibration magnitude, which can be presented by means of one of the forms presented in Table 2.
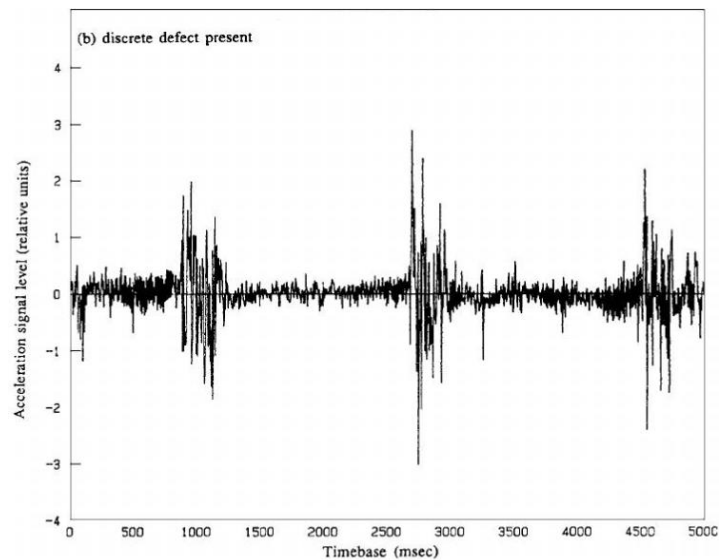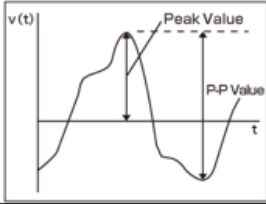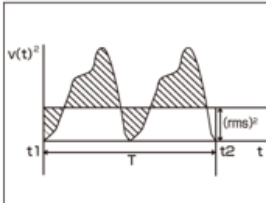

Figure 2. Acceleration time history with a noticeable discrete defect present [1]

Table 2. . Forms of vibration magnitude expression. Figures were taken from [3]

Magnitude function name	Magnitude function definition	Note
P (P-P)	$V_{PEAK} = \|v(t)\|_{max}$	- Maximum zero-to-peak or peak-to-peak value - Used for signal evaluation in case there is need to determine the magnitude of discrete excitations
RMS	$V_{rms} = \sqrt{\frac{1}{T}\int_{t1}^{t2} v(t)^2 \, dt}$	- Root mean square value - Used for signal evaluation in case vibration overall "power" is more important than the maximum amplitude

Crest factor

The measure of a signal impulsiveness and also a significant criterion for evaluating bearings condition is a function called crest-factor with following definition:

$$Crest\ factor = \frac{P}{RMS} \tag{3}$$

It is generally considered that a bearing in a good condition will give a vibration response in a form very close to random noise, so the peak and RMS values will be relatively close to each other. Obviously, if a bearing is withstanding an impulsive load caused by its internal damage, significant peaks will appear in the time history and the value of crest factor will be higher than it is for an undamaged bearing.

Crest factor values for different types of vibration signals taken from [1] are presented in Table 3.

Table 3. Crest factors values for different signal types

Signal	Crest factor
sine wave	1.414
random noise	<3
bearings in good condition	2.5-3.5

damaged bearings	>3.5
failure	~7

Probability density distribution and kurtosis

Another worth mentioning impulse presence indicator is kurtosis. This term is related to another time domain analysis technique - probability density distribution. The technique is based upon analyzing the probability of appearance of peaks over a range of amplitudes. Output of the analysis are the probability distribution curves, which, again, have their characteristic shape for the case of a sinusoidal signal, broadband random noise, etc. The other data which can be gained from this technique are four statistical moments, which can characterize the system condition. Their calculation is presented in [1]. Kurtosis happens to be the fourth statistical moment of a probability density distribution and, similarly, can be used to evaluate the bearing condition and detect fault presence.

Phase analysis

Phase analysis is an another highly valuable time-domain analysis technique, which allows for determination of a character of the overall vibration by analyzing how do the components move - radially and axially - with respect to each other.

Table 4 shows types of motion (different combinations of in-phase and out-of-phase axial and radial vibrations) that can be detected by vibration measurement proceeded on, for example, shaft bearings - by placing sensors in radial and axial direction on bearings on each side of a shaft. Third column presents a fault commonly associated with stated type of motion.

Table 4. Phase analysis possible outputs

Axial vibrations	Radial vibrations	Fault
out of phase	out of phase	misalignment, both radial and axial looseness
absent	opposite phase	couple unbalance
absent	in phase	force unbalance radial looseness
opposite phase	in phase	bent shaft

2.1.2.2 Frequency domain analysis techniques

These techniques use Fast Fourier Transform (FFT) to transfer a time domain signal of a complex vibration to a frequency spectrum, which provides important information about which frequencies contribute to the vibration the most. Again, the amplitude value assigned to each frequency over a spectrum may be expressed either as a peak value, or as an RMS value.

The most common form of a frequency domain analysis techniques is a baseband auto-spectral density analysis. The typical output spectrum is presented in Figure 3. Such issues as unbalance, structural resonances and various bearing damages can be detected by means of a frequency spectrum analysis.
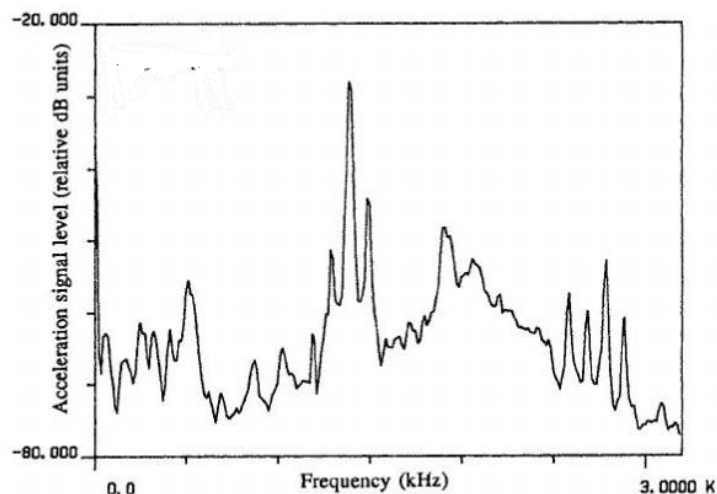

Figure 3. Vibration auto-spectrum example [1]

Unbalance means uneven mass distribution over a rotor assembly, which results in a centrifugal force acting on bearings. The force direction is continuously changing with the rotation of the shaft. Considering a constant rotational speed, one period of the acting centrifugal force and, consequently, of the induced vibration equals to time of one revolution. Thus, a frequency spectrum will depict a significant amount of unbalance as a peak at a shaft rotation frequency.

Various bearing damages can be detected by means of a frequency spectrum. As stated before, a bearing in satisfactory condition produces broadband and random vibrations at a relatively low amplitude level. Once a damage appears, it produces collateral forces resulting in an excessive vibration, which usually contains excitations at discrete frequencies.

They are sometimes clearly identifiable at a frequency spectrum afterwards – v. Figure 4. They can be related to definite bearing damage types and give a fairly explicit image of bearing's current condition. These characteristic frequencies are dependant both on a bearing geometry and running speed. Their calculation is provided in the chapter 0.
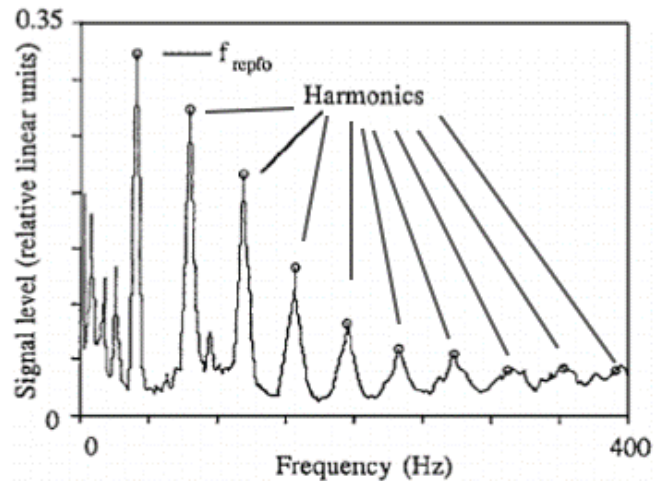

Figure 4. Bearing vibration auto-spectrum indicating a frequency correcponding to outer race damage [1]

It is important to notice that in general characteristic frequency peaks are clearly identifiable in the frequency spectrum only at a certain stage of a damage development and supposing that they are distinguishable from the background noise. Otherwise, the system gives a response on these frequencies, but it is harder to detect. In that cases, more advanced analysis techniques are used.

Bearings-related diagnostics problematics

Bearing is a crucial component of a spindle assembly, and the performance of the whole assembly very much depends on the condition of the bearings namely. Being a moving and dynamically loaded part makes them vulnerable to unwanted damaging effects, which can occur and develop over time, while bearing's (read: whole assembly's) performance will keep declining and might end up in product's quality loss, machine's damage, or failure. Calculation of bearing characteristic frequencies and the associated bearing defects is provided in the following series of equations, which were taken from [1]:

"Ball Passing Frequency Outer Race" – the rolling element pass frequency on a stationary outer race (the frequency at which a rolling element contacts a fixed point on a rotating outer race with a stationary inner race):

$$f_{BPFO} = \frac{N}{2} \cdot f_s \cdot (1 - \frac{d}{D} \cdot cos\beta) \tag{4}$$

"Ball Passing Frequency Inner Race" – the rolling element pass frequency on a stationary inner race (the frequency at which a rolling element contacts a fixed point on a rotating inner race with a stationary outer race):

$$f_{BPFI} = \frac{N}{2} \cdot f_s \cdot (1 + \frac{d}{D} \cdot cos\beta) \tag{5}$$

"Ball Cage Stationary Outer Race" - the rotational frequency of the ball cage with a stationary outer race (or the relative rotational frequency between the cage and the rotating outer race):

$$f_{BCSOR} = \frac{f_s}{2} \cdot \left(1 - \frac{d}{D} \cdot cos\beta\right)$$
$$= \frac{f_{BPFO}}{N} \tag{6}$$

"Ball Cage Stationary Inner Race" - the rotational frequency of the ball cage with a stationary inner race (or the relative rotational frequency between the cage and the rotating inner race):

$$f_{BCSIR} = \frac{f_s}{2} \cdot \left(1 + \frac{d}{D} \cdot cos\beta\right)$$
$$= \frac{f_{BPFI}}{N} \tag{7}$$

"Ball Speed Frequency" – the rotational frequency or a rolling element:

$$f_{BSF} = \frac{d}{D} \cdot \frac{f_s}{2} \cdot (1 - (\frac{d}{D} \cdot cos\beta)^2) \tag{8}$$

"Ball Fault Frequency" – frequency of a local fault of a rolling element (contact frequency between a fixed point on a rolling element with the inner and outer races):

$$f_{BFF} = \frac{d}{D} \cdot f_s \cdot \left(1 - (\frac{d}{D} \cdot cos\beta)^2\right)$$
$$= f_{BSF} \cdot 2,$$

(9)

where d is ball diameter, D is bearing pitch diameter, N is number of balls, β is the bearing contact angle, and f_s is the shaft rotational speed in rotations per second.

From the diagnostics point of view, vibrations caused by a bearing mechanical damage have four stages of development. As the damage progresses, vibration changes in character, and has a typical behavior at each of the stages giving out certain frequency spectrum patterns. These patterns appear at different frequency ranges, so different diagnostics techniques are available for their detection. Determination of the stage is helpful as an orientational point to determine the degree of potential risk. The description of the wear development stages with corresponding techniques is presented in the Table 5.

Table 5. Stages of bearing damage development

Stage	Description	Frequency spectrum characteristic patterns	Technique for pattern detection	Remaining bearing life [4]
1	An insignificant damage occurred and started producing high-frequency impulses	Peak in ultrasonic (20+ kHz) range of frequencies	Spike Energy, PeakVue	10-20% of L_{10} and more
2	The deterioration progresses and becomes capable of inducing resonant vibrations of the bearing.	Peak on bearing natural frequency in the high-frequency range (possibly with sidebands); peaks on bearing fault frequencies are seen in demodulation spectrum	Demodulation techniques (High-frequency resonance techniques)	5-10% of L_{10} and less
3	The bearing vibrates on the frequency of the appropriate component damage	Peaks on bearing fault frequencies in the main spectrum	Common frequency spectrum analysis	1-5% of L_{10} and less
4	Serious damage is present, vibration is at a significant level	Peaks decrease in amplitude and may become unrecognizable, whereas the overall noise increases to a high extent	Common frequency spectrum analysis, or RMS value assessment	Near-failure condition

Obviously, standard FFT spectrum analysis is helpful for bearing damage detection only at the last two stages, and the more advanced vibration analysis techniques have to be used to detect the damage at the earlier stages.

Demodulation techniques (High-frequency resonance techniques)

Demodulation techniques are able to detect mainly the information whether the bearing is experiencing the second stage of bearing wear development, according to the Table 5. At this stage, the characteristic fault frequency peaks are obscured in the frequency spectrum. The vibration caused by the bearing damage is not strong enough in amplitude so far, but it is already possible to identify the problem by means of these techniques.

According to the definition stated in [5], envelope detection, or amplitude demodulation is "the technique of extracting the modulating signal from an amplitude-modulated signal". The result of this process is the demodulated signal - the time history of the modulating signal, or the original signal envelope. The demodulated signal, in turn, can be transformed into the frequency spectrum (envelope spectrum, demodulation spectrum). The term "envelope analysis" is associated with the frequency domain signal interpretation.

Modulation itself is a process of varying of a periodic signal – carrier signal – depending on the other signal – modulating signal. There are two types of modulation: amplitude modulation, which is the variation of the amplitude of a signal at a constant frequency, and frequency modulation, which is the variation of frequency of the signal at a constant amplitude. Amplitude modulation is associated with the change of the loading conditions and frequency modulation is associated with the change of running speed.

In case there is a defect of one of the bearing's components, each time a rolling element passes over the defect, it produces an impact to the bearing. The generated impact is able to induce the bearing's vibration at its resonant frequency (from a range 1-20 kHz [6]), and the periodicity with which the impact is generated is the fault frequency corresponding to one of the bearing components' defects (v. equations (4 - (9). In other words, as there is a change in bearing's loading forces, the technique has to extract this defect-related information from the amplitude modulated signal, where the high-frequency carrier component is the structural resonance frequency, and the low-frequency modulating component is the bearing fault frequency.

The process of the demodulation involves three stages. In the first stage, pre-filtering, the vibration signal is filtered by a high-pass filter to get rid of the low-frequency high-amplitude signals. The second stage, enveloping, is performed by using either the appropriate analog electrical circuit arrangement, or digitally – typically, by means of the Hilbert

Transform. At this stage, the carrier frequency is stripped away, and the output of the procedure is the modulating signal in time domain. The third stage, analysis, includes applying FFT on the obtained signal and analyzing the information it comprises.

This technique, or, at least, its conventional implementations, has several limitations. One of them is the determination of the way to approach the choice of the frequency range for the high-pass pre-filtering stage. According to [7], this range is commonly determined by an ad hoc approach, i. e. series of experiments where filtering is performed in different frequency ranges, and the results are subsequently compared. Then, the author states another possible solution: "A rule of thumb proposed by Weller is to set the lower corner frequency to be higher than 10 times running speed and to set the upper corner frequency at circa 60 times the ball passing outer race frequency". The other and more direct method is to get the bearing natural frequencies via an impact hammer. The other limitation is that the technique will lose in efficiency, if more than one defect is present. Then, it is important to notice that the amplitude of the peaks in the obtained envelope spectrum contains just relative information, – how higher their amplitude is in relation to the background noise, – so it does not contain the information about the detected vibration magnitude itself. And finally, it is efficient only if the bearing is at the early stages of wear, otherwise the peaks are not so distinguishable and the other analysis techniques have to be applied.

Spike Energy technique

Spike Energy technique belongs to the filtered high-frequency signal enveloping methods. Xu [8] defines the concept of Spike Energy as „a measure of the intensity of energy generated by repetitive transient mechanical impacts". The technique performs amplitude demodulation by means of non-conventional Peak-to-Peak Detection. It proceeds with the PTP amplitudes and it is able to preserve the peaks' magnitude compared to the envelope detection methods, which use a low-pass filter to obtain the modulating frequency, as low-pass filters have a smoothening effect on the signal peaks. Thus, this technique is more sensitive to the defect frequencies.

The outputs of the Spike Energy processing might be: overall SE severity, SE time waveform, or SE frequency spectrum. Spike Energy severity is expressed in gSE, where g is a unit of acceleration, and „SE" indicates that the overall amplitude was taken from a bandpass frequency range. It is useful to follow up the trending of this value together with

the common vibration measurements – of acceleration and velocity. The certain indicator of the developing damage is the increase of the value of the gSE, whereas the acceleration and velocity vibration values are still in the acceptable range.

It is important to note that the SE values are very dependant on a sensor mounting location and conditions and the type of the sensor itself, i. e. if some of these factors differ from one measurement to another, the measurements will give out imcompatible results. The reason for that is difference in structural frequencies and amplitudes, which play a key role in the measurement. Another important fact is that sensor internal component natural frequency has to be near center of bandpass. [9]

Shock Pulse Method

The Shock Pulse Method is a diagnostics tool which is intended to detect shock (pressure) waves generated by metal-to-metal contact occurring during the rotating motion – typically, as a result of lubrication film breaks. The fact that there is a direct relation between the metal-to metal contact density and the lubrication condition makes the application of the SPM more oriented on estimation of the lubrication condition than the other techniques.

The principle of the measurement is based on, at the first place, using an accelerometer of a specific design, so its natural frequency is 32 kHz - [10], [11] (although some sources refer to the value of 36 kHz [9], [12]). This frequency is, in fact, a typical frequency of a shock pulse wave. The signal obtained by the measurement is then amplified, as its amplitude is rather small; then it has to pass through a bandpass filter to strip away the frequencies outside a near-32-kHz range. Finally, the signal is converted into analog electric pulses, which are used to produce an output in dB with a 100 µV reference value [9].

The SP measurement gives out two readings: SP carpet value, which is used for lubrication quality assessment and SP max value, which indicated a presence of a bearing damage. The SP Carpet Value is an indicator of the density of occurring shock impulses, this value tends to increase as more metal-to-metal contact occurs. This typically happens as the result of lubrication film breakdowns. SP max value is a value of the maximum shock amplitude. Obviously, a bearing damage produce an impact of an amplitude higher than the frictional vibrations, so the SP max value is outstanding from the carpet value. There are unified color-coded SP levels for the bearing condition assessment.

2.2 Bearing failure modes

As a mediator between rotating and stationary components, bearing as such is subjected to loads. As stated before, bearing damage is a common cause of spindles vibration. However, knowing/detection of the damage itself is not enough to provide a sufficient diagnostics, because the aim of quality assurance procedure it to ensure the product will functionate in an acceptable way – in other words, that the damages occurance probability will be dragged down to the lowest possible value.

Bearing manufacturers provide an estimated bearing life ratings based on laboratory fatigue tests' statistics. The decisive factor in bearing choice and rating is its fatigue life assessment expressed in L10 life rating. Paradoxically, as reasonably noted by Adams [13], the life of a bearing is usually dictated by other damages caused by factors, damage from which occurs before the bearing undergoes a fatigue failure. According to SKF [14], only one third of bearing failures is caused by fatigue, while the other main causes are lubricaion problems (circa 33%), contamination (circa 16%), and improper mounting (circa 16%).

ISO 15243:2004 states 6 bearing failure modes with more specific submodes to categorize the types of bearing failures (Table 6):

Table 6. Bearing failure modes

Bearing failure mode	Submodes
A) Fatigue	• subsurface initiated • surface initiated
B) Wear	• abrasive • adhesive

C) Corrosion	• moisture
	• frictional
	    ○ fretting
	    ○ false brinelling

D) Electrical erosion	• excessive voltage • current leakage
E) Plastic deformation	• overload • indentation from debris • indentation by handling
F) Fracture and cracking	• forced fracture • fatigue fracture • thermal ctacking

Commonly, a distinct cause is characteristical to each of the modes, thus,it is useful for bearing diagnostics by visual inspection.

In Appendix 1 each of the failure submodes is presented with the corresponding chain of causation (from right to left). Information used in the table was mainly taken from [14].

A simplified categorization of the above-presented bearing damage root causes by the type of affection is suggested in Table 7. The root causes, their damaging impact could be partly mitigated or eliminated in the post-production stage of the assembly, are groupped together under the thick line.

Table 7. Categorizing of the bearing damage root causes

Root cause	Category
Long operation	Wanted case
Inadequate lubrication	Proposal-affected
Light loads, speed diffrences	Proposal-affected
Ineffective insulation, Frequency variations	Proposal/opeation-affected
Bent shaft, surface imperfections	Technology-affected
Ingress of contamination	Proposal-, operation-, and handling-affected
Inadequate fits	Proposal-, and mounting-affected
Inadequate sealing	Proposal-, and mounting-affected
Inadequate handling/storage	(Itself)
Improper mounting procedure	(Itself)

2.3 Vibration measurement devices

To perform diagnostics, the vibration data are needed first to be obtained in the form of a registered signal, then appropriately treated to examine the objective characteristics of the vibration.

2.3.1 Measurement units

Vibration is a dynamic effect, and it can be characterized by correlative physical quantities - displacement, velocity, and acceleration. It is critical to choose the correct quantity to measure, due to certain limitations in sensors' construction and, thus, limitations of the range of values, where the measurement signal corresponds to reality. Thus, the measured value signal has to be strong enough to be distinguished from the background noise and assumed vibration frequencies and amplitudes have to match sensor's range of frequencies and amplitudes. The measurable ranges of frequencies are presented in Table 8.

Table 8. Common range of measurement frequencies. Values were taken from [2]

Unit	Range [Hz]
Displacement	0.1 – 1000 (2000)
Velocity	10 – 1500
Acceleration	1 – 30000

2.3.2 Measurement sensors

Displacement measurement sensors

Eddy current sensor is the most practical sensor for displacement measurement. The magnetic field of a coil contained in the sensor changes with the change of the distance between sensor tip and the rotating conductive material: eddy current loops magnetic field react to the change of the distance, as it influence the resistance of the field. The voltage at the output of the sensor is directly proportional to the gap between the sensor and the material.

The main advantage of eddy current sensor is that it is non-contacting, since that no wear occurs. In the field of diagnostics, it is commonly used to detect vibrations at relatively low frequencies (there is no lower frequency limit), and/or when it is impossible to mount an accelerometer. Besides that, it is used when the actual amplitude in micrometers is the target value, and there is no need to perform the frequency analysis – e. g. studying the dependence between bearing preload and the vibration amount.

Other displacement sensors – laser, ultrasound, capacitive, and inductive are rarely used for vibration measurement.

Velocity measurement sensors

Vibration velocity is a ratio of amplitude and frequency. So, it is undistinguishable from the measured velocity value, if the measured system is withstanding vibration of high amplitudes at low speed, or vibration of low amplitudes at high speeds. Namely velocity is used as an assessment criterion for determination of grades for vibration tolerances for rotors balancing in ISO 1940 [15] and in ISO 10816 [16].

Velocity measurement sensors work basing on the electromagnetic induction principle: the voltage produced on a coil is directly proportional to the relative velocity between the coil and the magnetic field. The sensor contains a permanent magnet, which is connected to a moving part. As the vibrations are transferred to the magnet, and the coil does not move, the inductive voltage is produced, and can be readily recalculated to the velocity value.

The advantage of this type of sensors is that they are cheap and sensitive. However, due to their fragile construction, their precision is limited, when used out of the laboratory conditions, and they also tend to wear. They also have a lower frequency limit of circa 10 Hz, to avoid usage on their resonance frequencies. These sensors are large and have special mounting requirements, and that could be another disadvantage.

Acceleration measurement sensors

Acceleration is directly proportional to the caused load. It is widely used for sophisticated applications requiring analysis in high-frequency range, especially for detecting frequencies caused by damaged bearings.

The vibration force is applied to a reference mass contained in the sensor, which is connected to a piezoelectric crystal, and a charge which occurs as a result of a mechanical deformation of a crystal is measured and subsequently recalculated to the acceleration.

These sensors exist in 3 types – compression-type, shear-type and triaxial, depending on the direction of the vibration force being detected.

Accelerometers come in a big variety of sizes. They are rugged and the precision of measurement is not influenced by a sensor orientation. The main disadvantage of this type

of sensors is that their sensitivity is low on low frequencies, and they resonance on high frequency, so they have a two-side limited frequency range, which is, however, usually large enough to obtain target values. Commonly, smaller accelerometers have a larger frequency range, but lower sensitivity. Thus, certain consideration has to be taken to determine the range of interest and to check if is actually covered by a chosen sensor.

2.3.3 Vibration analysis and diagnostics equipment

Every area of industry is familiar with vibration and with a need to reduce it to improve performance. Condition monitoring of the machines is highly reasonable for economy purposes. If a problem occures, it needs to be solved efficiently and quickly. Therefore, a large number of devices for vibration analysis and diagnostics were brought to the market to meet requirements of a potential customer in every field. These devices acquire vibration data from the sensors and then treat them in an appropriate way to perform analysis to the extent required. They differ in size, functionality and the level of protection.

Commonly used vibration measuring devices

It is very common that vibration measurement does not need to get further than checking if the vibration level is in a permitted range and if it is not, promptly assume the possible fault. Many manufacturers tend to suggest very easy and user-friendly devices for this case to save time on staff trainings and eliminate possible errors due to incorrect measurement. Fluke 805 [17] is used for such simple purposes as screening, or prompt go/no-go testing with such basic functions as overall vibration and temperature measurement and bearing condition assesment using crest factor value. Vibrio M by Adash [18] is a similar device, its functionality is though expanded also to fault source identification tool, signal display in time and frequency domain and a possibility to export measured data to special software for further analysis.

FACULTY
OF MECHANICAL
ENGINEERING
CTU IN PRAGUE

DEPARTMENT OF
PRODUCTION MACHINES
AND EQUIPMENT

Figures 5, 6. FLUKE 805 and Microlog analyzer in application. [17], [19]

Companies such as SKF and FAG mainly known for bearing production also have lines of vibration analysis equipment and software under their own development in this category: e. g. FAG's Detector II [20], SKF's QuickCollect [21], and some others.

For more complicated analysis and diagnostics purposes a large variety of more sophisticated equipment is offered: those devices offer an extended functionality, but commonly remain user-friendly like simplier ones. Their memory capacities and their processors are powerful enough to perform needed measurement data treatment and present it in an appropriate form, while the device is staying light and portable. Such devices are, for example, VIBSCANNER 2 [22] and VIBXPERT II [23] from Pruftechnik, which are able to measure overall vibration, do impact tests, and perform almost exhaustive range of time- and frequency domain analysis. These devices have plenty of analogs with similar functionality and parameters – FLUKE810 [24], Microlog analyzer by SKF [19], etc.

Starting with the simpliest ones, a temperature sensor could be integrated, as temperature monitoring is always important. It is also practical to have a rotations-per-minute (RPM) sensor. Such elements are highly useful and, fotrunately, easy-to-integrate. Many manufacturers also add a Bluetooth feature and/or possibility to share measurement results via email. Sometines automatic fault detection is integrated to measurement devices, but its relevance is limited. Most devices are also able to assess the overall vibration level according to the standard ISO 10816 [16]. There is also an opportunity to add an impact hammer element to measure the structural resonances, like it is available from Pruftechnik's VIBXPERT II [23].

It is not uncommon that a vibration measuring device is integrated with a balancing machine. It could be very helpful to perform in-situ balancing instantly after the measurement station has diagnosed an unbalance. Such devices as Schenk's Smart Balancer [25] can provide a vector diagram of the unbalance and other data for effective one- or two-plane balancing. That is practical since non-portable balancers are commonly not able to run at high rotational speeds; neither count they with thermal and multiple bearing interaction effects, which, in turn, typically occur at higher speeds. However, compared to non-portable balancers, which are designed primarily to isolate the rotating part from the vibrations as much as possible, in-place unbalance measurements have to be performed with certain degree of consideration – for instance, one must mind checking and filtering the background vibrations to make sure that namely unbalance is the problem. It is worth mentioning, that balancing procedures, especially in two planes, especially on big machines, have to be performed by experienced staff.

Figure 7. SCHENK SmartBalancer in application

Vibration measurement automation and customization opportunities

As the offer on vibration diagnostics equipment market is really extensive and diverse, equipment suppliers try to follow the progress as tightly as possible and introduce new, sometimes very useful and time-saving and error-limiting - generally by means of high degree of automation - features to remain a compelling competitor. Such technology is, for example, radio-frequency identification (RFID) tags at measuring spots for quick and practical route-based data collection. With the help of such technology, the device can identify each individual measuring point itself without a need to manually re-configure the

measurement setup and enter measuring parameters. Obviously, it is a great advantage for large plants with numerous machines or components to be monitored. Such feature is offered, for example, by FAG's Detector III [26]. Alternatively, the route-based data collection could be even fully eliminated by employing Industrial Internet of Things (IIoT) devices, which are able to share measured information online, so the monitoring can be performed constantly. Such device is, among others, VIBGUARD IIoT [27] offered by Pruftechnik. Pruftechnik also developed its own intelligent sensor VIBCODE [28] to ensure error-free data acquisition and transfer, also with automatic detection of a measurement place.

In many cases the monitoring is not enough, and measured data have be analyzed more deeply, especially as a base for consequent substantial performance improvements. Typically a vibration measurement equipment manufacturer enriches its offer with a software, which is compatible with the range of supplied devices. With the help of this software data can be stored, treated and analyzed using appropriate techniques, and, in case of IIoT devices, even monitored online. Such programs are, e.g. Analysis and reporting manager [29] from SKF, OMNITREND Center [30] from Pruftechnik, DDS [31] from Adash, etc.

Some companies use a strategy of making somewhat universal devices for vibration measurements with subsequent expanding its functions individually by offering a customer a special requirement set of modules. For example, VIBROPORT 80 and VIBROTEST 80 [32] offered by Schenk is able to perform a wide number of analysis techniques, balancing, diagnostics, data collection features with a possibility of further customization. Another example could be FAG's ProCheck [33] device with a large number of inputs and overall powerful parameters, which is flexible enough to provide a substantial vibrational analysis „in all industrial segments". Finally, there is also an attempt to customize less universal devices, for example, by offering an opportunity of sensors selection.

Vibration measurement devices overview

The overview of the chosen above-mentioned devices is presented in Appendix 2.

FACULTY
OF MECHANICAL
ENGINEERING
CTU IN PRAGUE

DEPARTMENT OF
PRODUCTION MACHINES
AND EQUIPMENT

2.4 Assembly and control processes of precise spindle bearings

2.4.1 Design considerations. Dimensions and geometrical tolerances control

Already at the stage of the spindle assembly proposal, the fits between the shaft, bearings and the housing have to be considered very judiciously. The consequences of the inappropriate resulting fit (too loose or too tight) are very likely to cause the bearing damage. Generally speaking, if the fit between the diameters is too loose, a relative motion between the components occurs and results in fretting corrosion, adhesive wear and, definitely, in excessive heat generation during bearing operation, which may lead to thermal cracking. If the fit is too tight, the rolling elements raceways may be distorted, or bearing's internal clearance will be reduced, which, again, may result in excessive heat and thermal cracking. Moreover, the excessive interference between components requires a high mounting force, which increase the risk of damage.

An important factor to consider is that in case of high-speed run of precision bearings, the impact of the centrifugal force cannot be neglected, and the fits become speed-dependent. The centrifugal force acts in the inner ring, forcing it to expand, which might result in clearance between moving parts, even though there was none in the moment of the assembly. The outer raceway and ring experience additional loading and become more vulnerable to contact deformations. The impact of the centrifugal forces in high-speed applications is usually larger compared to the impact of loading forces.

Bearing manufacturers define strict tolerances – dimensional and geometric for the bearing seats on the shaft and the housing. The dimensions may be measured either by a micrometer, or by a 3D measurement station.
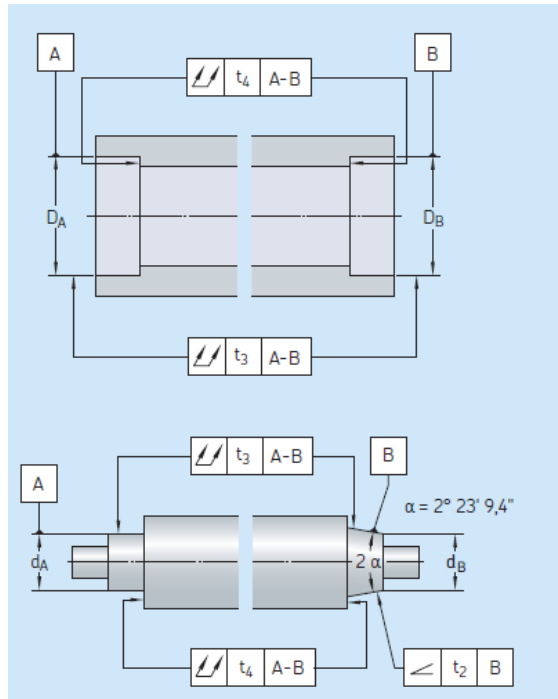
Figure 8. Bearing seats geometrical tolerances [34]

Another important spindle assembly design consideration is addition of mounting-related features. They are lead-in edges of the shaft and the housing, undercuts, maximum radius definition.
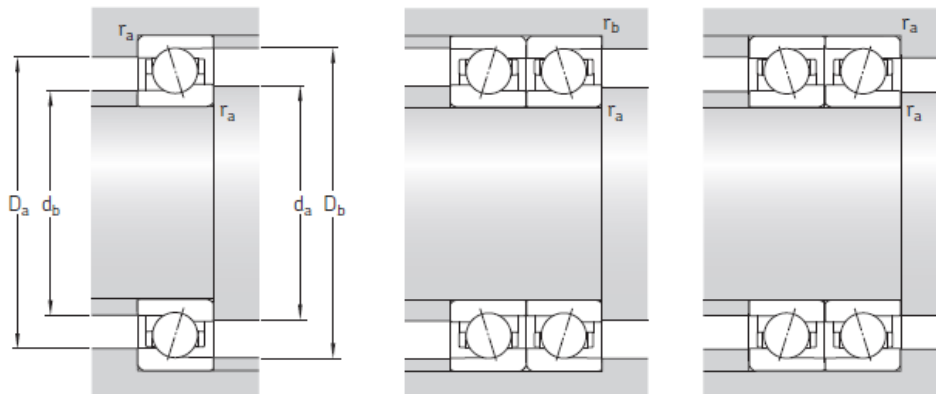
Figure 9. Abutment and fillet definitions [34]

2.4.2 Storage and assembly guidelines

Bearings strorage and handling is an important factor of bearing service life influence, since there a certain risk of contaminants ingress, or improper forces application. Bearing manufacturers produce useful guidelines in order to prevent this from happening.

FACULTY
OF MECHANICAL
ENGINEERING
CTU IN PRAGUE

DEPARTMENT OF
PRODUCTION MACHINES
AND EQUIPMENT

Cleanliness is a very important factor, especially for lightly loaded super-presicion bearings. The ingress of contaminants affect bearing performance very badly, causing vibration and operating tempertaure to increase. This may result in abrasive wear, surface fatigue damage, moisture corrosion, or plastic deformation from indentation from debris. Even a small amount of dirt on a bearing seat can cause a significant bearing misalignment. The contaminants may be transferred to the bearing by air (smoke, dust, moisture), by touching surfaces (hands, tools, packages), or they may be included into a bad quality lubricant. The bearing have to be stored in a clean, dry, dust-free area, or appropriately wrapped in order to protect them from the contaminants.

The area of storage also has to be free of shocks or vibrations. Bearing have to be stored horizontally, especially in case some vibrations are present – othewise, they are more vulnerable to the surrounding vibrations, which, in turn, might result in false brinelling. Bearings with grease-for-life lubrication have a limited shelf life, as the grease tends to deteriorate with time.

Before mounting procedure, again, one has to make sure that the work area is, dry and dust-free. It is practical to arrange an area with surfaces made from easy-to-clean materials, which do not tend to chip or rust. All of the mounted surfaces have to be clean and undamaged. The fitting dimensions have to be within appropriate tolerances.

While induction heating application is preferable for bearings of a rather large size (over 100 mm outer diameter), for the small- and medium-size bearings so-called „cold mounting" is used, which means, they are mounted by mechanical force application. Hence, there is a risk of damaging the bearing by improper force application.

As far as the mounting forces are concerned, there are several aspects to be considered. The first one is that the fit between two diameters has to be proposed and controlled appropriately – as described in section 2.4. Secondly, the force has to be applied on the proper bearing ring – it is always the ring corresponding to the diameter being mounted. The force must be applied evenly in a proper direction (i. e. at right angle). The rolling elements and the raceways must be isolated from the impact force, especially those made from fragile ceramics. Then, the proper amount of force has to be applied – the concept of a „proper amount" is difficult to define and it is usually based on the experience of the person who performs the mounting.

The proper tools have to be used. The combination between an impact sleeve and a dead-blow hammer with a nylon head is able to ensure the efficient force transmission and reduce the risk of damage of rolling elements and raceways. It might also be practical to apply a thin oil film on a shaft before mounting a bearing.

2.4.3   Bearing rigidity and preload

Bearing are preloaded to ensure that such interconnected factors as dynamic stability, stiffness and accuracy of the system are acceptable. Moreover, preload value is directly proportional to the the first order natural frequency of the system. [35] By applying preload to the bearing, bearing's deflection under load is minimized, so are the vibrations and the risk of rolling elements' skidding in the raceway. However, the amount of preload has to be carefully controlled, because too light preload results in insufficient stability of the system, and a too high preload generates excessive heat during the operation. Lighter preloads are acceptable for high-speed operating spindles, though they might show a performance decrease on lower speeds.

Fixed position axial preload is reached by applying either the matched bearing sets, or the precise bearing rings. Requirements for their tolerances are stated in the bearing manufacturer's catalog. The alternative to this preloading method is a fixed pressure preload obtained by spring components pushing on the bearing rings. The benefit of this arrangement is reducing of the thermal efects.

Radial preload is obtained by removing the bearing's internal clearance during the mounting procedure and depends on the proposed tolerances and fits. Radial preload cause load to distribute between more rolling elements, so the load amount applied on each element is reduced.

2.4.4   Grease distribution run

Greased-for-life precision bearings have to undergo a grease distribution run before the assembly can start to be used in the machine operation. Grease distribution run has to be performed according to the procedure prescribed by the bearing manufacturer. This procedure has a great impact on the bearing's life and future performance. This procedure consists of a series of start-stop operations to ensure the even distribution of grease. Stops are performed in order to prevent excessive heating and preload of bearing contact areas. Nevertheless, there is a risk of bearing overheating, so it is recommended to control the

temperatures of the bearings during this procedure. A distribution is even and completed as soon as the bearing temperature becomes stable.
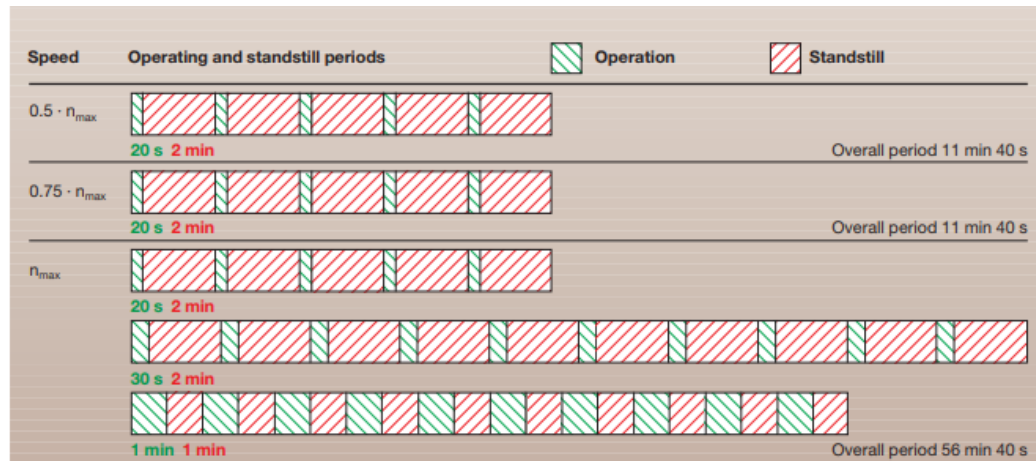
Figure 10. Grease distribution run procedure diagram [36]

Precision bearings life is limited rather by the properties of the lubricant, than by the loads and fatigue. Although, if the lubricant is unable to prevent sliding of the roller element on the bearing's raceway, this process may produce a tangential load (in addition to the normal load), which causes higher subsurface stresses and may lead to a premature subsurface fatigue failure.

2.4.5 Temperature monitoring

The bearing operating temperature is a very important performance-affecting factor, that should be monitored to make sure excessive heat is not generated during bearing operation. It is important to have a stable operating temperature; even more important that the value itself. The temperature trends have to be controlled and followed continuously. The unstable behavior of the temperature (rising and falling) may be related to end of grease service life. A rapid increase of the temperature during a short period of time is a sign of an occurred bearing damage.

The bearing temperature is usually measured at the stationary ring, and the sensor should be placed as close to the bearing as possible.

2.4.6 Geometric accuracy of axis of rotation

The rotational accuracy of the spindle directly impacts the resulting condition of the machined surface, i. e. the quality of the product. Deflections of the spindle axis occur due to external dynamic loads and elastic deformation of the assembly components and can be

minimized by correct assembly design and mounting, especially as far as clearances and preloads are concerned. Every clearance in the assembly fits may affect the rotational accuracy, enabling the unwanted and uncontrolled motion between the components. The accuracy is also influenced by RPM. This parameter is measured by displacement sensors at different speeds.

Generally speaking, the rotational accuracy is a function of the mated parts' manufacturing qualty precision, their dimensional and geometric tolerances, the surface roughness, and the mounting procedure. The bearing rotational accuracy affects the accuracy of the whole assembly. The main factor of the bearing's rotational accuracy is the runout of the inner ring's orbite. Its shape can be affected during the mounting procedure.

2.5 Methods of assembly and control currently employed at Viking CNC

This section takes into consideration Viking CNC FG-15 spindle assembly. FG-15 is a 6-axis single-purpose CNC tap flute grinder equipped with oil cooled direct drive Fanuc servo spindle motor with programmable speed from 0 to 15.000 RPM. The nominal power 15kW with 19kW peak performance.
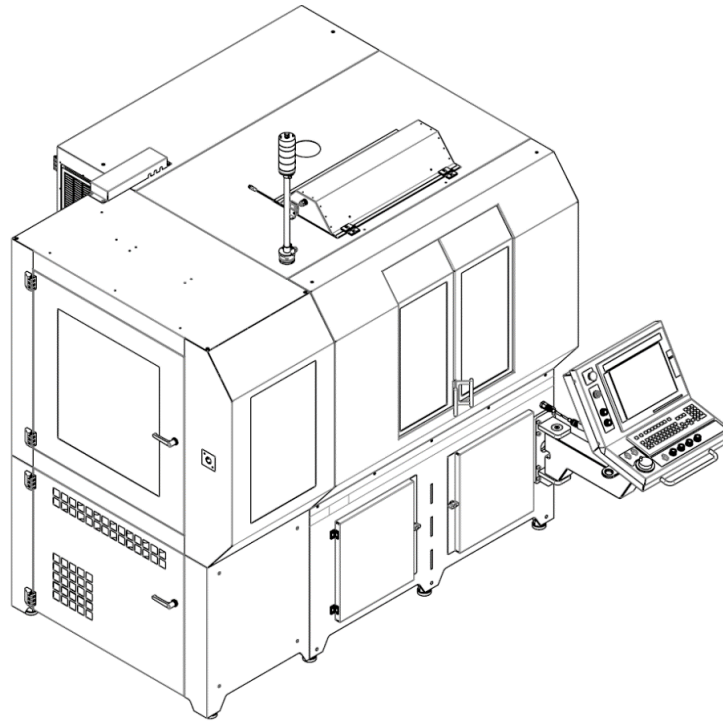
Figure 11. FG-15
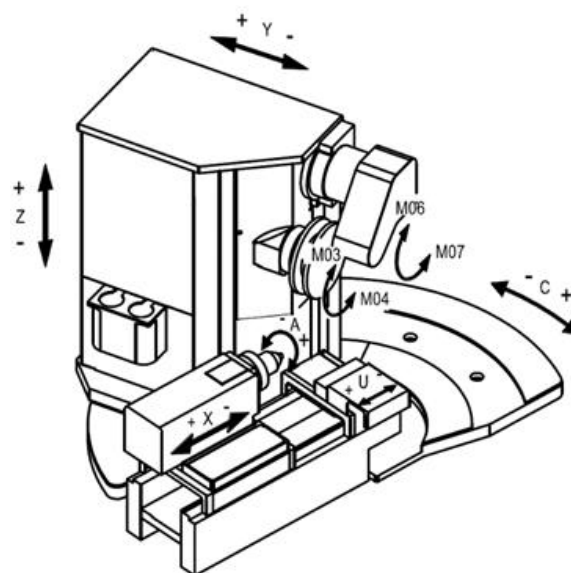
Figure 12. FG-15 Axes

43

The FG-15 spindle assembly consists of the precise shaft with two SKF's super-precision sealed single-row universally matched angular contact ball bearings with ceramic balls in the front part of the assembly and the radial sealed single-row deep groove ball bearing with ceramic balls in the rear part of the assembly. The exact type of bearings is defined in the Figure 14 and Figure 15. The spindle is directly driven by an electric motor, which is connected to the assembly via a coupling.
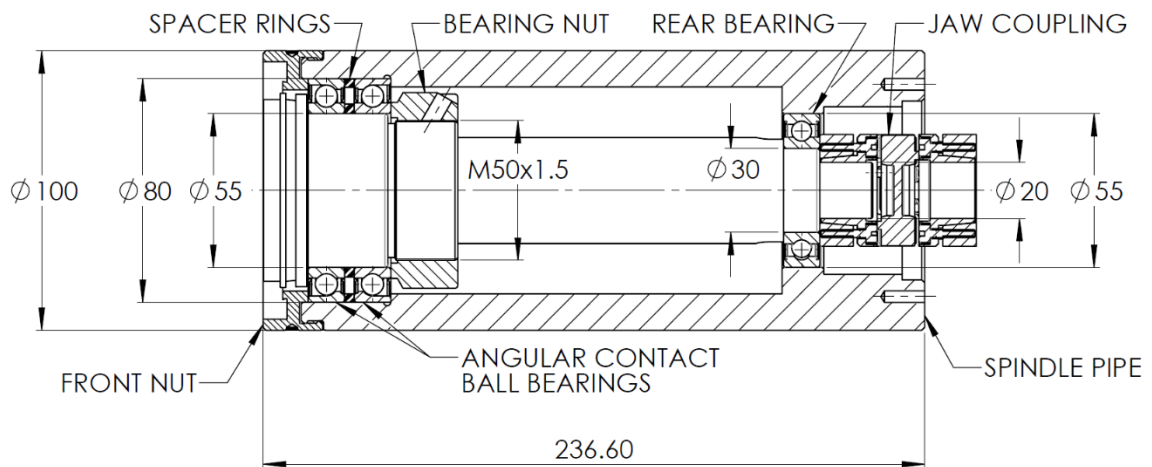
Figure 13. Spindle assembly
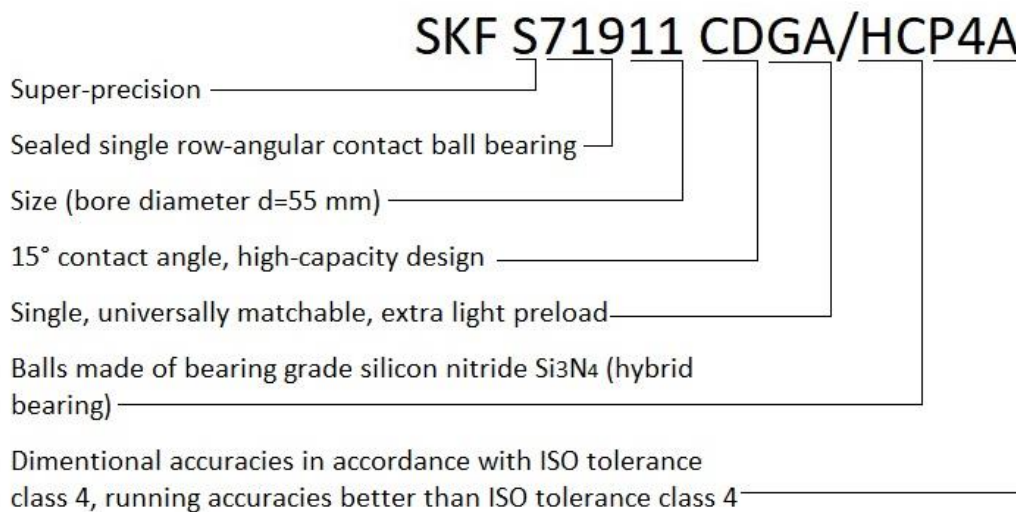
Figure 14. Front bearings type

6006 2RZTN9/HC5C3WT

Single row deep groove ball bearing
Size: (Bore diameter d=30 mm)
Non-contact seal, NBR, on both sides
Glass fibre reinforced PA66 cage, ball centred
Rolling elements made of silicon nitride
Radial internal clearance greater than Normal
Grease specification (Long-lasting high-temp lubricant)
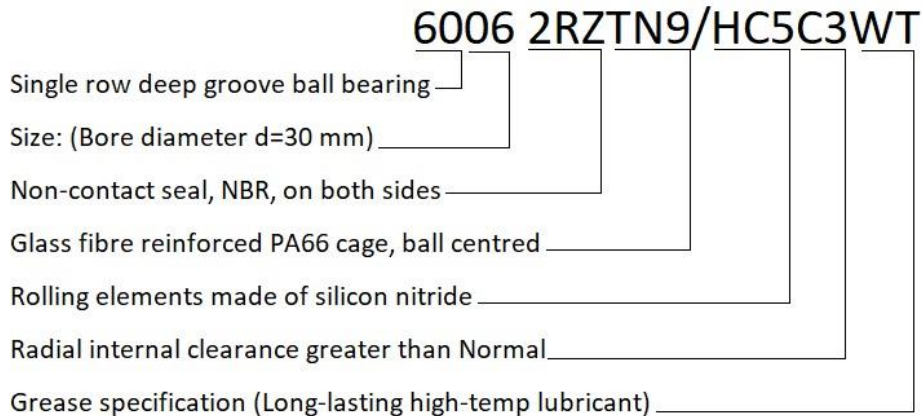
Figure 15. Rear bearing type

2.5.1 Dimensions and geometrical tolerances control

The shaft dimensions that require measurement, such as bearing seats, are numbered in the drawing, as shown in the Figure 18 and Figure 19. The dimensional control of the shaft is performed at the manufacturer's facilities in Italy, and the manufacturer provides Viking CNC with resulting measurement protocols. All dimensions with geometrical tolerances are measured on Zeiss Contura 3D measurement station (Figure 16). The circularity of the diameters is measured on the Mitutoyo Roundtest RA-2100 measurement station (Figure 17). The diameters are then measured with a digital micrometer.
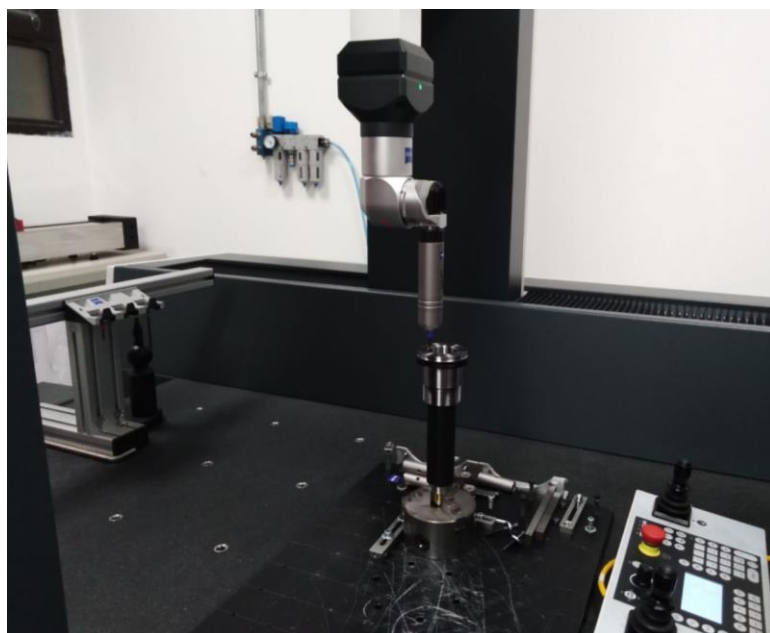
Figure 16. Zeiss Contura 3D measurement station

Figure 17. Mitutoyo Roundtest RA-2100 measurement station
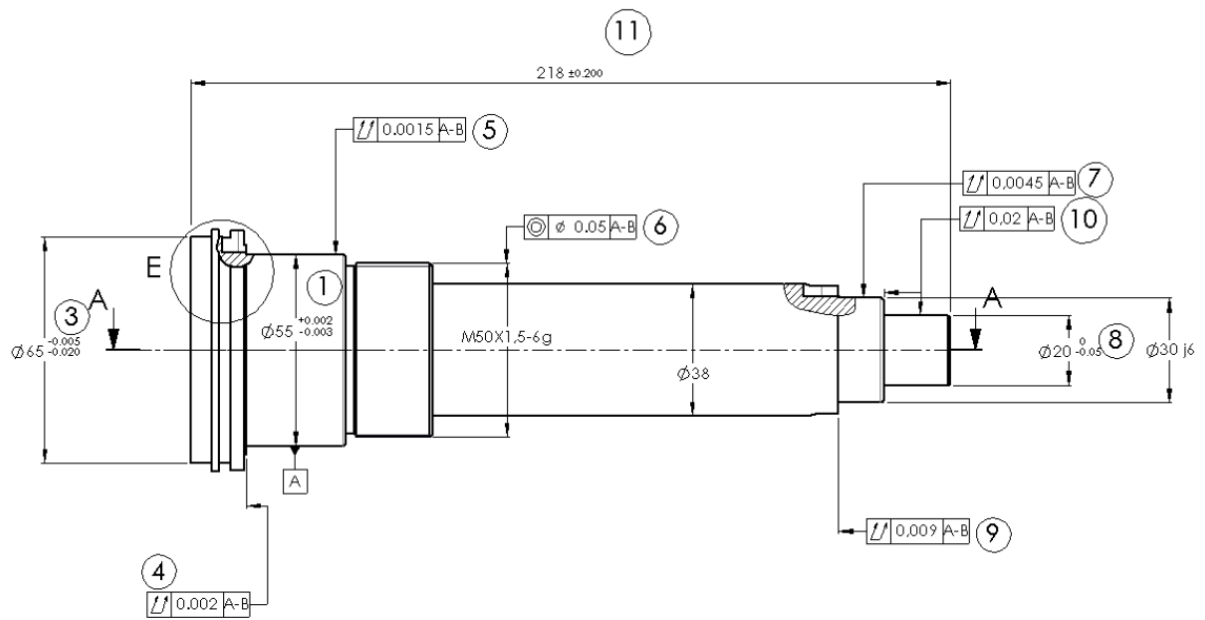
Figure 18. Geometrical tolerances and dimensions to be measured on the shaft

FACULTY
OF MECHANICAL
ENGINEERING
CTU IN PRAGUE

DEPARTMENT OF
PRODUCTION MACHINES
AND EQUIPMENT
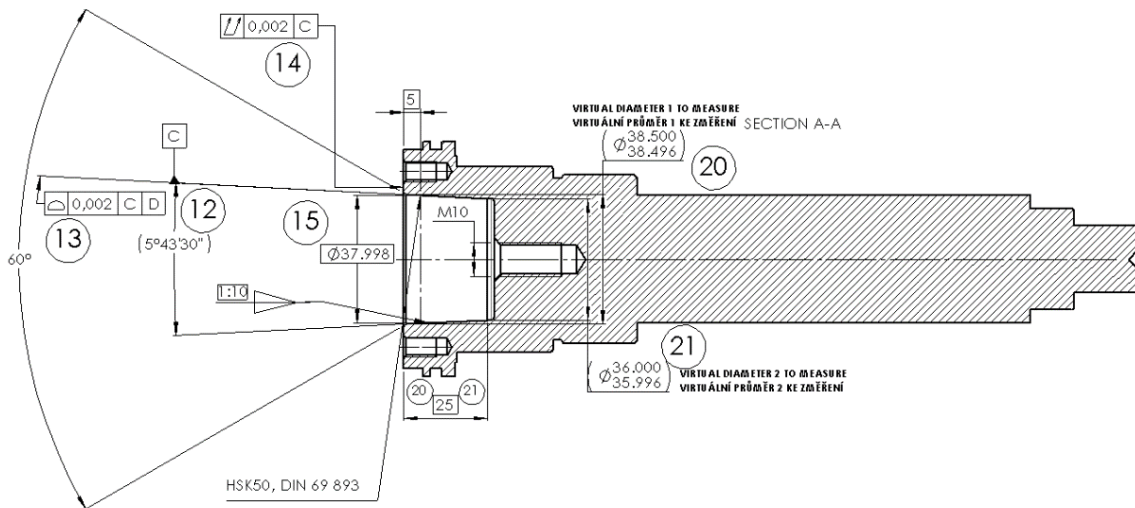
Figure 19. Geometrical tolerances and dimensions to be measured on the shaft

Bearing spacer rings are measured with a micrometer to have the same height (maximum deviation of 5 μm is tolerable – v. Figure 20).
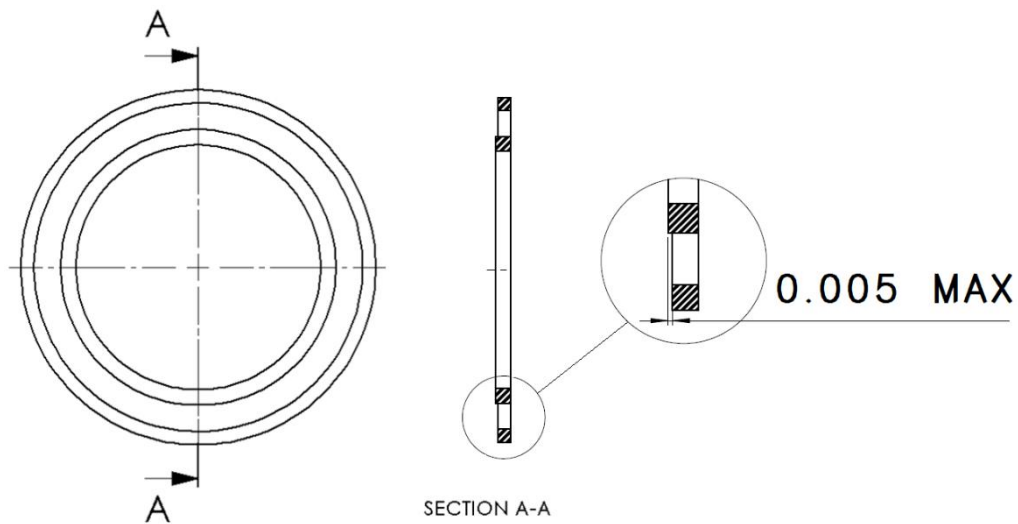
Figure 20. Bearing spacer rings

There is no special procedure currently employed regarding spindle pipe bearing seats geometry measurement.

2.5.2 Assembly procedure and notes

The assembly procedure is performed according to the Appendix 3.

2.5.3 Control procedures and test run

Grease distribution run and test procedures are performed after the spindle is mounted to the machine. Grease distribution run is performed according to the procedure described in section 2.4.4. until the temperature is stable and stays under 40 °C on 6000 RPM.

Figure 21. Grease distribution run procedure diagram [36]

The subjective assessment by listening is performed during the spindle assembly's test run on the machine. The principle of the assessment could be described in the following way: in case the bearings run without problems, they give out a "rustling" sound. Every deviation from the "normal" sound is considered as a problem. Typically, the "squeaking" sound signalizes that balls are skidding in the bearing raceway, or that the bearing outer ring is turning.

Spindle temperatures are monitored via a sensor placed in the rear part of the spindle motor and the results are displayed in the machine's HMI. The temperature has to be stable at different RPM.

2.5.4 Axial clearance control

The assembled spindle has to undergo an axial clearance control: a tensile or compressive force is applied to the shaft axially by pushing it in with hands, or by pulling it with screws put in the front holes. The shaft's displacement is measured during the procedure by a dial indicator. The acceptable result of the measurement is a displacement within 0.01 mm, which has to return to zero value once the shaft is released.

3. **Practical section**

This section describes practical application of the vibration analysis stated in the research section. The analysis is applied to the series of 5 spindle assemblies, which is a yearly production of the company. This section includes the proposal of the spindle test stand, where the spindles are going to be measured and tested, the measurement procedure instructions and description, along with the measurement results assessment and the evaluation of different factors' impact on spindles quality.

3.1 FG-15 spindles quality issues

FG-15 spindles are assembled at Viking CNC using second-party supplied components. The spindle is characterized by a light structure, as it does not withstand loads more than hundreds of newtons in radial direction during the grinding process.

The majority of quality issues the company faces is bearing-related. Typically, it is associated with an uneven noise coming from the bearings. Several typical patterns have been detected, although their cause has remained unclear most of the time. The typical „problematic" bearings behavior and possible reasons are, firstly, that bearings might „rattle" as a result of an unproper fit, as well as the angular contact ball bearings' outer rings might turn. Then, the typical for this spindle bearing-related quality issue is that bearing balls do not roll at constant speed and skid in the raceway. Besides undesired noise, these issues result in exstensive vibration and heat, which has a bad impact on the spindle performance.

Initially, there was no testing environment, so most of the problems have been revealed already at the moment when the spindle had been installed into the machine. So, if a problematic spindle is installed into the machine, and the test run shows that the spindle performance is not normal, the spindle is pulled out and disassembled. Parts which are supposed to be causing the problem are replaced with spare different ones, and the procedure of test in the machine is repeated until the satisfactory performance is reached. Obviously, such procedure might be very time-taking, especially in cases when it is hard to detect, which parameter exactly is causing the problem.

The aim of this section is to bring a systematic approach to the spindle quality assurance procedure and to reduce the uncertainties associated with this process.

3.2 Spindle test stand concept

The stand (Figure 22) has a concrete base on the anti-vibration feet in order to isolate the stand and, thus, the measurement equipment, from the surrounding vibration of the working hall, where the stand is situated. They are also used for height adjustement, which has to be controlled using a spirit level. The tested spindle assembly is clamped on a steel plate with T-slots.

Figure 22. Spindle test stand

Spindle is run by a Fanuc servo motor, its speed is controlled by Fanuc control system. The spindle is run coaxially, which corresponds to its final arrangement in the machine and provides the conditions similar to the ones in the macine. Furthermore, by using the direct drive, such effects as additional forces induced by the belt tightening, or additional vibrations such as belt trembling, are eliminated. The spindle and the motor shafts are coupled by the jaw coupling with a rubber insert.
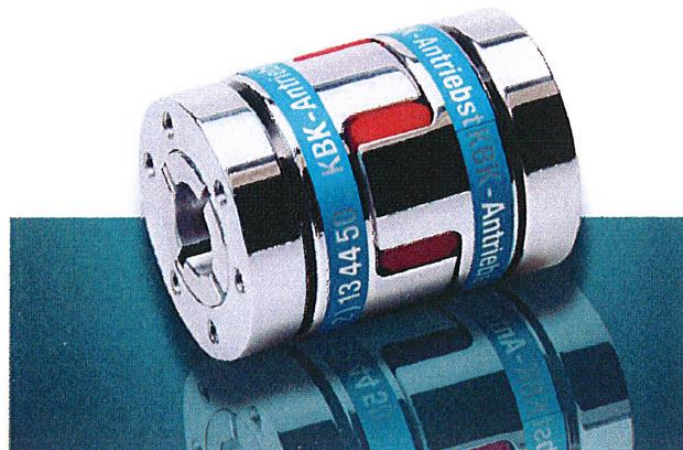
Figure 23. Spindle coupling [37]

The test stand arrangement is shown in the Figure 24. Spindle is placed into the two thin housings. They are designed to have a light structure, so that they have a minimum impact on the spindle vibration signal. A spring element is placed between the spindle and the housing surfaces, again, to isolate the vibrating spindles from the other masses and to get stronger vibration signal. Furthermore, the spring spindle placement is advantageous concerning its actual placement in the machine – the spindle assembly is fitted in a glide bushing.
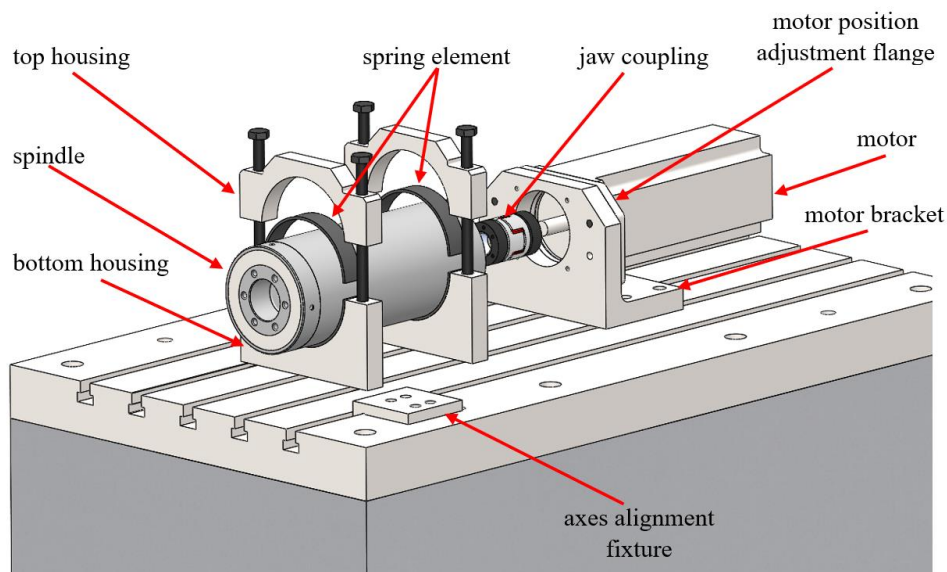
Figure 24. Spindle test stand arrangement

The sensor holders are magnetic, and their lower surface is prismatic, so that it nearly coinsides with the outer surface of the spindle pipe. The accelerometers are screwed into the holders and sticked to the assembly.

3.2.1 Axes setup

The tolerance of the axes misalignment should not exceed the maximum misalignment allowed by the coupling – 0.1 mm of radial misalignment. The motor axis is set up to be parallel with the base plate T-slots and remains fixed for the whole cyclus of measurement or testing procedure. After the motor is set up, the following measurements have to be taken:

1. The coupling actual diameter d_c
2. The motor axis actual height h_m – the coupling height h_c is measured by an altimeter. The motor axis height is then:

$$h_m = h_c - \frac{d_c}{2} \tag{10}$$

3. The motor axis actual distance b_m from the motor bracket side surface: the coupling distance b_c is measured by a depth gage. The motor axis distance is then:

$$b_m = b_c - \frac{d_c}{2} \tag{11}$$

The concentricity between the spindle and the motor axes is ensured by manipulating exclusively with spindles using the following procedure:

1. The spindle pipe actual outer diameter D_s is measured.
2. The shafts of the spindle and the motor are connected by a coupling.
3. The distance b_s between the motor bracket side surface and the spindle pipe is measured and then adjusted to be

$$b_s = b_m + \frac{D_s}{2} \tag{12}$$

by hammering to the rear housing in the appropriate direction.
4. A dial indicator is fixed on the setup fixture. It is used to measure the runout in the horizontal direction by moving the setup fixture in a T-slot. The runout in the

horizontal direction is adjusted by hammering to the front housing in the appropriate direction.

5. The height of the spindle pipe is measured at two points and then adjusted to be

$$h_s = h_m + \frac{D_s}{2} \tag{13}$$

by tightening the housings' screws.

6. Measurement of b_s and of the horizontal runout is done again to control that the values did not change after proceeded manipulation.

3.3 Vibration measurement

Generally, typical problems, which have been already detected on this type of spindles are associated with excessive noise, vibration, and bearing heat. Despite the fact that the quality of the spindle performance can be assessed to be acceptable or not acceptable, it is quite a problem to detect the root cause and eliminate it.

Measured vibration signal is able to provide useful information about the vibration character. Thus, vibration signal analysis is a very promising tool to determine the vibration causes. The application of the vibration diagnostics on the FG-15 spindles is supposed to provide the information about the vibration patterns, which are typical for the acceptably and not acceptably manufactured spindles. Because of the fact that 5 spindles are going to be measured, some statistical information can be collected. Followingly, the parameters correlating with the certain vibration spectrum patterns are supposed to be stated, basing on the acquired information.

3.3.1 Measurement equipment

Experimental measurements of the vibrations were performed using NI 9234 vibration input module (Figure 25 (a)) and 4 CTC AC105-2A IEPE accelerometers (Figure 25(b)). NI 9234 vibration input module has four analog input channels which can be sampled simultaneously at the 51.2 kS/s/channel sampling frequency. Acquired signal is proceeded to a PC with installed NI software, where the signal is processed and recorded.

(a)   (b)

Figure 25. Measurement equipment: (a) NI-9234 input module [38] and (b) installed IEPE accelerometer

3.3.2 Measurement process

The vibration was measured in 2 planes, each of which corresponded to the bearings location, as shown in the Figure 26 and Figure 27. The measurement of each bearing was performed in 2 radial directions (horizontally and vertically). RPM value is measured by an optical RPM sensor, triggered by a reflective tape placed on the motor surface. Table 9 descripes the sensor location and direction.

Table 9. Sensors locations and directions

Channel Number	Position	Vibration direction
Channel 0	Front	Vertical
Channel 1	Front	Horizontal
Channel 2	Rear	Vertical
Channel 3	Rear	Horizontal
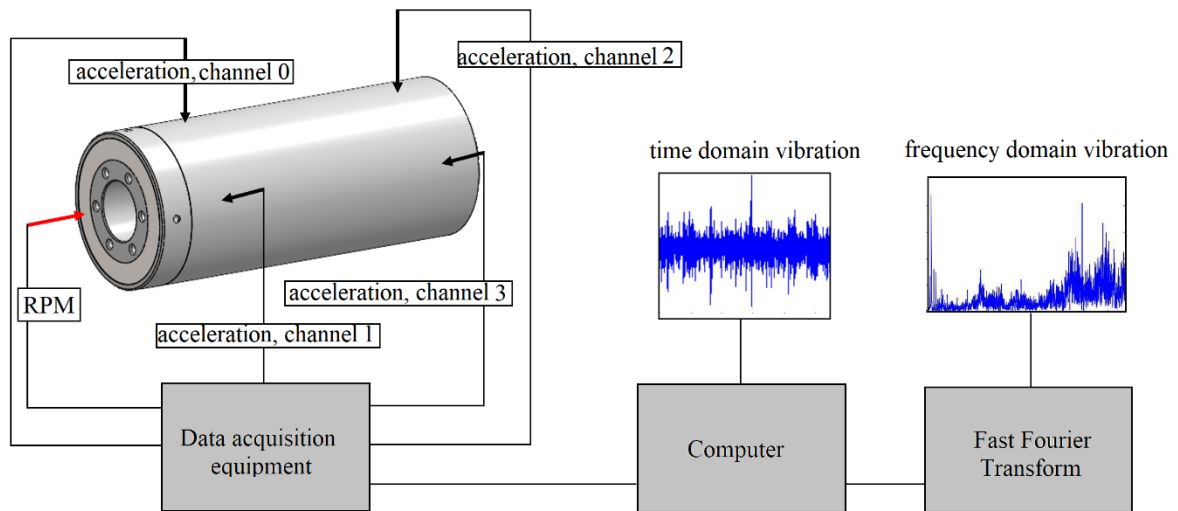
Figure 26. Measurement scheme (vibration signal illustrations are taken from [39])
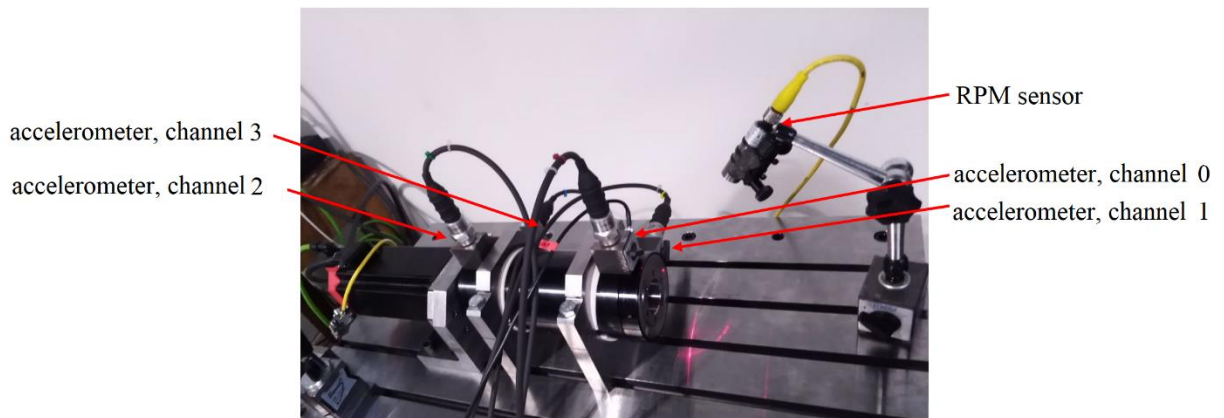
Figure 27. Measurement arrangement

The measurement was realized for maximum spindle rotational speed of 6000 RPM and included measurement on different RPM levels, each of the measurement recording time was 20 s. Two of five spindles were chosen to perform an experiment to study the effect of the front nut tightening on the vibrations.

3.4 Spindle components dimensions and geometry. Resultant fits.

Among the factors which are supposed to affect the vibration, there are different parameters of spindle components geometry related to bearings, such as bearing fits, and bearing seats geometry. Then, spacer rings flatness and height difference affect bearing preload and might also affect vibrations. Different dimensional and geometric configurations generate different vibrations character. The dimensional parameters used in the investigation are shown in the Figure 28.
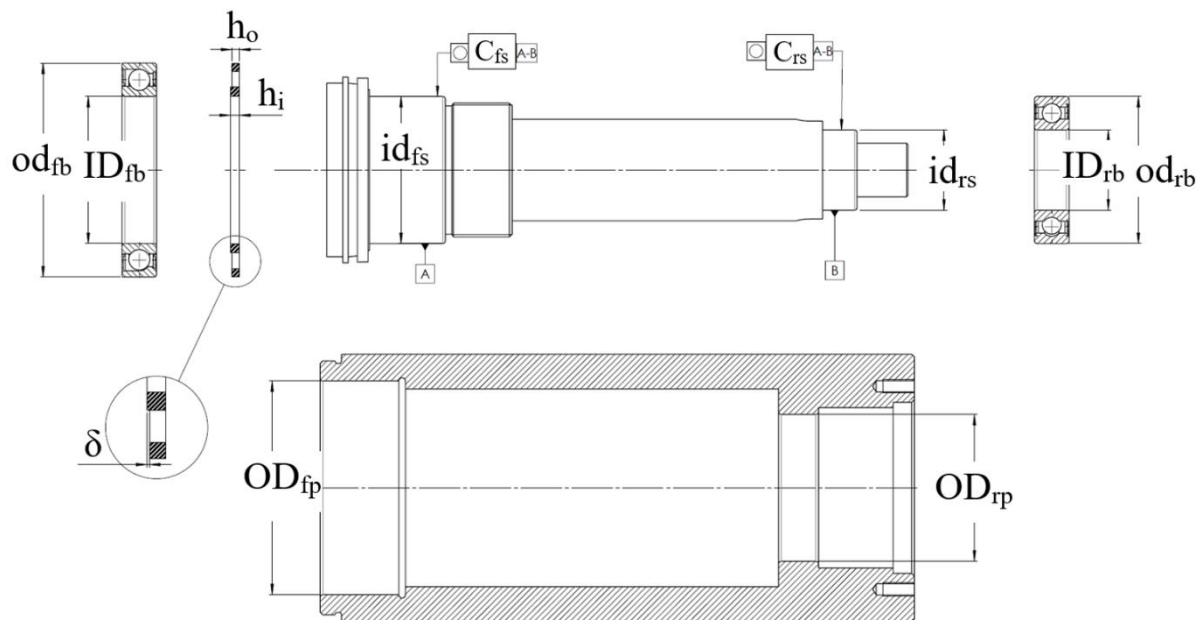
Figure 28. Spindle parameters

The tolerances for these parameters are stated in the Table 10:

Table 10. Spindle parameters tolerances

Parameter	Nominal dimension	Lower limit	Upper limit	Description
ID_{fb}	55	-0.007	0	Front bearing Inner Diameter (ID)
od_{fb}	80	-0.007	0	Front bearing Outer Diameter (OD)
id_{fs}	55	-0.003	+0.002	Front bearing ID seat (shaft)
C_{fs}		0	0.0015	Front bearing ID seat circularity
OD_{fp}	80	+0.001	+0.007	Front bearing OD seat (pipe)
h_o	3.5	0	0.010	Outer spacer ring height

56

h_i	3.5	0	0.010	Inner spacer ring height
δ		0	0.005	Spacer rings height difference
ID_{rb}	30	-0.008	0	Rear bearing ID
od_{rb}	55	-0.011	0	Rear bearing OD
id_{rs}	30	-0.004	+0.009	Rear bearing ID seat (shaft)
C_{rs}		0	0.0045	Rear bearing ID seat circularity
OD_{rp}	55	-0.030	0	Rear bearing OD seat (pipe)

Then, bearings' fits values on the inner and outer diameters are calculated in the following way:

$$Front\ bearing\ ID\ fit = ID_{fb} - id_{fs}; \quad Rear\ bearing\ ID\ fit = ID_{rb} - id_{rs} \qquad (14), (15)$$

$$Front\ bearing\ OD\ fit = OD_{fb} - od_{fs}; \quad Rear\ bearing\ OD\ fit = OD_{rb} - od_{rs} \qquad (16), (17)$$

Actual spindle dimensions measurement

Spindle shaft geometry measurement is performed at shaft manufacturer's facilities, and the measurement protocol is provided. The shaft bearing-related dimensions and geometry measured values were taken from these protocols: id_{fs} and id_{rs} were measured on Zeiss Contura 3D. The circularity of the diameters C_{fs} and C_{rs} was measured on Mitutoyo Roundtest RA-2100. The other values available for measurement were measured at Viking CNC facilities: for inside diameters (ID_{fb}, OD_{fp}, ID_{rb}, OD_{rp}) three-point bore gages of appropriate size were used; for outside diameters (od_{fb}, id_{fs}, od_{rb}, id_{rs}) outside micrometers of appropriate size were used. Bearings were fixed on a small vise stand before measurement.

Bearing spacer rings height was also measured by digital outside micrometer. During measurement, a measured ring was fixed on a small vise stand. Bearing spacer rings height was measured at 4 points over the ring circumference located 90° from each other. Because of the fact that the ring's height deviation was varying sometimes reaching the value of 0.007 mm, the spacer rings height difference δ was calculated as a difference between the two rings average height values.

Measured actual dimensional values of the investigated spindle components are stated in Table 11:

Table 11. Spindles parameters – measured actual values

Spindle no.	Spacer rings average height difference [mm]	Inner ring height deviation [mm]	Outer ring height deviation [mm]	Front bearings ID fit [mm]	Front bearings OD fit [mm]	Front bearing ID seat circularity	Rear bearing ID fit [mm]	Rear bearing OD fit [mm]	Rear bearing ID seat circularity
2001	0.0015	0.001	0.006	-0.002 / -0.001	0 / 0.001	0.0003	-0.006	-0.002	0.00052
2002	0.001	0.003	0.007	-0.002 / -0.001	0.015 / 0.016	0.0007	-0.0035	-0.003	0.00092
2003	0.001	0.004	0.004	-0.004 / -0.003	0.008 / 0.008	0.00025	-0.0055	0.001	0.0018
2005	0.004	0.005	0.007	-0.004 / -0.003	0.015 / 0.015	0.0016	-0.006	0.002	0.00048
1937	0.002	0.004	0.004	0.0005 / 0.003	0.013 / 0.013	0.003	0	-0.002	0.0025

It is expected that the bearing characteristic frequencies will manifest themselves on the frequency spectra, which may happen in case of a bearing race deformation. Bearings parameters are presented in the Table 12, and their characteristic frequencies calculated according to the equations (4) - (9) are presented in the Table 13:

Table 12. Bearings parameters

	Front	Rear
N [1]	23	11
d [mm]	8	7.1
D [mm]	67.5	42.5
β [°]	15	0
$\cos\beta$ [1]	0.9659	1

Table 13. Bearings characteristic frequencies

	rpm \ f [Hz]	1000	2000	3000	4000	5000	6000
Front bearings	f_{BPFO}	169.7	339.4	509.2	678.9	848.6	1018.3
	f_{BPFI}	213.6	427.2	640.8	854.4	1068	1281.6
	f_{BSF}	1	1.9	2.9	3.9	4.9	5.8
	f_{BFF}	1.9	3.9	5.8	7.8	9.7	11.7

	f_{BCSOR}	7.4	14.8	22.1	29.5	36.9	44.3
Rear bearing	f_{BPFO}	76.4	152.7	229.1	305.4	381.8	458.1
	f_{BPFI}	107	214	320.9	427.9	534.9	641.9
	f_{BSF}	1.4	2.7	4.1	5.4	6.8	8.1
	f_{BFF}	2.7	5.4	8.1	10.8	13.5	16.2
	f_{BCSOR}	6.9	13.9	20.8	27.8	34.7	41.6

3.5 Vibrations measurement assessment

The obtained vibration signal was processed in LabView environment to perform the FFT, then Matlab and Microsoft Excel software was used for the following vibration analysis and other vibration data processing.

3.5.1 Preliminary assessment – overall vibration severity over the 10-1000 Hz range

The vibration velocity RMS values over the range 10-1000 Hz were calculated from the obtained signal on 1000, 2000, 3000, 4000, 5000, and 6000 RPM. Figure 29 shows these values for the tested spindles on different spindle speed for the front bearings and for the rear bearing in both directions. It is evident, that the spindle 2003 is showing significantly higher vibrations than the other spindles. Spindle 2002 is showing the lowest RMS values. Vibrations of the spindles 2001, 2005 and 1937 are quite similar on the front bearings; as for the rear bearing, there is a worth-mentioning difference between the 1937 spindle vibrations compared to the 2001 and 2005 spindles vibrations. Hence, it might be supposed that the 2002 spindle had the most successful dimensional configuration along with a properly performed assembly procedure, whereas the spindle 2003 had, contrariwise, the worst configuration. This fact should be taken into account for the further detail analysis of the measured data. However, one has to keep in mind that spindle is a complex unit, so even if the vibration RMS amount is similar for two different spindles, the causes of the vibration might be different, as well as the degree of complicatedness of their elimination.

FACULTY
OF MECHANICAL
ENGINEERING
CTU IN PRAGUE

DEPARTMENT OF
PRODUCTION MACHINES
AND EQUIPMENT
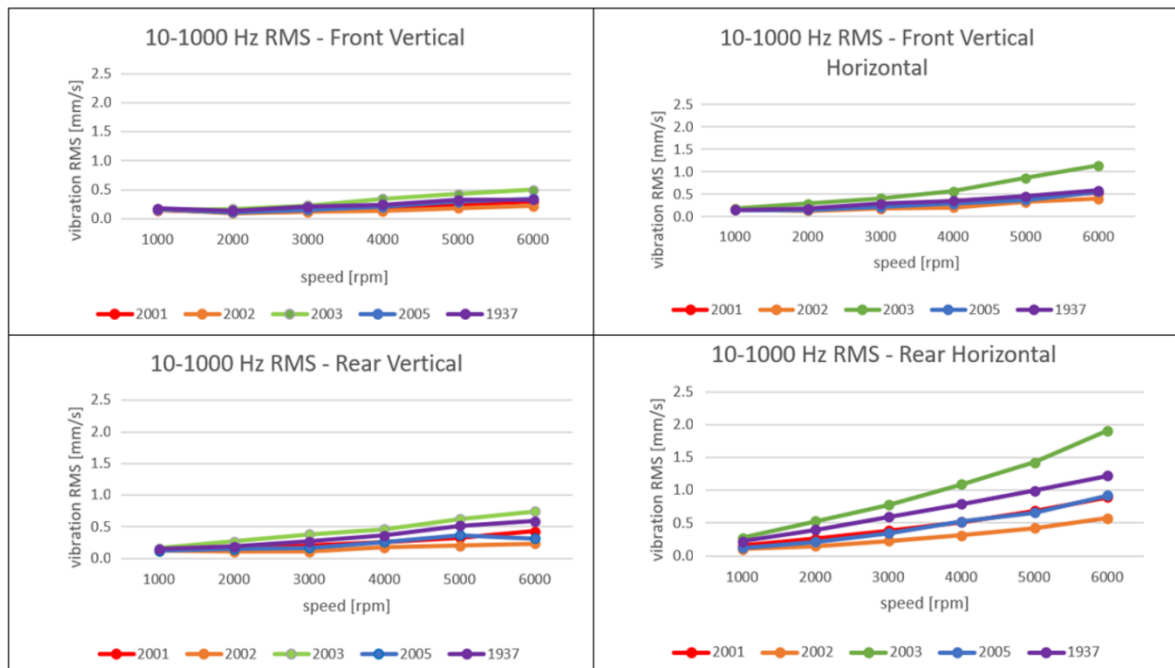
Figure 29. Spindles RMS values over 10-1000 Hz comparison

3.5.2 Overview of the vibration character observed on frequency spectra

The vibration of a running spindle is complex, so it is reasonable to divide the obtained vibration signal into the following categories:

- Spindle rotation speed frequency and its multiples
- Structural resonances spreaded over a wider rande of frequencies (low frequencies)
- Bearing fault frequencies
- High-frequency excited ranges

Vibrations which come under one of these categories have common attributes, patterns, and root causes, which are typically associated with each of the categories. Hence, vibrations of each category are considered separately in order to evaluate the degree of influence of the vibration-causing factors typically associated with the categories, and find out, which spindles were affected more by these factors. The cause of the degree of the factors' impact is supposed to be traced back to the spindles dimensional, geometrical and assembly parameters.

3.5.2.1 Spindle rotation speed frequency and its multiples

Values of the rotational speed frequency (first harmonic - 1H) amplitudes and its multiples (2H, 3H, etc.) over the different RPM levels were analyzed for each spindle, and then followingly compared.

1H of the spindle 2001 has significantly larger amplitudes both for front and rear bearings vibration. It shows the most significant increase at rear bearing in horizontal direction. Rear bearing vibration amplitude in vertical direction is approximately half-valued and the main reason for this is probably the spindle housing construction, where two parts of it are being pulled together with tightening force acting in the vertical direction. The magnitudes of the 2H and 3H do not manifest themselves at so high amplitudes and their values remain similar over all the RPM levels, with 2H always having a slightly higher amplitude, except the Rear Horizontal channel, where the 3H frequency tends to prevail in amplitude and shows a slight increase – v. Figure 30.
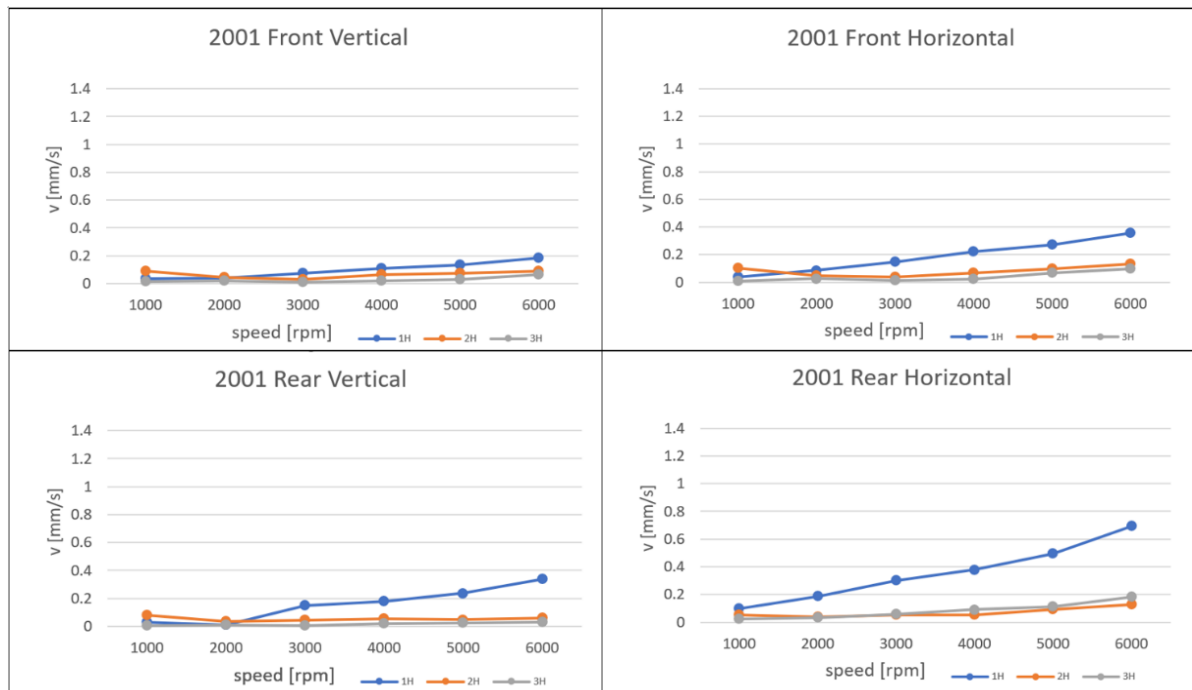
Figure 30. Rotational speed frequency and its harmonics amplitude values – spindle 2001

Spindle 2002 has generally low vibration amplitudes at harmonic frequencies, showing only a slight increase with RPM at front bearings. 1H has a higher vibration amplitude. 1H and 3H vibration amplitudes are generally higher in horizontal direction, and 3H increases at high speeds in horizontal direction. 2H remains almost unexcited at front bearing in horizontal direction and at rear bearing in vertical direction. The most rapid increase with the highest amplitude of 1H is at rear bearing in horizontal direction – v. Figure 31.
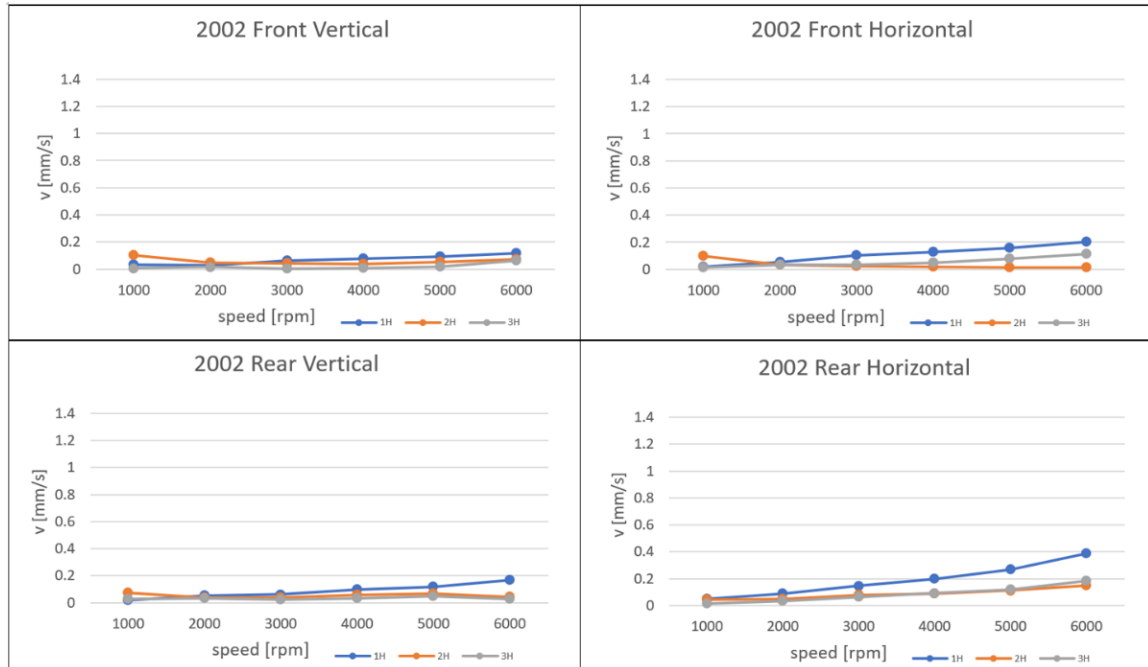
Figure 31. Rotational speed frequency and its harmonics amplitude values – spindle 2002

What is unique about the 2003 spindle is prevailing 3H amplitude over all the other harmonics, including 1H, which amplitude is typically the highest. 2H is excited at rear bearing; 2H and 3H peaks are also present at front bearing, but with a relatively low amplitude and a relatively slight increase with RPM. These vibrations are possibly transmitted from the rear bearing considering the amplitudes trend and ratio. 4H and 5H are excited at front bearings besides the other harmonics at high speeds (which might be related to the structural resonances excitement) – v. Figure 32.
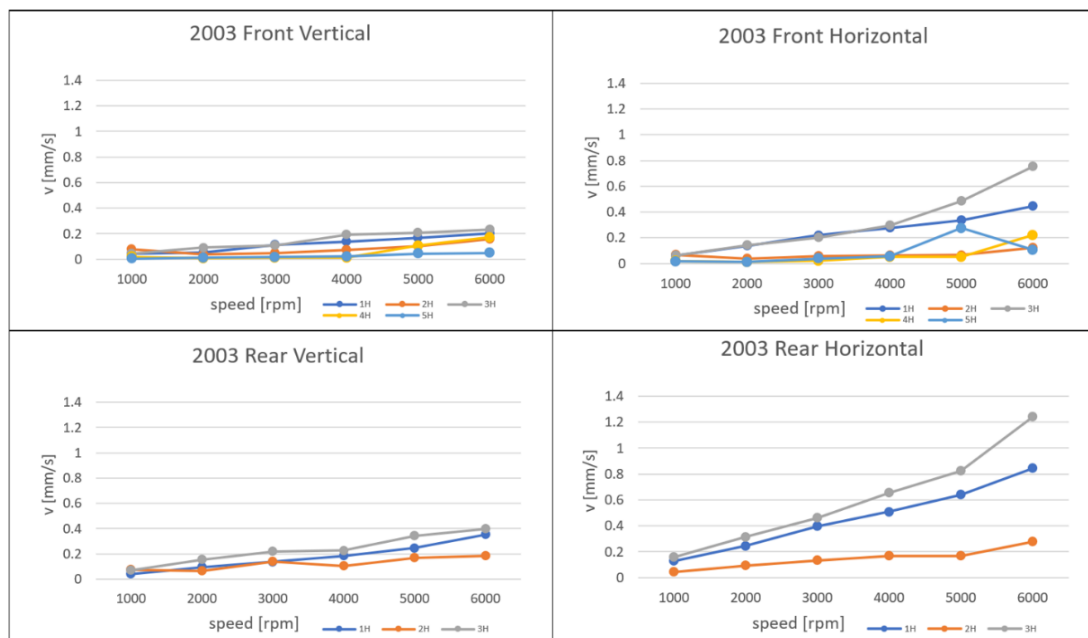
Figure 32. Rotational speed frequency and its harmonics amplitude values – spindle 2003

Spindle 2005 shows generally low vibration at harmonic frequencies in vertical direction, as it is shown in the Figure 33. There is a significant excitement of 3H at rear bearing, especially in horizontal direction, which is subsequently transmitted to the front bearing. Front bearings have also excited 4H, 5H, 6H though with relatively low amplitudes. 2H is also excited at rear bearing and its magnitude is comparable with the 1H and 3H. 2H is excited at front bearing in vertical direction. It is excited more than the other harmonics at front bearings in vertical direction. 1H is excited more in horizontal direction. Rear horizontal has the highest amplitudes with the most rapid increase.
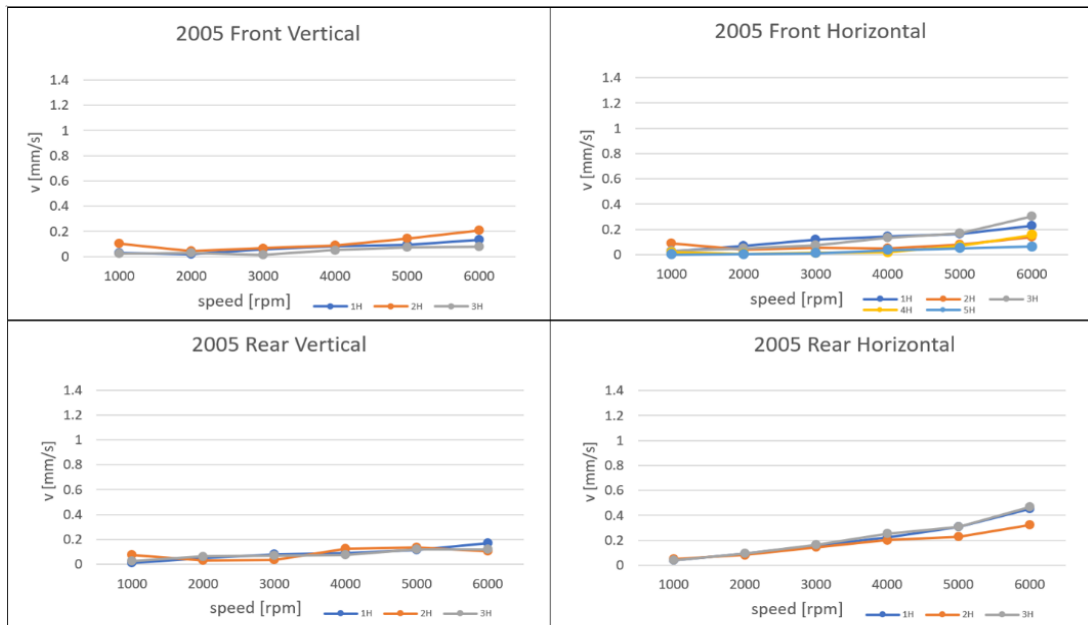
Figure 33. Rotational speed frequency and its harmonics amplitude values – spindle 2005

Spindle 1937, as illustrated in the Figure 34, shows a rapid increase of 1H amplitude with RPM at all vibration channels; the most significant one is at the rear bearing in horizontal direction, then at rear bearing in the vertical direction. There is also excited 3H at front bearings. 2H vibrates at approximately same amplitude and character at all channels. There are also slightly excited harmonics of 4H and 5H at the front bearings in vertical direction at higher speeds.
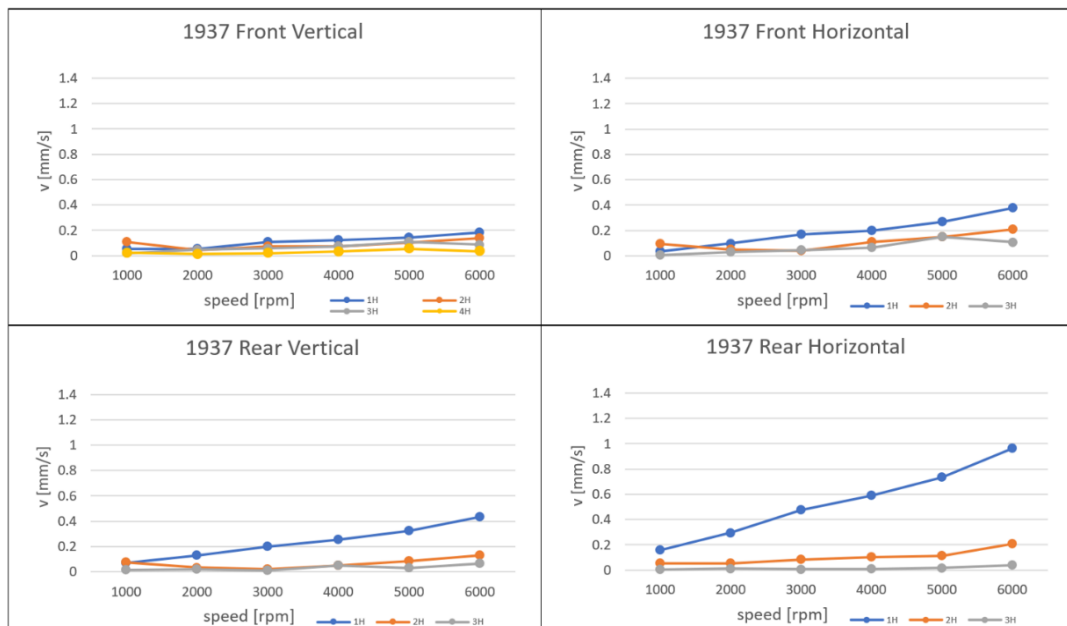
Figure 34. Rotational speed frequency and its harmonics amplitude values – spindle 1937

General tendentions

General behavior at 1, 2 and 3 harmonics is summarized in the Table 14.

Table 14. Spindles behavior summary over RPM - spindle rotational speed frequency and its harmonics

	2001		2002		2003		2005		1937	
1H	yellow	red	yellow	yellow	yellow	red	yellow	yellow	yellow	red
	red	red	yellow	red	red	red	yellow	red	red	red
2H	green	yellow	yellow	green	yellow	yellow	yellow	yellow	yellow	red
	green	yellow	green	yellow	yellow	red	yellow	red	yellow	red
3H	yellow	yellow	yellow	yellow	yellow	red	yellow	red	yellow	yellow
	green	yellow	green	yellow	yellow	red	yellow	yellow	yellow	yellow

[red] - significant excitement, [yellow] - slight excitement, [green] - generally low vibration level

Colored cells correspond to the bearings in the following order:

Front vertical	Front horizontal
Rear vertical	Rear horizontal

1H magnitude is one of the most important criteria as this peak is the largest one in most cases. As it is evident from the table, the measured spindles have 2 patterns of 1H peak behavior:

1. Significant vibration amplitudes at the rear bearing and at the front bearings in horizontal direction and a slight amplitude increase at higher speed at front bearing in the vertical direction. (2001, 2003, 1937)

2. Significant amplitudes at rear bearing in horizontal direction and slight increases at higher speeds at the front bearing and at the rear bearing in the vertical direction. (2002, 2005)

65

The rotational speed frequency course has a similar character for spindles 2001, 2003 and 1937: the 1H amplitude has a tendention increase rapidly with the rise of the speed, and the curve resembles a rather exponential dependency between the speed and the vibration amplitude value. Furthermore, for 2001 and 1937 the velocity curve is characterized by similar ratio between the magnitudes of the vibration on the first, second and the third harmonics.

The excited 1H might be caused by unbalance. This means, the spindles 2001, 2003 and 1937 might have the similar amount of an unbalanced mass which might generate an unwanted centrifugal force during the rotation. Balancing might fix the problem and eliminate the excessive spindle vibration at the 1H frequency. If 2H and 3H peaks were generated by the unbalance vibration, balancing might fix this issue as well.

Then, 2002 and 2005 have the similar course of the 1H vibration with relatively low amplitudes. The most rapid increase of the amplitude is, for both spindles, at the rear bearing in the horizontal direction, but the magnitude of the vibration is still lower than it is for the spindles 2001, 2003, and 1937.

The effect of the dimensional parameters on the rotational speed frequency and its harmonics degree of excitement has been assessed, and it has been figured out that 1H frequency higher amplitude values correspond to the spindles with higher circularity deviation on the rear bearing seats on the shaft. Besides, it is in accordance with the fact that 1H amplitude is generally higher at the rear bearing. This constitutes a reasonable assumption that the rear bearing inner diameter seat circularity is a factor which participates on the magnitude of the 1H vibration. The described correlation is shown in the Figure 35. Correlation between bearing seat ID circularity and 1H amplitude value at rear bearing in (a) horizontal direction (b) vertical direction

(a)

(b)
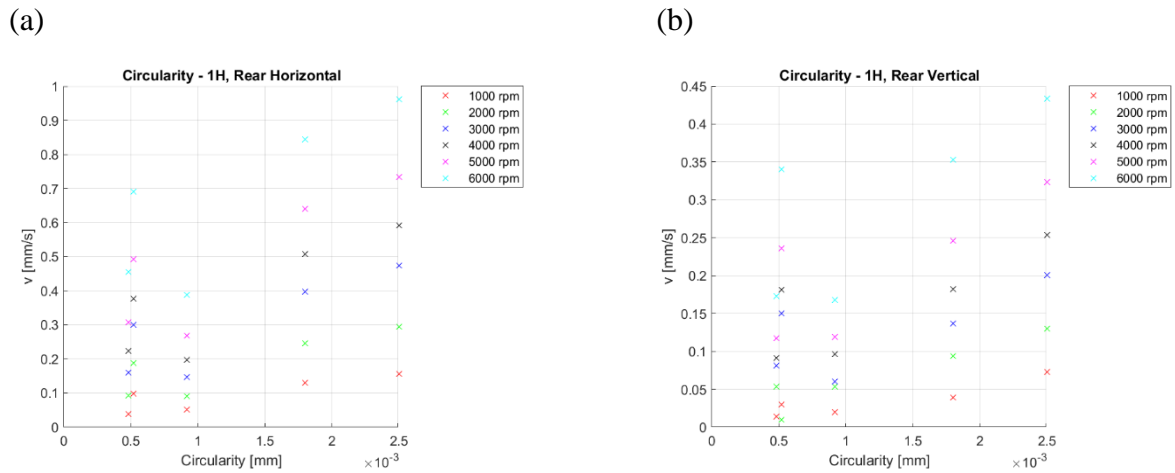
Figure 35. Correlation between bearing seat ID circularity and 1H amplitude value at rear bearing in (a) horizontal direction (b) vertical direction

There are three patterns of the 2nd harmonic peaks behavior:

1. The 2H is either not excited, or keeps having low amplitudes with a slight icrease at higher speeeds. (2001, 2002)

2. The 2H amplitudes are low and show a slight increase at higher speeds at the front bearings in both directions and at the rear bearing in the vertical direction, but there are significant amplitudes at the rear bearing in horizontal direction. (2003, 2005)

3. The 2H has relatively significant amplitudes in horizontal direction and show a slight increase at higher speeds in vertical direction. (1937)

For all of the measured spindles, 2H tends to manifest itself more in the horizontal direction. Its amplitudes are generally rather low, although they show an increase with the increasing speed. For example, for 2005 spindle the 2H and 1H amplitudes are generally comparable, and for the front bearing, vertical direction it is excited even more than the 1H. The excited 2H frequency is typically associated with looseness in the assembly, or axes misalignment. Another possible reason is that it might be additionally excited by the rotor unbalance. For 2005 spindle the reason for the prevailing 2H in amplitude might be misalignment, as the characteristic sound has been noticed during the measurement.

As far as the geometry dependences are concerned, as the vibration on 2H typically represents looseness in the assembly, it might be related to the bearing-related dimensions and geometry. Figure 36 show that 2H magnitude correlates with (a) shaft front bearing seat

circularity and (b) inner spacer ring deviation at the front bearings and with (c) bearing outer diameter (OD) fit at the rear bearing: It is shown that 2H is excited more for larger dimensional deviations at the front bearings and for looser fits at the rear bearing.

(a)   (b)   (c)
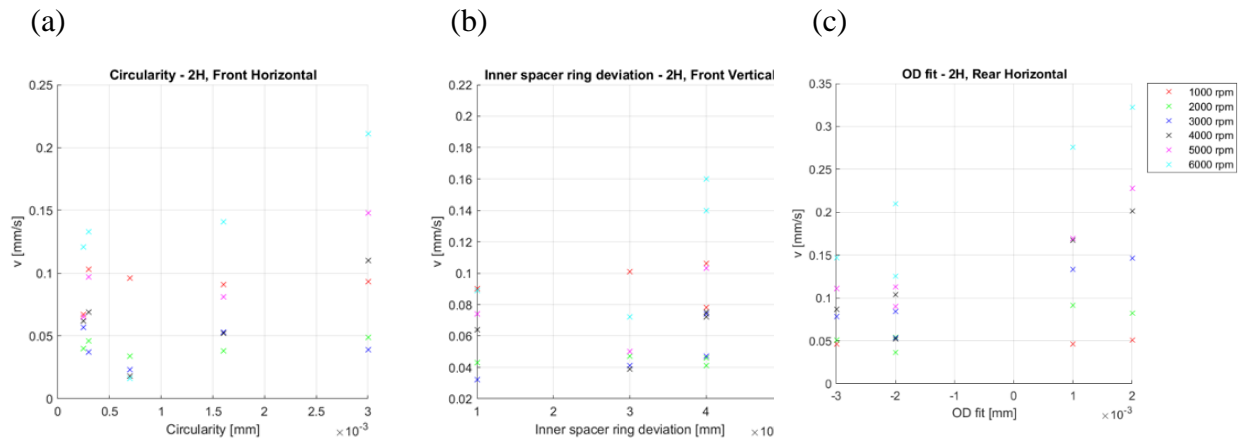
Figure 36. Correlation between 2H amplitude value and (a) front bearing seat ID circularity in horizontal direction, (b) front bearing inner spacer ring deviation in vertical direction (c) bearing OD fit in horizontal direction

The 3H frequency vibration manifests itself in 3 patterns:

1. The 3H is either not excited or keeps having low amplitudes with a slight icrease at higher speeeds. (2001, 2002, 1937)

2. The 3H has relatively significant amplitudes in horizontal direction and show a slight increase at higher speeds in vertical direction. (2003, 2005)

3H might be excited because of misalignment and looseness. Again, another possible reason is that it might be excited by the rotor unbalance. As a result of the dimensional parameters influence assessment, it has been figured out that the highest 3H values generally correspond to the tighter rear bearing ID fit, as shown in Figure 37. The reason for this might be the higher deformation of the bearing by press-fit itself, or by the irregularities brought during the assembly procedure.
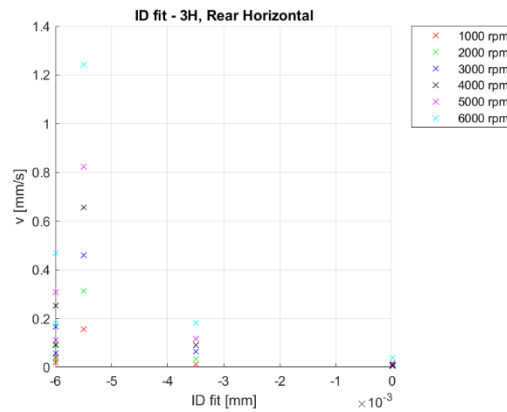
Figure 37. Correlation between 3H amplitude value and rear bearing ID fit

Summary

The spindles, performance quality of which was overly affected by the vibration excited on the rotational speed harmonics, are listed in the Table 15:

Table 15. Spindles affected by the vibration excited on the rotational speed harmonics

Frequency	Affected spindles	Possible causes
1H	2003, 2005, 1937	• Unbalance • Bearing ID seat circulatity
2H	2003, 2005, 1937	• Misalignment • Unbalance • Rear bearing loose fit • Front bearing spacer ring deviation
3H	2003,2005	• Misalignment • Looseness • Unbalance • Rear bearing ID fit
4H, 5H	2003, 2005, 1937	• Resonance of spring spindle placement

Condition of each spindle in terms of the factor of vibration at rotational speed frequencies and their harmonics can be assessed in the following way – v. Table 16:

69

Table 16. Spindles condition assessment - rotation speed harmonics

Spindle	2001	2002	2003	2005	1937
1H					
2H					
3H					

- favorable condition,   some issues are present

The table states that the spindles 2001 and 2002 are in the optimal condition regarding rotation speed frequency and its harmotics excitement.

3.5.2.2 Bearing characteristic frequencies

Spindles with bearings being slightly deformed due to the geometry and assembly irregularities might give out low-amplitude vibrations at bearing characteristic frequencies (v. Table 13). It is assumed that the degree of the deformation can be evaluated by the magnitude of the vibration on these frequencies. Due to the fact that the magnitude of the excited characteristic frequencies (if there are any) is distinguishable only at higher rotational speeds (though they do not necessarily increase with the RPM), only the measurement results at 4000 rpm – 6000 RPM is provided, which is enough to estimate the trend.

A comparison between the spindles BPFO and BPFI amplitudes is shown at the Figure 38. It is evident that, with few exceptions, all spindles have the vibration at the characteristic bearing frequencies with similarly low amplitude values. Then, there are relatively large values at the BPFO at 5000-6000 RPM at 2003. 2005 and 1937. front bearings. It is possible that the front bearings of 2003, 2005 and 1937 spindle are deformed, with bigger deformation of the outer race. It might be related to the fact that the spindles 2003, 2005 have relatively tight fits on the front bearings, which might have brought complications to the assembly process, while the fit of the 1937 front bearings is, conversely, relatively loose.

Vibration on the rear bearing characteristic frequencies are lower compared to the vibrations on the front bearings. The chart shows that the 2003 spindle has an excitement of

the BPFO at the 5000-6000 RPM. This might mean that the outer race of 1937 spindle rear bearing could be also deformed more than in the other cases.
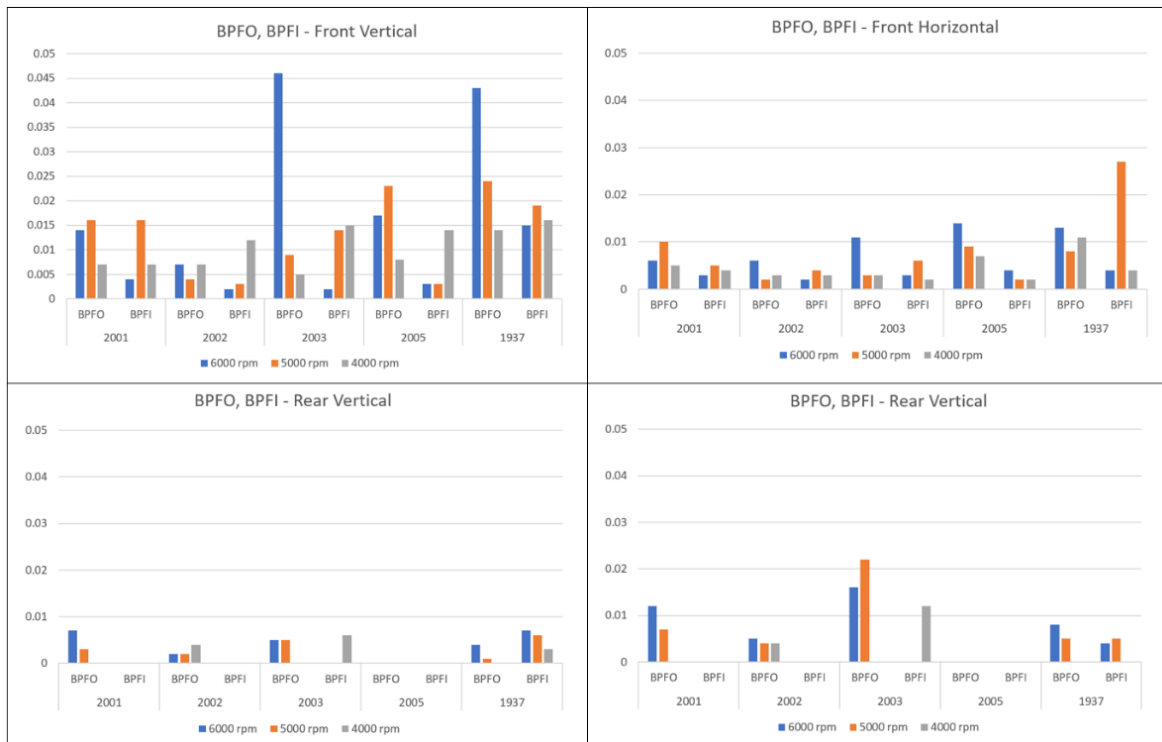
Figure 38. Bearing characteristic frequencies vibration amplitudes

Several assumptions of the relation between the dimensional and geometrical parameters and the magnitudes of the bearings characteristic frequencies are presented below in the Figure 39 and Figure 40. Figure 39 and Figure 40 (a) show that the vibrations at BPFI in vertical direction both at the front and the rear bearings have higher amplitudes for spindles with larger ID seat interference and ID seat circularity deviation. There is also a relation between the rear bearing OD fit and the BPFO vibration amplitudes at rear bearing in horizontal direction – asshown in the Figure 40 (b). However, due to the fact that in case of rear bearings the most of these frequencies had zero amplitude value, so there is not enough data to propose a comprehensive estimation.

(a)   (b)
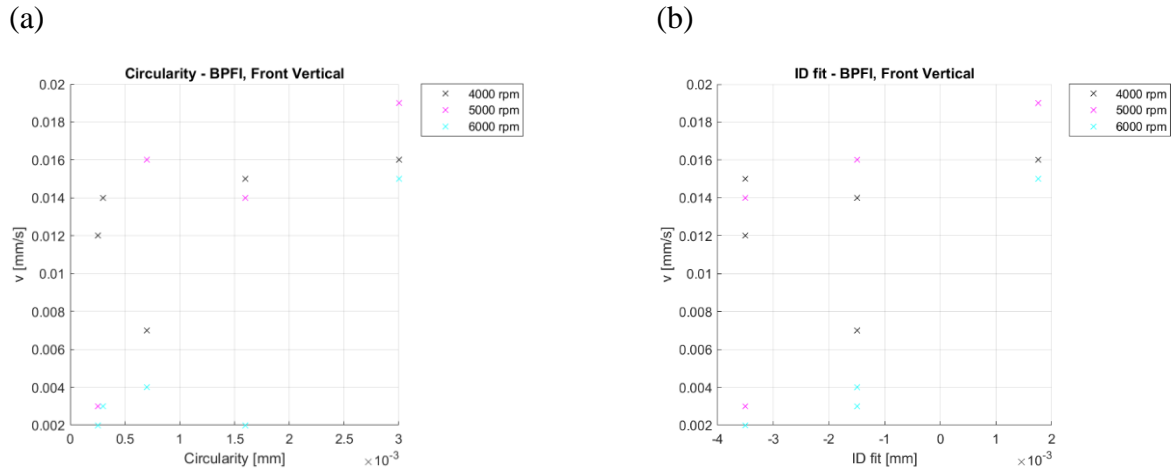
Figure 39.Correlation between BPFI amplitude value and (a) front bearing seat ID circularity (b) front bearing ID fit

(a)   (b)
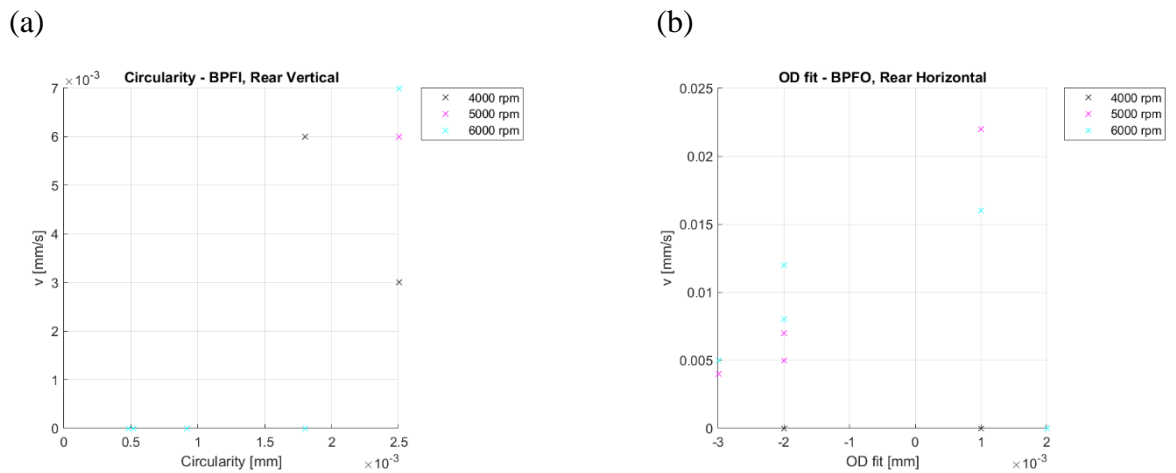
Figure 40.Correlation between rear bearing (a) BPFI amplitude value and bearing seat ID circularity (b) BPFO amplitude value and bearing OD fit

Cage frequency does not itself occur as a peak on the frequency spectra, but some spindles (2001, 2003, 1937) have isolated harmonics (starting from the 4H and higher) modulated by sidebands of BCSOR (FTF). The example of such sidebands is demonstrated in the Figure 41. The issue is present at both bearings. The corresponding sidebands location is stated in the Table 17. + or – indicates whether the BCSOR occurs to the left (-), or to the right side (+) of the harmonic peak. The amplitude values are summarized in the Figure 42.
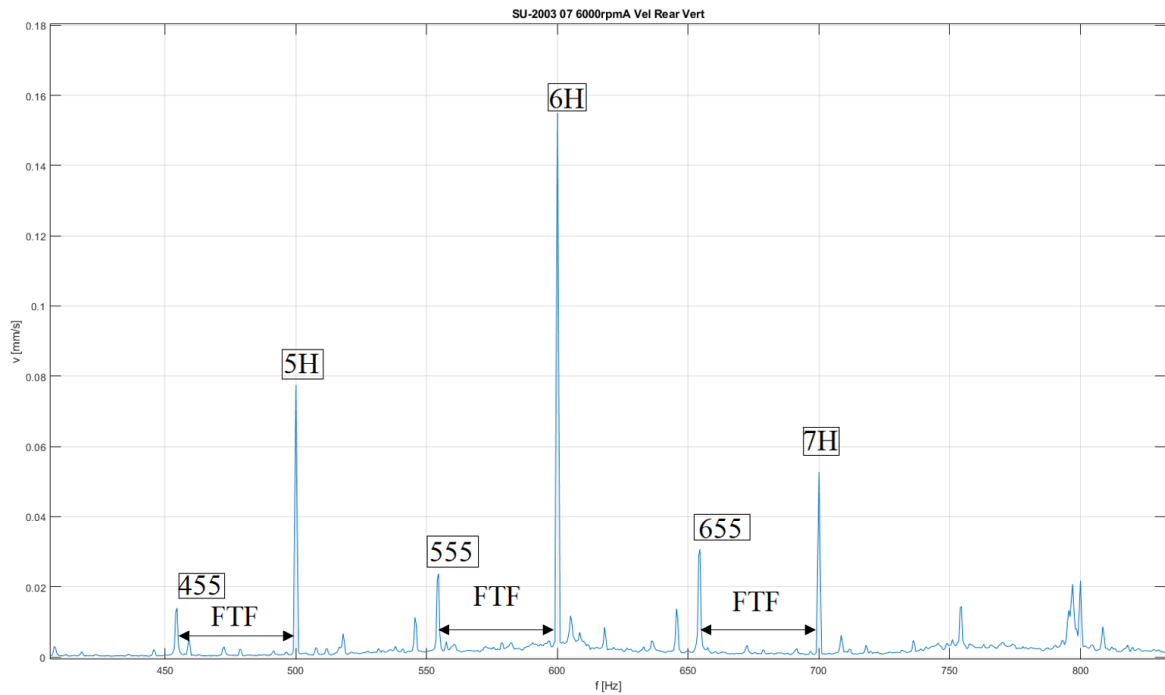
Figure 41. Cage frequency modulation - 2003 spindle, 6000 RPM, rear bearing, vertical direction

Table 17. Cage frequency modulation attachment frequencies

Speed [RPM]	Front Vertical			Front Horizontal			Rear Vertical			Rear Horizontal		
	6000	5000	4000	6000	5000	4000	6000	5000	4000	6000	5000	4000
2001	-	-	-	-	-	-	5H+	5H-	-	5H-	5H-	-
2002	-	-	-	-	-	-	-	-	-	8H-	8H-	-
2003	6H-	4H-	9H-	4H-	4H-	7H-	9H-	7H-	9H-	8H-	9H-	7H-
2005	-	-	-	-	-	-	4H+	-	-	6H-	-	-
1937	-	7H+	-	-	-	-	4H+	4H+	-	4H+	4H+	-

73
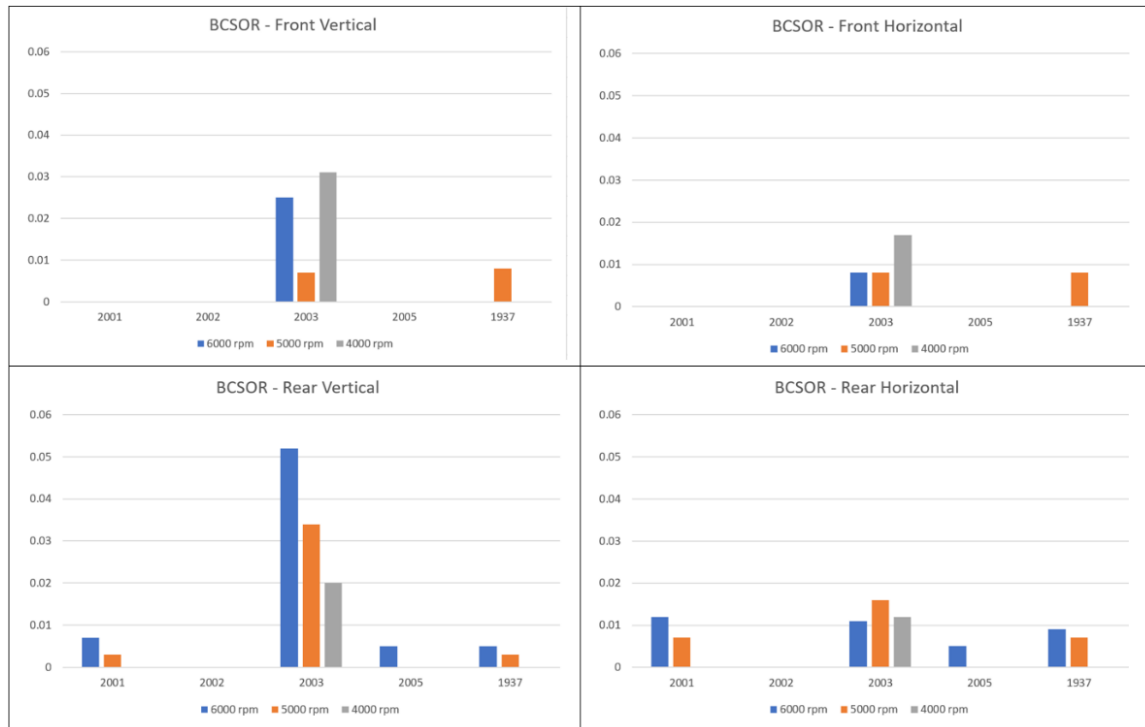
Figure 42. Cage frequency sidebands vibration amplitudes

Although cage frequency occurs in the spectra as a sideband, no correlation with these sidebands' amplitudes and the measured dimensional parameters has been revealed. Thus, it may be assumed that in this case assembly conditions have a greater influence on cage deformation. If a frequency manifests itself on the spectrum, that meant the component (cage, race) is crooked during the assembly. This is possibly the 2003 spindle's case.

Summary

Table 18 represents the summary of the spindles which showed relatively high excitement at the bearing characteristic frequencies along with the possible causes.

Table 18. Spindles manifesting vibration excited on bearing characteristic frequencies

Frequency	Affected spindles	Possible causes
BPFO	2003, 2005, 1937	• Bearing OD fit • Assembly conditions

BPFI	1937	• Bearing ID fit • Bearing ID seat circulatity • Assembly conditions
BCSOR	2003	• Assembly conditions

The bearings' components condition assessment basing on the gained data is provided in the Table 19.

Table 19. Spindles condition assessment -bearing characteristic frequencies

	2001		2002		2003		2005		1937	
BPFO	🟩	🟩	🟩	🟩	🟥	🟩	🟥	🟩	🟥	🟩
	🟩	🟩	🟩	🟩	🟩	🟥	🟩	🟩	🟩	🟩
BPFI	🟩	🟩	🟩	🟩	🟥	🟩	🟥	🟩	🟥	🟥
	🟩	🟩	🟩	🟩	🟩	🟩	🟩	🟩	🟩	🟩
BCOR/ BCIR	🟩	🟩	🟩	🟩	🟥	🟩	🟩	🟩	🟩	🟩
	🟩	🟩	🟩	🟩	🟥	🟩	🟩	🟩	🟩	🟩

🟩 - favorable condition,   🟥 - some issues are present

3.5.2.3   Structural resonances spread over a wider range of frequencies

In order to analyze the vibrations spread over the rest of the 10-1000 Hz spectrum without reference to any of the specific or characteristic frequencies, the frequency spectrum was divided into the 100 Hz intervals, and the velocity RMS values were calculated for each of the intervals, so that it is possible to identify more and less excited ranges and compare the spindles reciprocally by this parameter. The excitement of the wider frequency ranges was additionally demonstrated by waterfall plots on the example of the front bearing vibrations in horizontal direction – for each spindle. Other waterfall plots are presented in Appendix 4.

As demonstrated in the Figure 43, the highest RMS value happens to be at the ranges 10-100 Hz and 100-200 Hz range of the spindle 2001 – mainly because of the high amplitude of the rotational speed frequency and its multiples. At the front bearings the range 200-300 Hz is more excited than at the rear bearings. There is also a slight excitement of the range 400-500 Hz at the front bearings in the horizontal direction – v. Figure 44. At the rear bearing the range 300-400 Hz becomes excited at the higher speeds (from 5000 RPM). This range is also excited at the front bearings, but the amplitudes are larger at the rear bearing, so this resonance is likely to refer to the rear bearing.
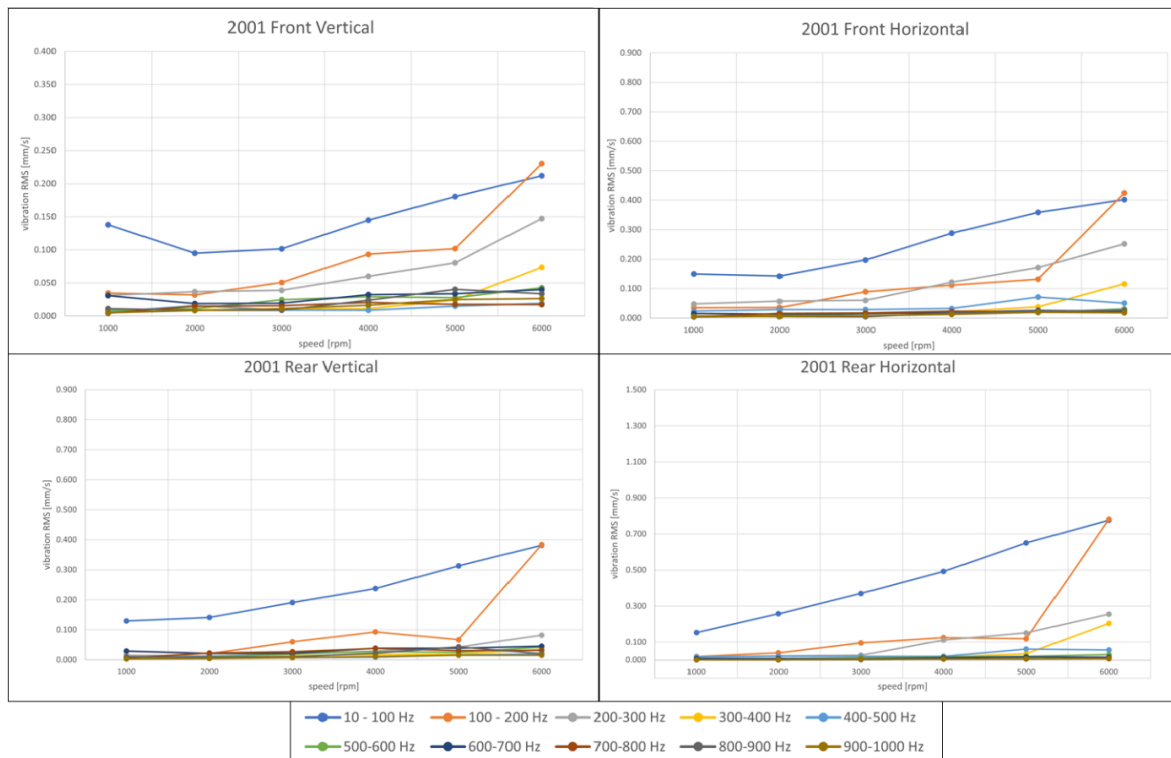
Figure 43. RMS values over 10-1000 Hz – spindle 2001
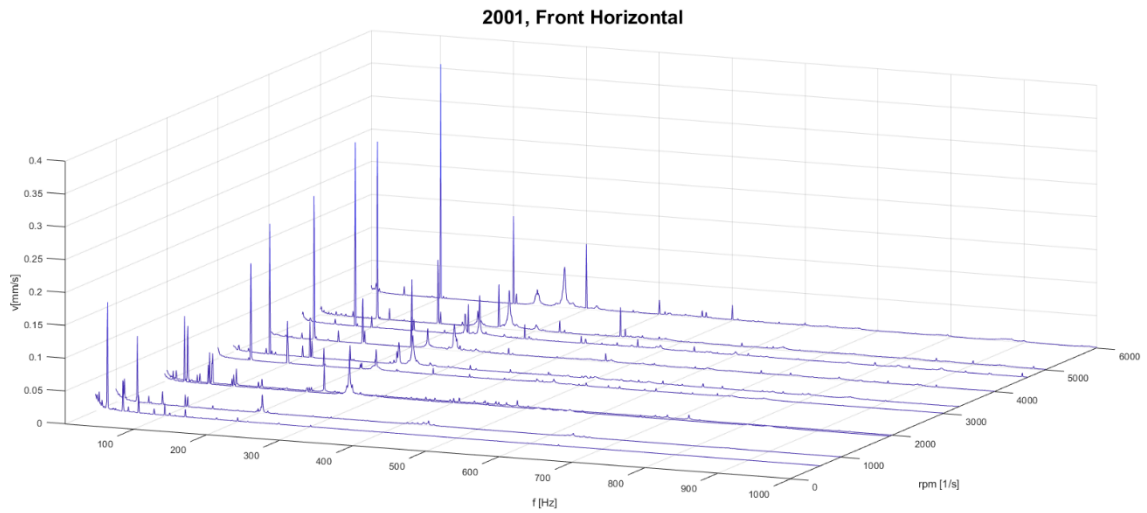
Figure 44. 2001 spindle waterfall plot – front horizontal

Spindle 2002 vibration at the mentioned frequency ranges has a similar character as the vibration of the 2001 spindle, but with generally lower amplitudes (v. Figure 45). It is worth-mentioning that the 400-500 Hz range becomes excited, but still with relatively low RMS value, already at 3000 RPM at the front bearings in the horizontal direction – v. Figure 46.
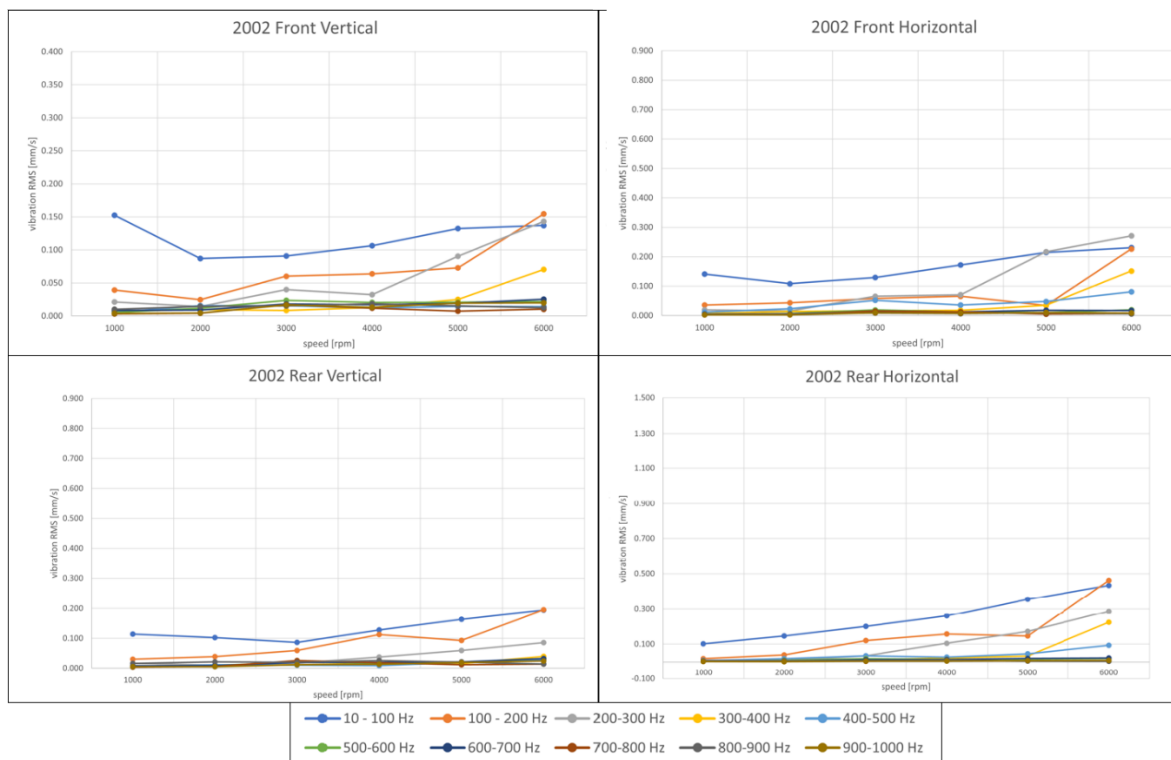
Figure 45. RMS values over 10-1000 Hz – spindle 2002

2002, Front Horizontal
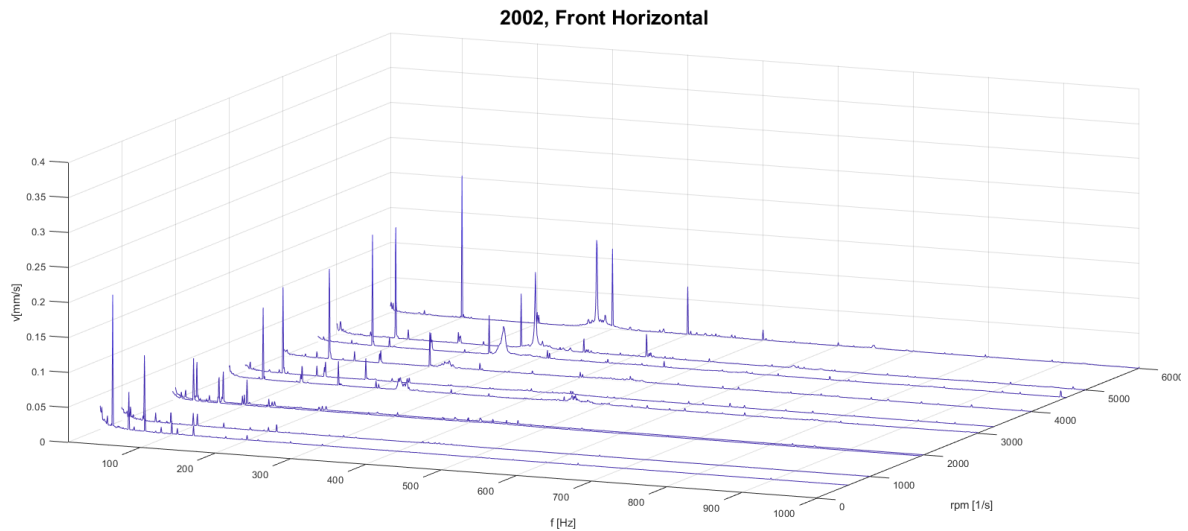
Figure 46. 2002 spindle waterfall plot – front horizontal

Spindle 2003 has the highest number of the excited resonance ranges and the highest RMS values over these ranges from all of the measured spindles, as shown in the Figure 47, Figure 48. The range 200-300 Hz at 5000 and 6000 RPM has the highest RMS value at both bearings; and this value is higher at the rear bearing. The range of 300-400 RPM becomes significantly excited at 6000 RPM, and this value is higher at the rear bearing. The range of 400-500 Hz also becomes excited at the higher RPM with similar values for both bearings, where the horizontal direction has approximately two times larger RMS values. Vibrations from 500 Hz to 1000 Hz are generally excited more in the vertical direction, which is an expected effect of the test stand housing construction. Ranges from 600 Hz to 900 Hz show a slight increase with RPM in horizontal direction, while 900-1000 Hz range remains unexcited.
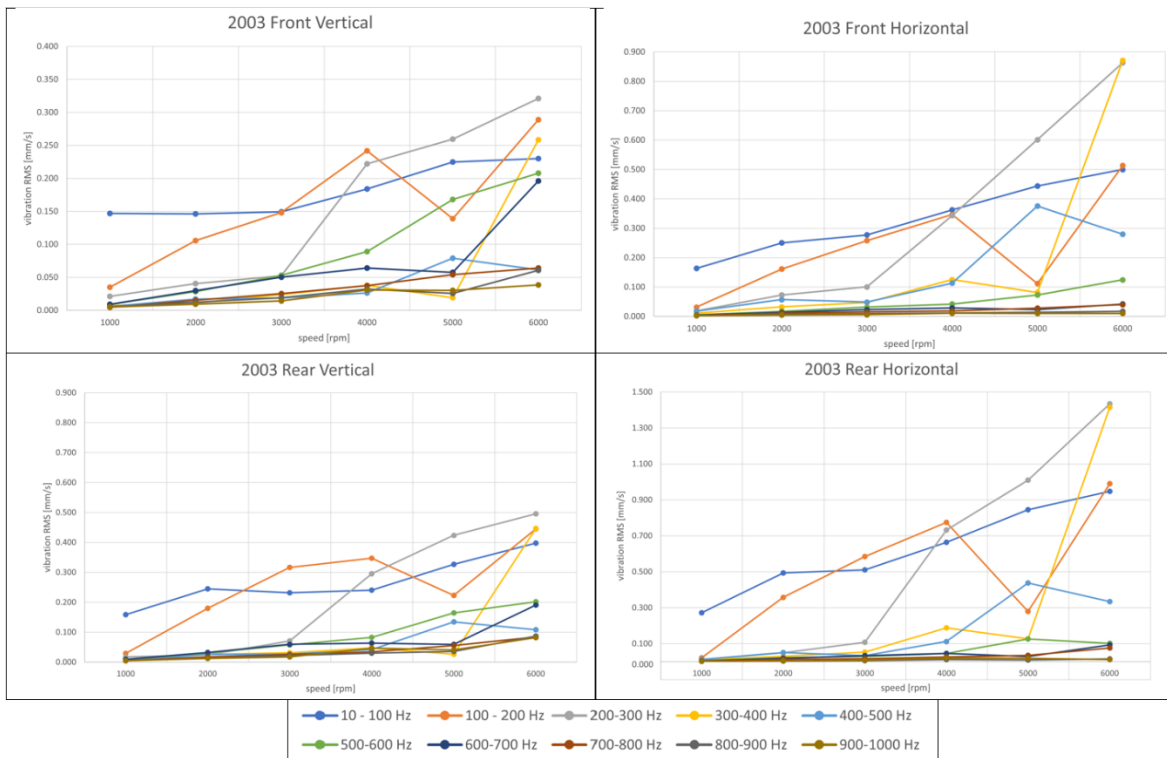
Figure 47. RMS values over 10-1000 Hz – spindle 2003
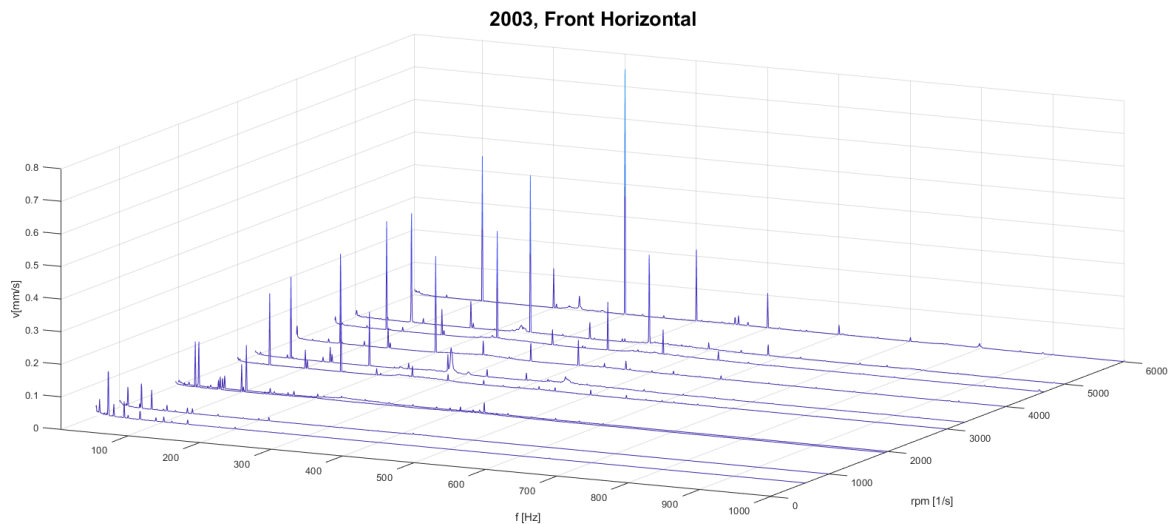
Figure 48. 2003 spindle waterfall plot – front horizontal

Spindle 2005 vibrations have a significantly excited range 200-300 Hz as shown in the Figure 50, with the largest amplitudes in horizontal direction and at the rear bearing – v. Figure 49. The 300-400 Hz range is excited at higher speeds with higher values on the rear bearing and in horizontal direction. The range of 400-500 Hz also becomes excited at the higher RPM with similar values for both bearings and directions. Higher frequency ranges

are excited mainly in vertical directions, with the amplitudes remaining relatively low. The 600-700 Hz range excitement is quite significant from ranges from 5000 RPM and higher.
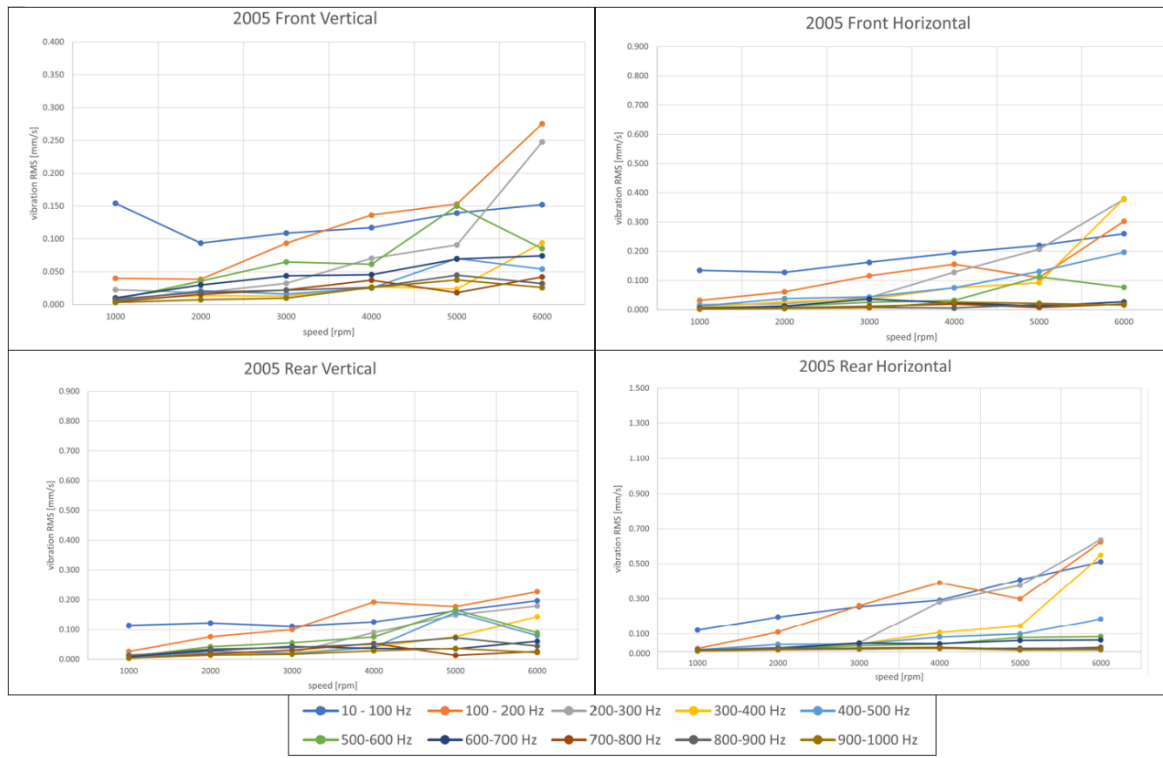
Figure 49. RMS values over 10-1000 Hz – spindle 2005
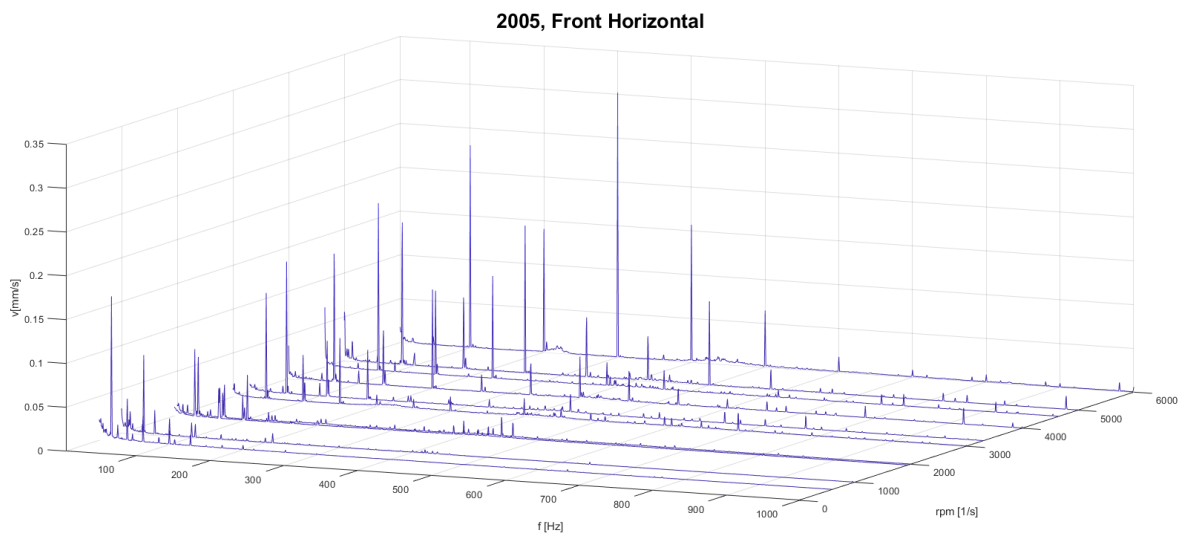
Figure 50. 2005 spindle waterfall plot – front horizontal

Spindle 1937 results show a significant excitement at the range of 200-300 Hz, with the highest RMS values at the front bearing in the horizontal direction, as shown in the Figure 52. Front bearings also show the excitement of 300-400 Hz and 400-500 Hz range in the

horizontal direction, which is also present in the vertical direction with lower RMS values. Higher frequency ranges are excited to a smaller degree in vertical direction, while remaining almost unexcited in horizontal direction – v. Figure 51.
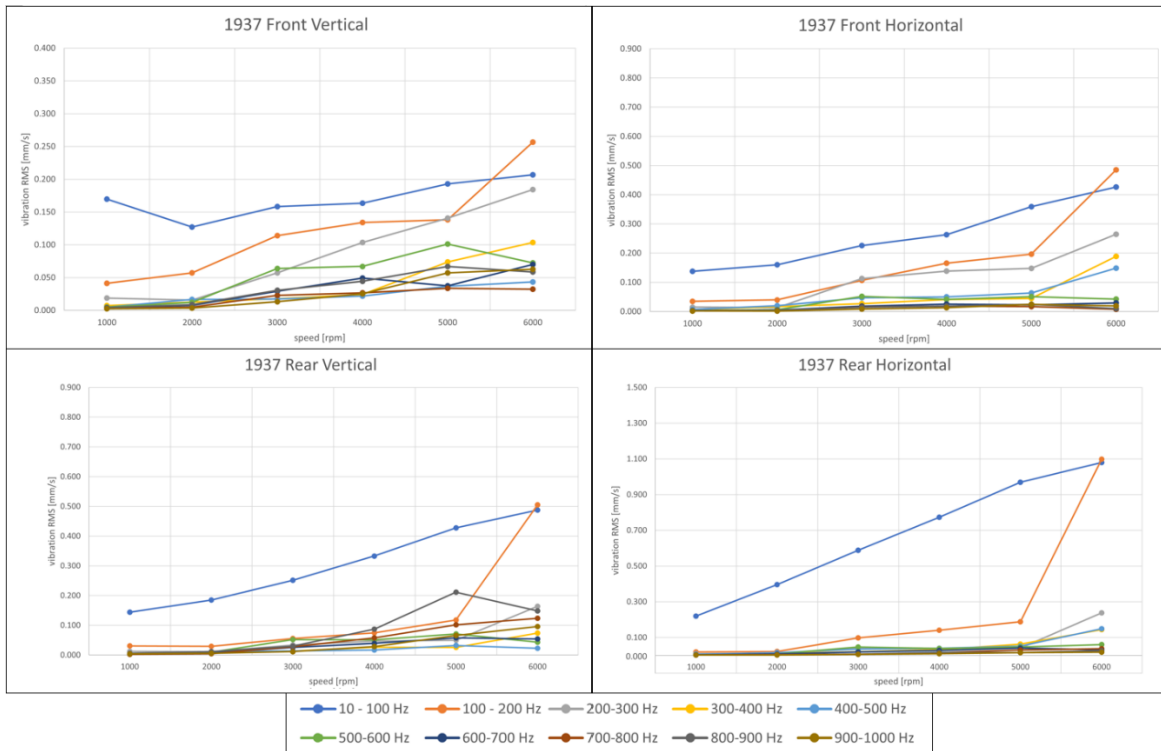
Figure 51. RMS values over 10-1000 Hz – spindle 1937
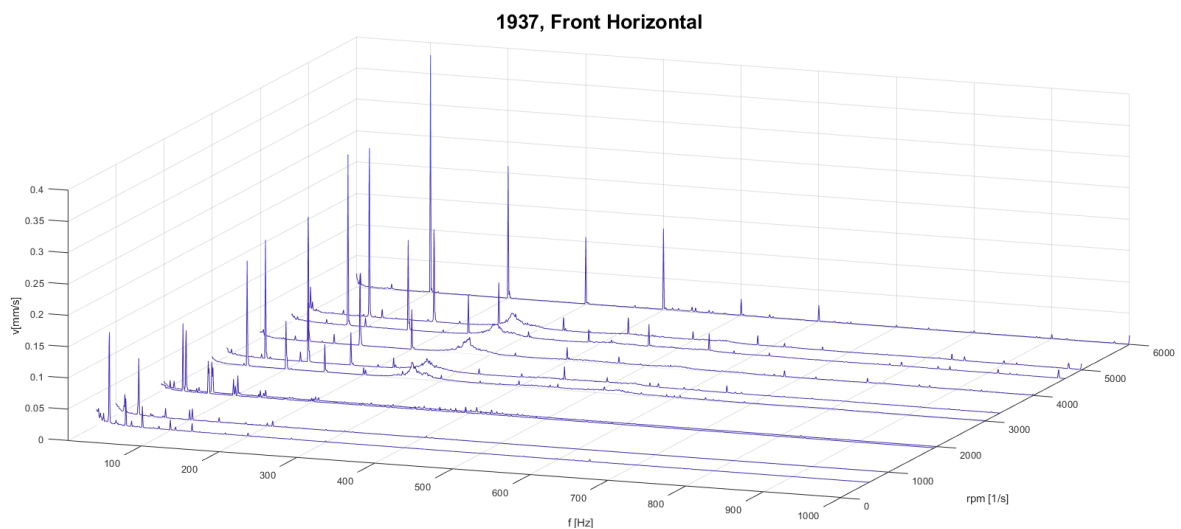
Figure 52. 1937 spindle waterfall plot – front horizontal

The above stated information about the RMS values for different frequency ranges is summarized in the Table 20:

Table 20. Spindles behavior summary over RPM - RMS values over 10-1000 Hz

The following table reproduces the colored cells. Within each year column the four colors are listed in the order: Front vertical, Front horizontal (top sub-row) / Rear vertical, Rear horizontal (bottom sub-row). Legend: R = significant excitement (red), Y = slight excitement (yellow), G = generally low vibration level (green).

	2001	2002	2003	2005	1937
10-100 Hz	R R / R R	R R / Y Y	R R / R R	R R / R Y	R R / R R
100-200 Hz	R R / R R	R R / Y Y	R R / R R	R R / R Y	R R / R R
200-300 Hz	R R / Y Y	R R / Y Y	R R / R R	R R / Y Y	R R / Y Y
300-400 Hz	Y Y / G Y	Y Y / G Y	R R / R R	Y R / Y Y	Y R / Y Y
400-500 Hz	G G / G G	G Y / G Y	Y R / Y Y	Y Y / Y Y	Y Y / Y G
500-600 Hz	G G / G G	G G / G G	R Y / R Y	R Y / Y Y	Y G / Y G
600-700 Hz	G G / G G	G G / G G	R Y / R Y	Y G / Y Y	Y G / Y G
700-800 Hz	G G / G G	G G / G G	Y Y / Y Y	Y G / G G	Y G / Y G
800-900 Hz	G G / G G	G G / G G	Y G / Y G	Y G / Y Y	Y G / Y G
900-1000 Hz	G G / G G	G G / G G	Y Y / Y Y	Y G / G G	Y G / Y G

🟥 - significant excitement, 🟨 - slight excitement, 🟩 - generally low vibration level

Colored cells correspond to the bearings in the following order:

Front vertical	Front horizontal
Rear vertical	Rear horizontal

There are two patterns of the vibration behavior at the 10-100 Hz rms:

1. Vibration in both bearing plane is significant over the mentioned range (2001, 2003, 1937)

2. Vibration is less significant at the rear bearing. (2002, 2005)

There are two patterns at the 100-200 Hz range:

1. Vibration in both bearing plane is significant over the mentioned range (2001, 2003, 1937)

2. Vibration is less significant at the rear bearing. (2002, 2005)

These two ranges are excited mainly because of the high amplitude of the rotational speed frequency and its multiples, thus in the terms of investigation of the excitement frequency ranges they are going to be treated rather as an additional information.

There are two patterns at the 200-300 Hz range:

1. Vibration in both bearing plane is significant over the mentioned range. (2003)

2. Vibration is less significant at the rear bearing. (2001, 2002, 2005, 1937)

When examining the 200-300 Hz range vibration character in detail and comparing its character and behavior among all spindles and bearings, it is obvious that for the spindles 2001 and 2002, and, partly, for 1937 this range is not as excited at rear bearings as it is in the front ones while for the spindles 2003 and 2005 it is excied even more on rear bearings.

What is common for the 2003 and 2005 rear bearings fit configuration is that they have a tight fit (0.006 mm) on the inner diameter combined with a clearance fit on the outer diameter. The OD clearance might be the reason for the rear bearing vibration. From the Figure 53 (a) it is obvious that for interference fit the vibration RMS is lower, although there is no direct dependency between the fit and the vibration. The reason for lower RMS at bigger clearance might be explained by a more favorable assembly configuration of the 2005 spindle. This is also valid for higher frequency ranges, such as 400-500 Hz, as illustrated in the Figure 53 (b).

(a)   (b)
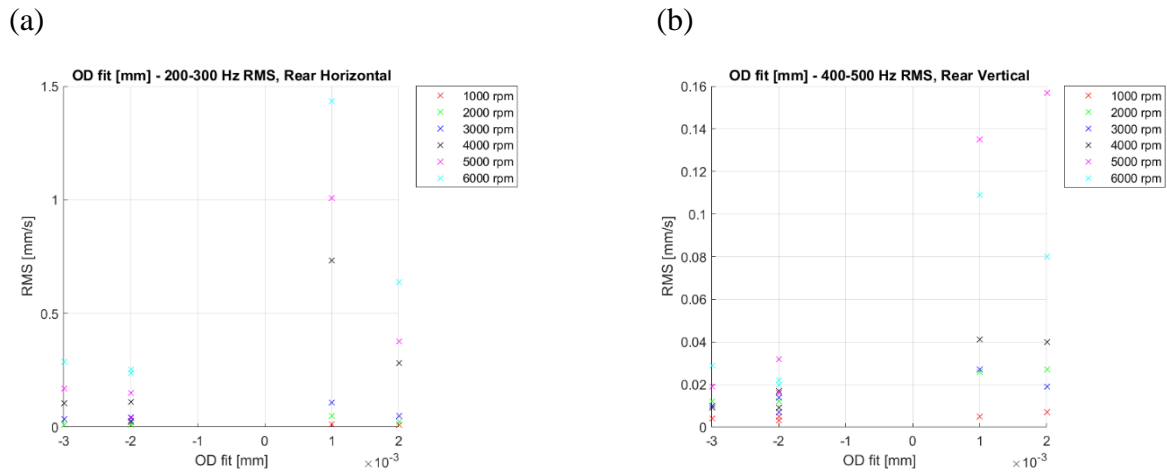
Figure 53. Correlation between 200-300 Hz range RMS value and rear bearing OD fit (a) in horizontal direction, (b) in vertical direction

Vibrations at the front bearings might be affected by such parameter as spacer rings average height difference – the correlation between these two parameters is shown in the Figure 54 (a). The 2003 spindle large amplitude of vibration might be caused by a combination of other parameters which are not related to dimensions. There is also a correlation between the inner spacer ring deviation and the excitement over this range – v. Figure 54 (b).

(a)   (b)
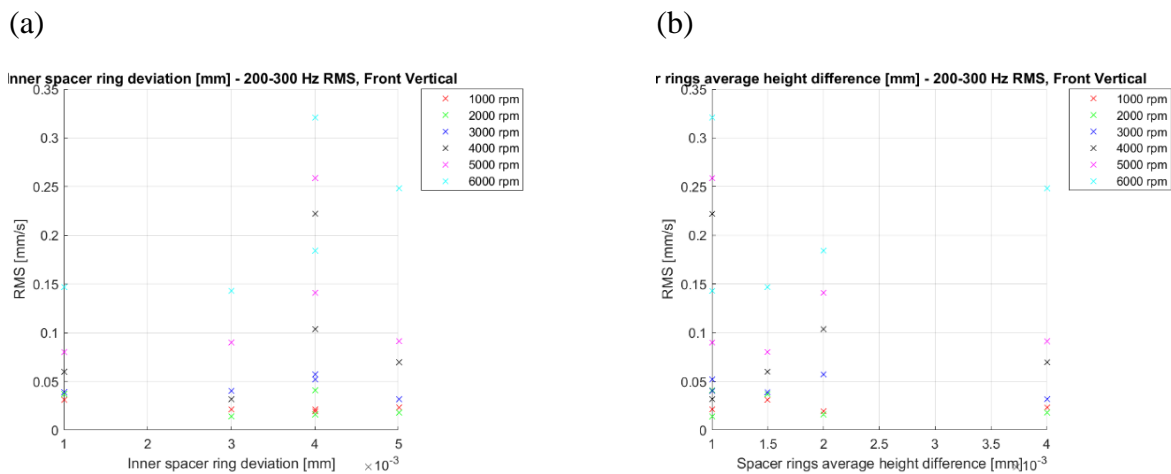
Figure 54. Correlation between 200-300 Hz range RMS value and front bearings (a) inner spacer ring deviation (b) spacer rings average height difference

Generally, there are 3 patterns for the 300-400 range:

1. The range is excited at the front bearings with a relatively low amplitude and vibration is also present in horizontal direction at the rear bearing. (2001, 2002)

2. The range is excited more at the front bearings and shows a slight excitement at the rear bearings. (2005, 1937)

3. The range is excited to a relatively high degree at both bearings in both directions (2003)

Analogously as for the range 200-300 Hz, there is a correlation between the rear bearing OD fit and the vibration RMS value at the range of 300-400 Hz – v. Figure 55.

(a)   (b)
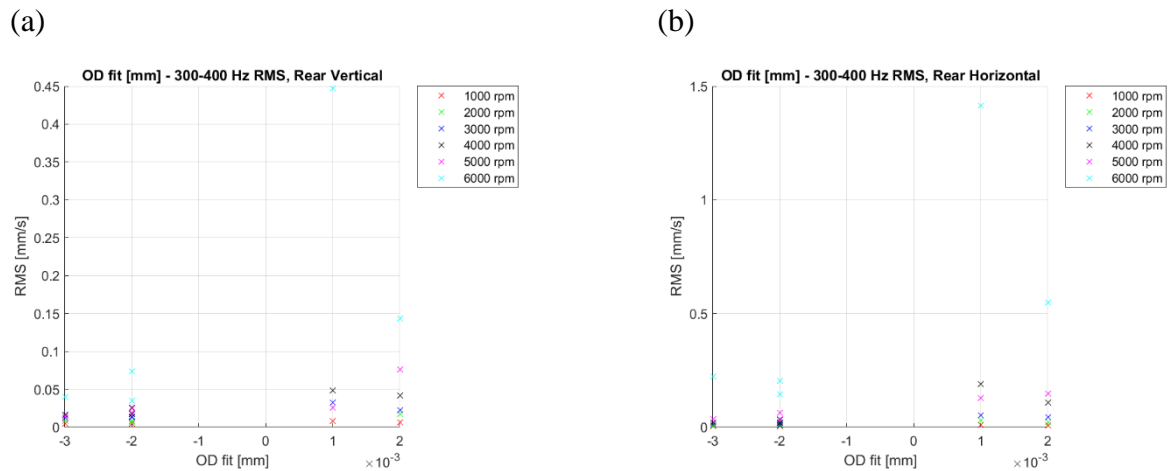
Figure 55. Correlation between bearing seat OD fit and 300-400 Hz range RMS value at rear bearing in (a) vertical direction (b) horizontal direction

There are no characteristic patterns for vibration at 400-500 Hz. This range might get excited because of the excitement of the structure or the resonances of the spindle spring placement, or by a resonant of one of the spindle components (cage, rings). Then, there might be a correlation between the RMS value and the inner spacer ring deviation (Figure 56), because larger deviation creates differently loaded parts of the surface which can have effect on the vibration level by contributing to the bearings resonances excitement.
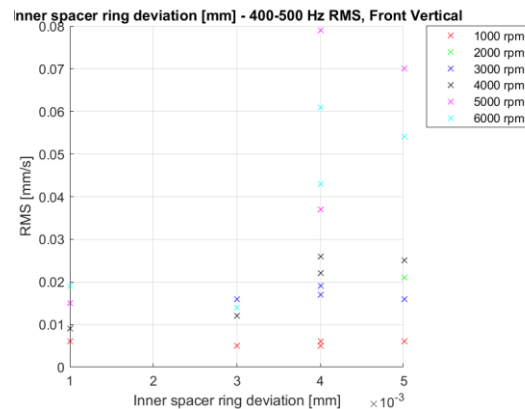
Figure 56. Correlation between front bearing inner spacer ring deviation and 400-500 Hz range RMS value

As far as the higher frequency ranges(500-600 and higher) are concerned, generally, there are 2 patterns (which, in fact, could be also considered as levels) of their excitement character:

1. They remain unexcited (2001, 2002)

2. They show a slight excitement in the vertical direction. (1937, 2005, 2003)

For the correlation charts, refer to Appendix.

The frequency of the vibrations in the same bearings plane might differ from each other in horizontal and vertical direction. This is related to several factors, particularly to the vibrations' modal form vector. The vibration direction is also to a certain degree influenced by the structure itself – i. e. by flatness, parallelism of the meeting surfaces, and the assembly process.

For the test stand used for the experiment, the vibration amount in different directions is likely to be influenced by the spindle housings construction. A separated top- and bottom-parts screwed together and underlaid by a spring rubber element result in a different pressing force in horizontal and vertical directions (Figure 57). This force is larger in the vertical direction – in the direction of the screws tightening, and it impacts against the vibrating motion. Hence, a larger vibration amount on the lower frequencies is expected in the horizontal direction, as this direction is more compliant.
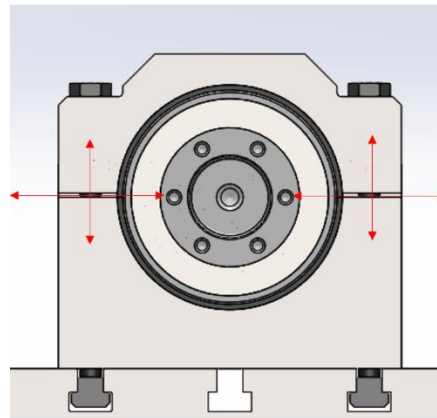
Figure 57. Vibration amount in different directions illustration

Summary

The result of the investigation of the vibration-affecting parameters is presented in the table. The estimation of the spindle condition in context of excited frequency ranges is presented in the Table 21.

It is also importatnt to note that the measurement was performed on a series of new spindles, so it is possible that some of the bearing components'(cage, rings) resonant vibrations will be mitigated with the components surfaces natural polishing after some operation period, and the excitement will not be so prominent.

Table 21. Spindles affected by the vibration excited at the 10-1000 Hz frequency range

Frequency range	Affected spindles	Possible factor
10-100 Hz	2001, 2003, 1937	• Complex set of factors
100-200 Hz	2001, 2003, 1937	• Complex set of factors
200-300 Hz	2003, 2005, 1937	• Spacer rings height difference • Rear bearing OD fit • Front bearing spacer ring deviation
300-400 Hz	2003, 2005, 1937	• Rear bearing outer diameter fit • Resonance of spring spindle placement/bearing component resonance

400-500 Hz	2003, 2005	• Rear bearing outer diameter fit • Front bearing spacer ring deviation • Resonance of spring spindle placement/bearing component resonance
500-600 Hz	2003, 1937	• Resonance of spring spindle placement/bearing component resonance
600-700 Hz	2003, 1937	• Resonance of spring spindle placement/bearing component resonance
700-800 Hz	2003, 1937	• Resonance of spring spindle placement/bearing component resonance • Front bearing spacer ring deviation
800-900 Hz	2003, 1937	• Resonance of spring spindle placement/bearing component resonance
900-1000 Hz	2003, 1937	• Resonance of spring spindle placement/bearing component resonance • Bearing ID seat circulatity

Table 22. Spindles condition assessment - - RMS values over 10-1000 Hz

	2001	2002	2003	2005	1937
10-100 Hz	red	green	red	green	red
100-200 Hz	red	green	red	green	red
200-300 Hz	green	green	red	red	red
300-400 Hz	green	green	red	red	red
400-500 Hz	green	green	red	red	red
500-600 Hz	green	green	red	red	green
600-700 Hz	green	green	red	green	red
700-800 Hz	green	green	red	green	red
800-900 Hz	green	green	red	green	red
900-1000 Hz	green	green	red	green	red

green - favorable condition, red - some issues are present

3.5.2.4 High-frequency excited ranges

Vibrations on the frequencies after 1000 Hz in most cases have some wide excited ranges, though with amplitudes generally lower than it typical for the vibrations on frequencies under 1000 Hz. That is why it is reasonable to assesss the vibrations on the frequencies higher than 1000 Hz at wider frequency ranges. RMS values for three ranges of 1000-2000 Hz, 2000-3000 Hz, and 3000-5000 Hz were calculated for each spindle, and then the results were compared consequently.

Figure 58 shows that 2001 spindle vibration on high-frequency ranges show moderate increase with RPM. The highest values has the 2000-3000 Hz, which is increases the most rapidly at rear bearing in horizontal direction.
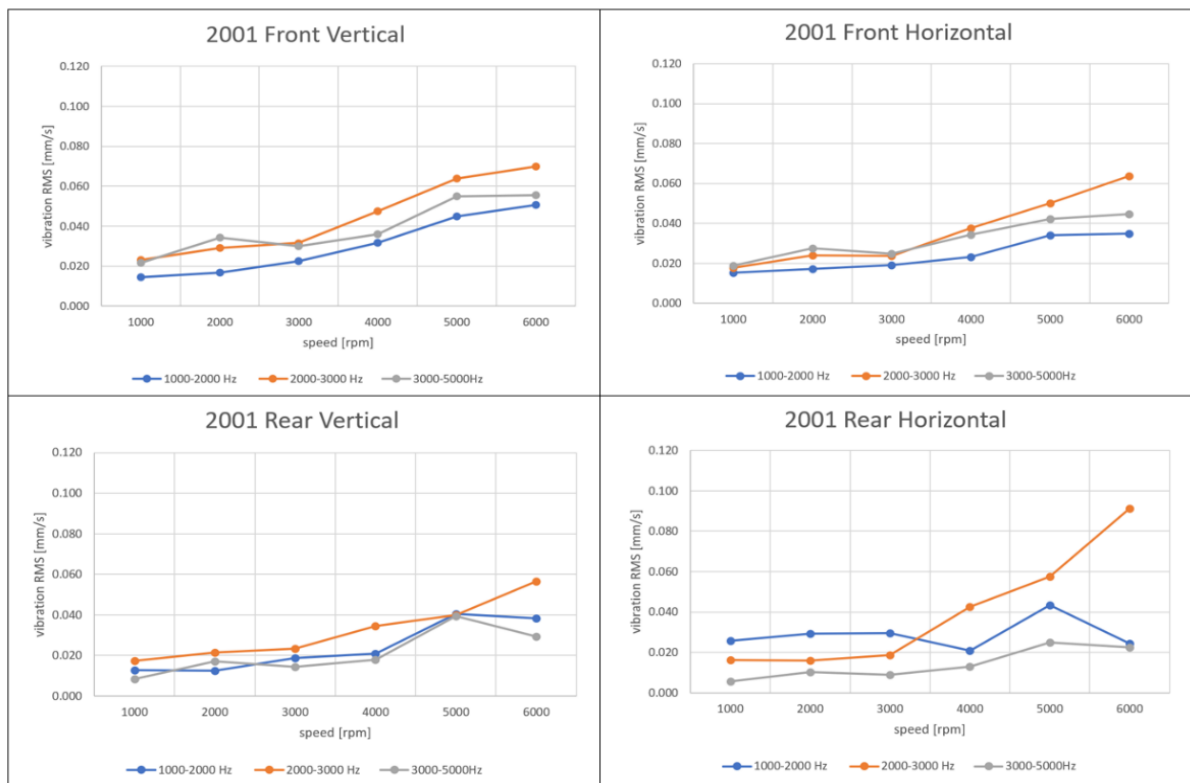
Figure 58. High-frequency ranges RMS – spindle 2001

As for the spindle 2002, all three of the examined ranges are excited to a approximately same degree at the front bearings, as shown in the Figure 59. The 2000-3000 Hz and 3000-5000 Hz ranges are excited more at the front bearings, while the RMS values of the 1000-2000 Hz are higher at the rear bearing, and they are relatively high already at 2000 RPM.
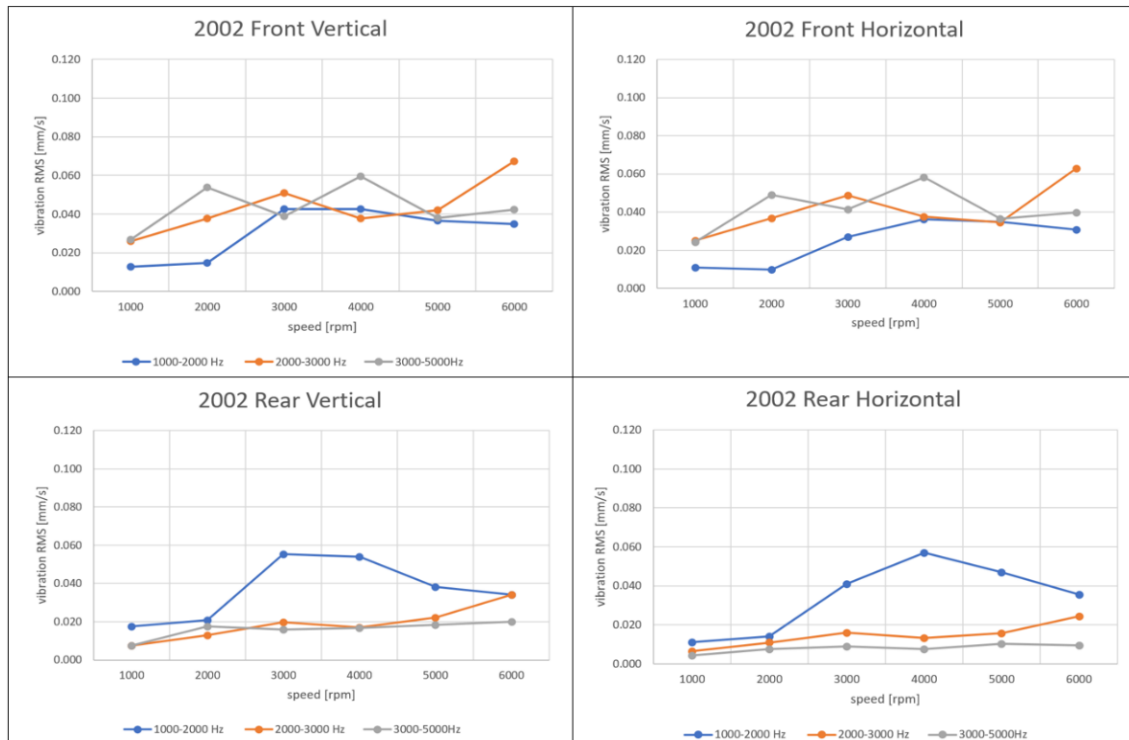
Figure 59. High-frequency ranges RMS – spindle 2002

2003 spindle show a rapid vibration increase at the ranges 1000-2000 Hz and 2000-3000 Hz, especially at high RPM – v. Figure 60. The 2000-3000 Hz range show the largest amplitudes at the front bearings in vertical direction, while 1000-2000 Hz range is excited the most at the rear bearing in vertical direction. The high-frequency ranges are not excited much in the horizontal direction.
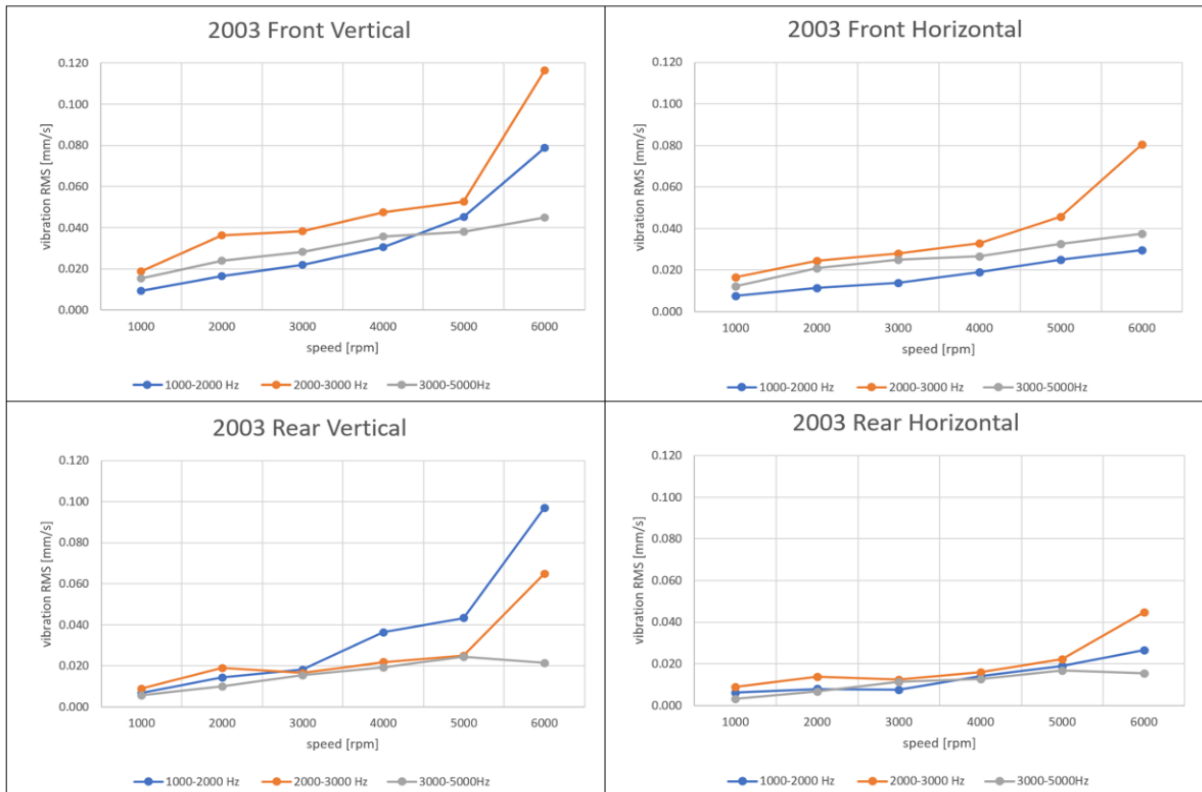
Figure 60. High-frequency ranges RMS – spindle 2003

Spindle 2005 has a relatively excited 1000-2000 Hz range with different courses at the front bearing and at the rear bearing, v. Figure 61. Higher frequency ranges are excited with rather low amplitudes and show a slight increase over the RPM at the front bearings, while remaining unexcited at the rear bearing.
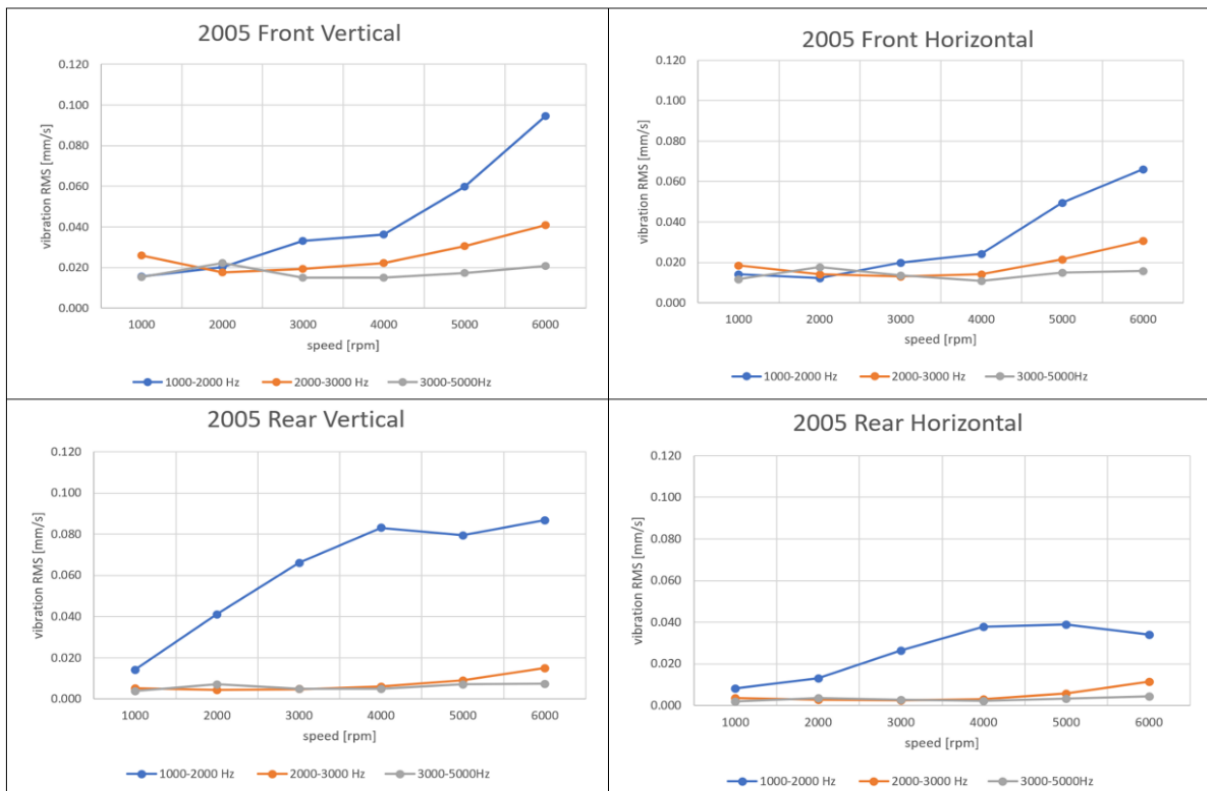
Figure 61. High-frequency ranges RMS – spindle 2005

1937 spindle is characterized by the 3000-5000 Hz range excited on the front bearings. This rapid step at 4000 RPM corresponds to a high-frequency excited range with peaks distributed rather randomly, as shown in the Figure 62. The 2000-3000 Hz and 3000-5000 Hz frequency ranges show a rather moderate excitement at the rear bearing, while 1000-2000 Hz course is very similar for the front and the rear bearings in both directions.
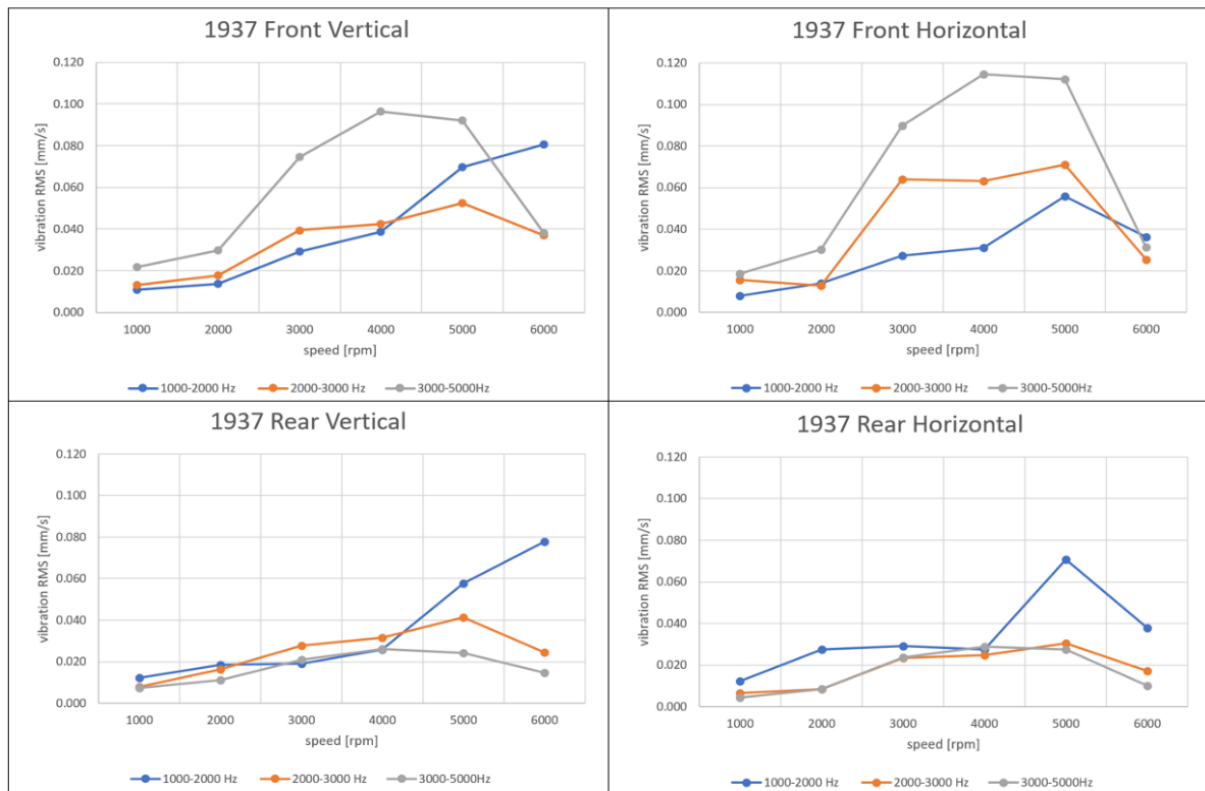
Figure 62. High-frequency ranges RMS – spindle 1937

General tendentions

For the measured spindles the following tendention is generally valid: frequencies higher than 1000 Hz are generally excited with smaller amplitudes. These ranges contain the highest ones of bearings fault frequencies on high RPM, and resonances of components with lower mass and stiffer structure placement, such as spacer rings. This could also be and vibration generated by electrical components, such as spindle motor or components of its control system. The differences between excitement of these ranges between different spindles is provided using the example of the frequency spectrum of front bearings in vertical direction at 6000 RPM.

As it is evident from the Figure 63 RMS values at the range 1000-2000 Hz always increase at higher RPM because of bearing characteristic frequencies peaks occurrence. All spectra contain bearing characteristic frequencies excited to a different degree (these frequencies and their impact is analyzed in chapter 703.5.2.2), along with their harmonic frequencies and the rotational speed harmonic frequencies. Obviously, spindles 2001 and 2002 are slightly and evenly excited over the 1000-2000 Hz range. Spindles 2003 and 1937 has significant peaks at frequencies 1020, 1080 (which could be an 11H with a 20 Hz

93

sideband). Additionally, spindle 2003 has an excited range only in vertical direction, and an excited range with a 1166 Hz frequency peak on the front bearings. Spindle 2005 has its highest peaks at 1280 Hz and sidebands – this spindle has the largest number of excited peaks. It is also characterized by a peak with a 1773 central frequency and 100 Hz and sidebands, which is present at the lower RPM as well with a frequency change.
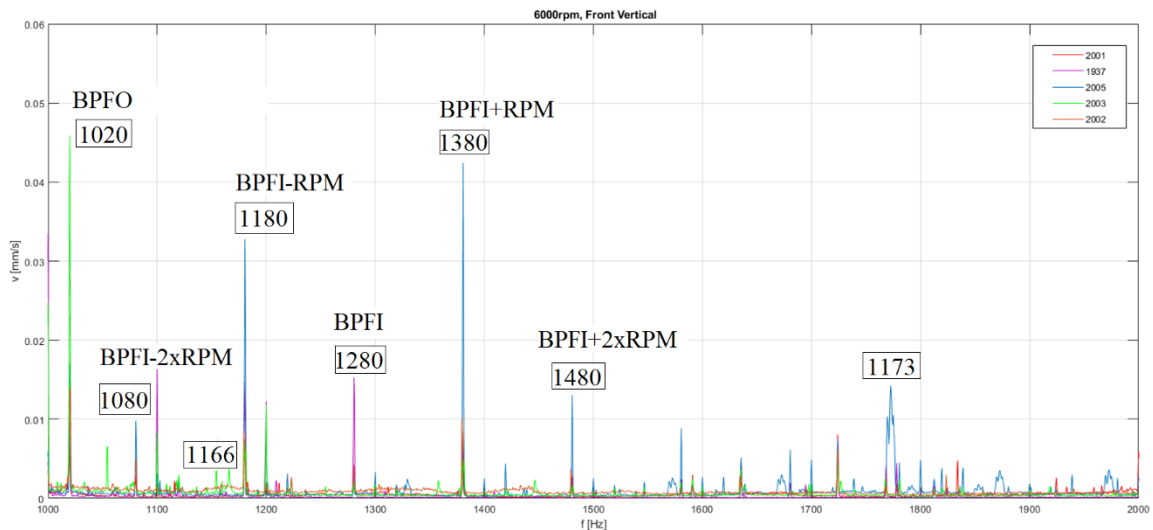
Figure 63. 1000-2000 Hz frequency spectrum

As far as the dimensional parameters are concerned, the RMS over the 1000-2000 Hz range tends to show higher values for larger inner rings average height difference at the front bearings (Figure 64 (a)) and for looser bearing OD fit (Figure 64 (b)), (although the correlation is not strict and there are values which do not correspond with this assumption).

(a)   (b)
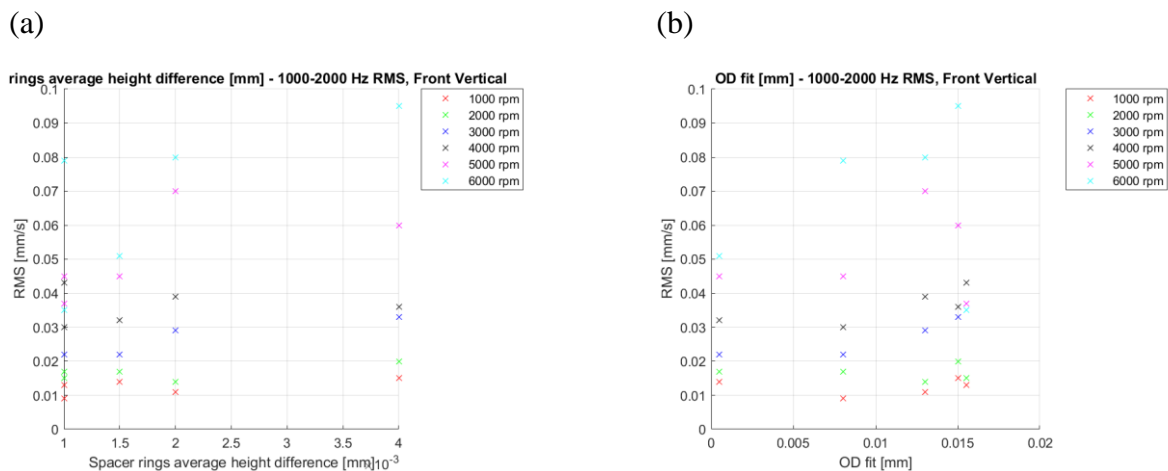
Figure 64. Correlation between 1000-2000 Hz RMS range value and front bearing (a) spacer rings average height difference and (b) OD fit

Some spindle have a slightly raised noise level over the range of 2000-3000 Hz, as shown in the Figure 65. Then, this range also contains frequencies which correspond to the bearings characteristic frequency multiples and their sidebands, e. g. 2564 Hz is a second multiple of the front bearing BPFI , 2040 is a second multiple of the front bearing BPFO, 2361 Hz, 2461 Hz, and 2661 Hz are sidebands, 2296 is a multiple of a BPFI sideband.
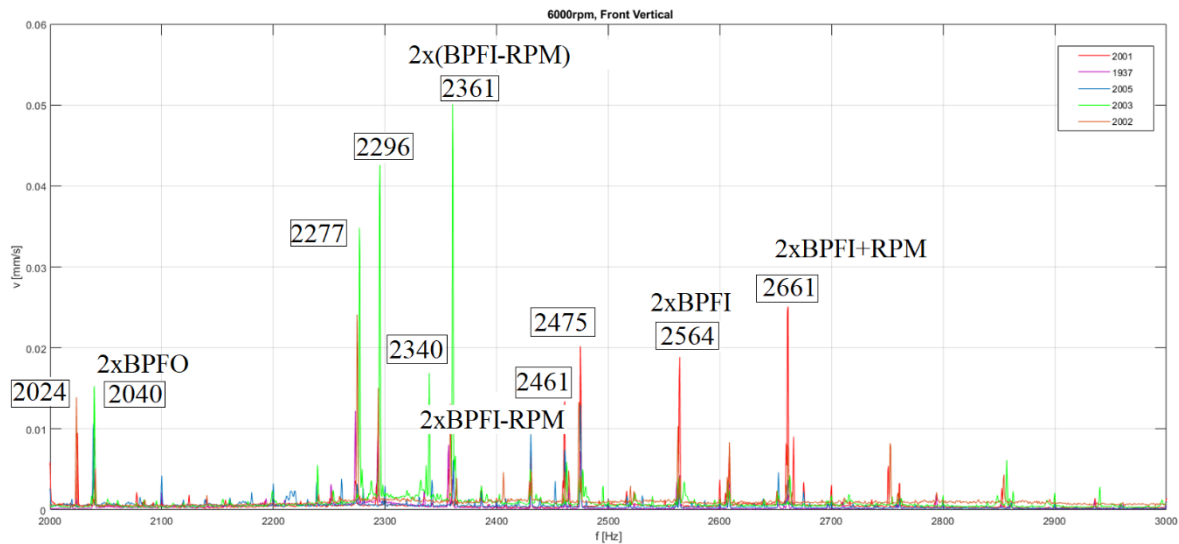
Figure 65. 2000-3000 Hz frequency spectrum

The range 3000-5000 Hz has a range (3000-3800 Hz), which is excited for all spindles in the approx. same manner, although the amplitudes are not the same, v. Figure 66. This range also contains randomly distributed peaks which are unique for different spindles. The rest of the spectrum is unexcited; small peaks are not taken into consideration.
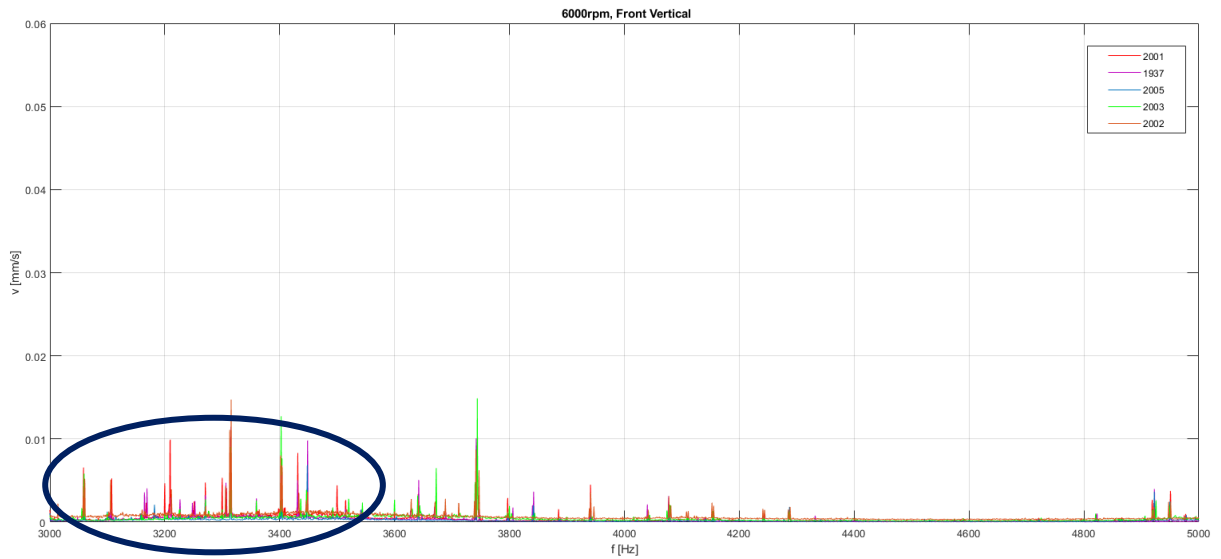
Figure 66. 3000-5000 Hz frequency spectrum

The high-frequency vibration character assessement is summarized in the Table 23.

Table 23. Spindles behavior summary over RPM - high-frequency ranges

- significant excitement,   - slight excitement,   - generally low
vibration   level

Colored cells correspond to the bearings in the following order:

Front vertical	Front horizontal
Rear vertical	Rear horizontal

Summary

To sum up the information about the high-frequency vibration character,Table 24 is presented. It was includes additional division the vibration by its type: P – occurence of singular peaks in the spectrum, R –character of excited wide ranges.

Table 24. Spindles condition assessment- high-frequency ranges

	2001	2002	2003	2005	1937
1000-2000 Hz	R	R	R, P	R, P	P
2000-3000 Hz	P	P	R	P	R
3000-5000 Hz	R, P	R, P	R, P	R	R

         - favorable condition,   some issues are present

Obviously, the degrees of high-frequency ranges excitement of the measured spindles is not significantly different, especially concerning frequencies under 3000 Hz. All spindles are showing out a certant degree of excitement over these ranges due to the reasons discussed above. Those reasons are summarized in the Table 25.

Table 25. Spindles affected by the vibration excited at 1000-5000 Hz frequency range

Frequency range	Affected spindles	Possible factor
1000-2000 Hz	2002, 2003, 2005, 1937	• bearing-related frequencies and their harmonics • Spacer rings height difference • Front bearing OD fit • resonances
2000-3000 Hz	2001, 2002, 2003, 1937	• bearings related - mounting
3000-5000 Hz	1937	• bearings-related • electrical

3.5.2.5 Time history evaluation

The desired character of the vibration acceleration time history is when the amplitudes are low and vary within the small range, without any significant peaks occurence. The time history of the measured acceleration signal has been investigated, and in most of the cases the signal course did not have a preferable character. The time histories of an acceleration signal is provided in Appendix.

To demonstrate the difference between the desired time history character and the faulty character, the time history of the spindle 2002 and the spindle 2003 vibration at the 4000 RPM are compared at the figure. Obviously, the 2002 spindle signal has peaks with the amplitude approximately three times larger than the average vibration level. These peaks indicate the presence of impulsive forces impacting on the bearings during the rotation. The occurence of the peaks is related to the scratching noise coming from the front bearings, which has been noted during the measurement. There are 2 types of the peaks character, thin - Figure 67 and thick - Figure 68, each of them corresponds to different type of vibration sound, and, supposingly, the different degree of an impulsive impact.
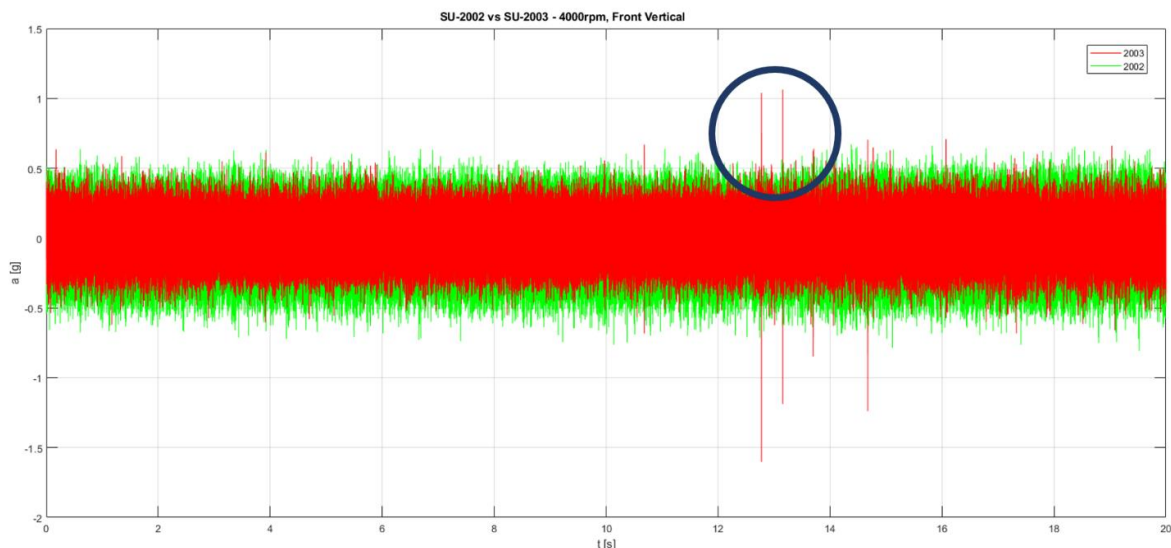
Figure 67. Desired and faulty time history characters comparison – singular peak
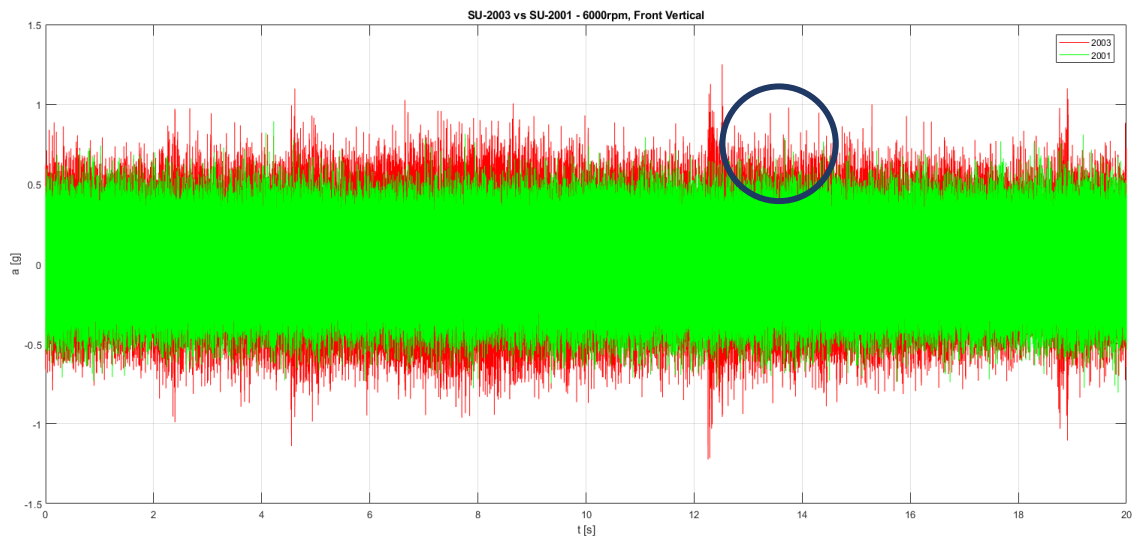
Figure 68. Desired and faulty time history characters comparison - thick peak

Time historiy measurements of the rear bearings of the spindle 2005 on several RPM levels and singular measurements of the 2002 and 1937 spindles has showed out a visually recognisable amplitude modulation at a low frequency (0.4 Hz) – v. Figure 69. This frequency is likely to be related to some of the assembly irregularities, such as a difference between front bearings' rotational speeds.
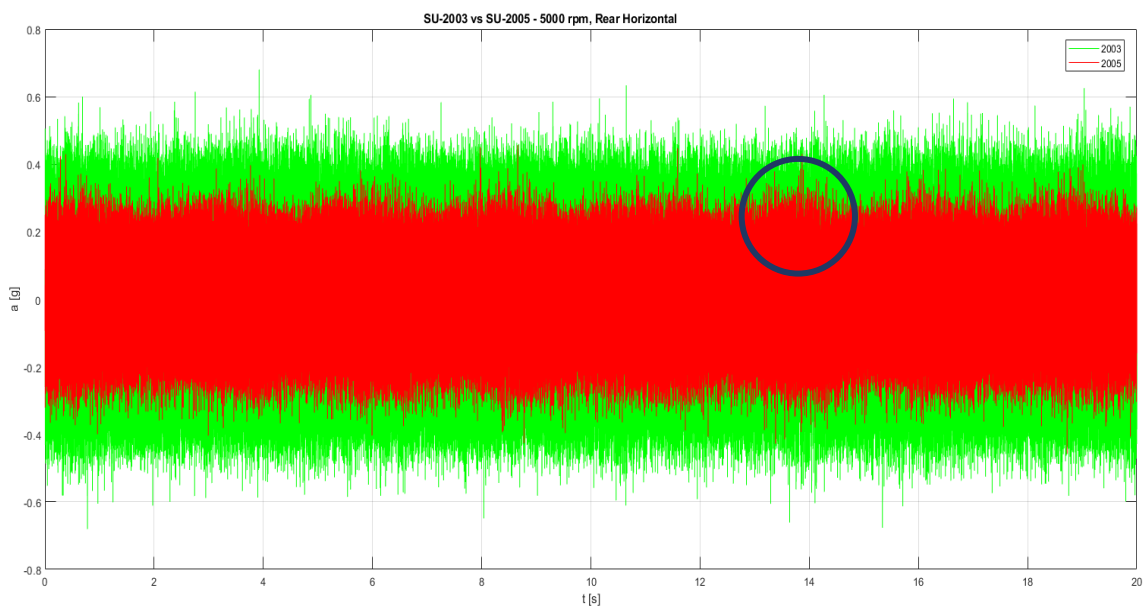
Figure 69. Time history amplitude modulation

Abnormal patterns

During the measurement of some of the spindles, 1937 in particular (2001 to a smaller extent), the effect of a sudden vibration self-excitement occurred, which is demonstrated in the Figure 70. :he part of the measurement record consists of an even noisy time history with a relatively low acceleration level without peaks (which is a desirable spindle vibration character), and then it a sudden vibration level raise occurs. The figure shows the time histories of all of the channels, and it is evident that the vibration level raise is more prominent at the front bearings.
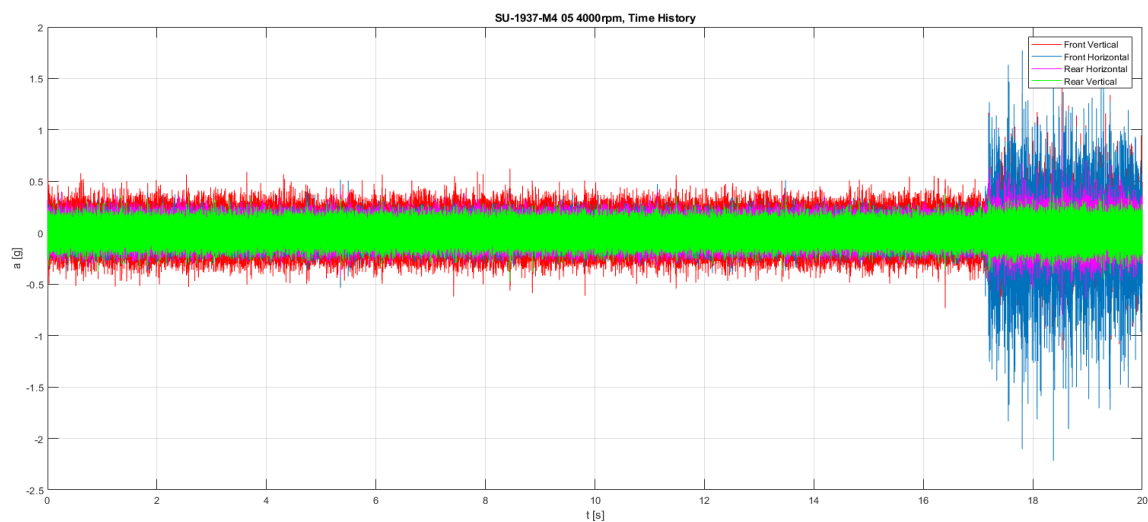
Figure 70. Self-excited vibration time history

The comparison of the FFT spectra of the first, „Low" part of the measurement and the „High" part is shown in the Figure 71. It is obvious that the raised vibration level corresponds to the wide frequency ranges excited, with central frequencies of approx. 300 Hz, 600 Hz, 800 Hz., and then keeping a raised level of noise. In the meantime, harmonics amplitudes have slightly lower values; and the bearing characteristic frequency peaks have similar values.
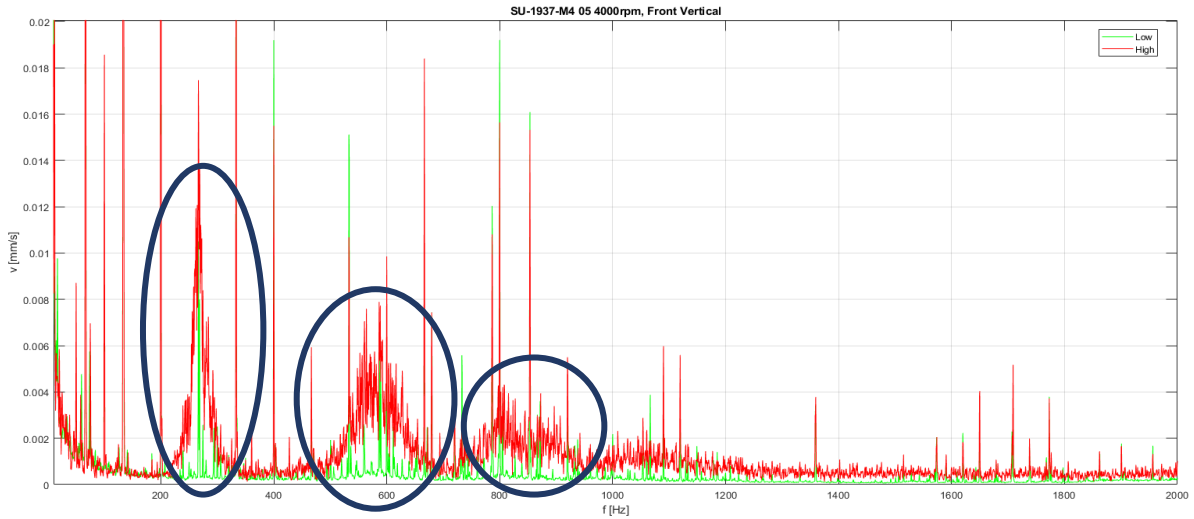
Figure 71. FFT spectra of the low-amplitude and high-amplitude acceleration signal

Summary

The evaluation of time history character from the peaks presence and peaks-to-average ratio point of view is presented in the Table 26.

Table 26. Spindles behavior summary over RPM -time history character

	2001		**2002**		**2003**		**2005**		**1937**	
Time history	🟨	🟥	🟨	🟨	🟥	🟥	🟥	🟨	🟥	🟥
character	🟨	🟥	🟨	🟨	🟨	🟥	🟨	🟨	🟥	🟥

🟥 - significant peaks presence,   🟨 - satisfactory character

Colored cells correspond to the bearings in the following order:

Front vertical	Front horizontal
Rear vertical	Rear horizontal

The higher peaks amplitude correspond to the larger force or impulse acting at the bearings, so this might have negative consequences on the bearing condition after a number of operating hours, as in this case the bearngs are experiencing higher cyclical loads. Such undesired time history character might symbolize the uneven load distribution, which causes

unconstant velocity of bearings' balls motion in the raceway. If a sudden change of the load occurs, the balls tend to change their velocity – accelerate or decelerate, and this might generate a vibration effect of the balls in the raceway, or induce the collision between the rolling elements and the cage, which might induce the shock impulse. The change of loads occurs due to the spindle manufacturing irregularities. However, sometimes the raised noise level might be related to the grease distribution, and be considered an allowable effect. Then, some of the peaks are not necessarily related to the bearing issues and might be caused by the coupling problems.

Some of the spindles have given out favorable time history patterns, such as 2003 spindle at 4000 RPM in the Figure 67. Such pattern could be used as a sample of a desirable spindle vibration output for the quality assurance procedure.

3.6 Summary and correlations overview

The final spindle quality assessment is presented in the Table 27. It is evident that the 2001, 2002, and 2005 spindles show relatively low vibration level in almost all the vibration categories, whereas the 2003 and 1937 spindles show a raised (though not dramatically excessive) level of the vibration among all the categories.

Table 27. Final spindle quality assessment

	Rot. speed frequency and its harmonics	Bearing characteristic frequencies	10-1000 Hz ranges excitement	1000-5000 Hz ranges excitement
2001	🟩	🟩	🟩	🟩
2002	🟩	🟩	🟩	🟥
2003	🟥	🟥	🟥	🟥
2005	🟥	🟩	🟩	🟩
1937	🟥	🟥	🟥	🟥

The overview of the assumed vibration-affecting factors is presented in the Table 28.

Table 28. Correlations overview

Parameter	Rot. speed frequency and its harmonics	Bearing characteristic frequencies	10-1000 Hz ranges excitement, [Hz]	1000-5000 Hz ranges excitement, [Hz]
Bearing ID circularity	1H	BPFI		
Rear bearing ID fit (less interference)	3H	BPFI	900-1000	
Rear bearing OD fit (less interference)	2H	BPFO	200-300, 300-400, 400-500	
Front bearing spacer ring deviation (inner)	2H		200-300, 400-500, 700-800	
Spacer rings height difference			200-300	
Assembly conditions		BPFO, BPFI, BCSOR		1000-3000
Placement	4H, 5H		200-1000	
Electrical				3000-5000

Basing on the experimental results, the quality assurance has to be focused on minimizing the looseness in the assembly and the dimensional or geometric deviation of the important bearing-related components, such as bearing spacer rings, or bearing seats. The presented table could be used as a diagnostic material to identify or confirm the problematic component causing the excessive vibration of the spindle.

3.7 Quality assurance procedure proposal

3.7.1 Design considerations

Referring to the assembly procedure, it is highly recommended that the spindle components' edges chamfering is included into the manufacturing process, and, consequently, manual edges breaking procedure is excluded from the assembly process. This step is not only time-saving, but it also prevents chips gathering in the assembly area and reduces the risk of particles getting inside of the assembly.

Basing on the spacer rings dimensions measurement, the surface flatness and parallelism geometric tolerances and have to be revised and corrected to comply with the bearing manufacturer's recommendations.

Regarding front bearings, it is also recommended to consider using bearings with different parameters, such as balls/cage material combination. It is possible that other cage/balls material combination would be less sensitive to varying loads, hence less vibration-prone.

3.7.2 Before assembly

This stage is aimed to ensure defected components to be excluded from the assembly process and describes the control procedures that have to be performed before the assembly process.

Front bearing spacer rings height difference and each rings' height deviation has to be controlled. The spacer rings have to be ground together to have 0.002 mm maximum deviation and packed and delivered in sets. Before the assembly, the bearing height has to be measured with a micrometer at minimum 4 surface points and the deviation should not exceed 0.002 mm.

Shaft bearing seats diameters runout have to be measured in centers, using the micrometer dial indicator to double-check that the runout is the same as stated at the manufacturer's protocols.

3.7.3 Assembly guidelines

This stage of the proposed quality assurance process is aimed to bring improvements to the already established process of the spindle mounting.

Special attention has to be paid to the front nut and the back nut bearing fitting surfaces flatness during the rubbing procedure, as these surfaces are most likely important vibration-affecting factors.

The spindles' performance has to be tested with the various nut tightening moments, and the correct value of the nut tightening moment has to be defined. Then, it will be ensured that all of the spindle bearings have the same preload amount

3.7.4 Grease distribution run

The very first time spindle is installed on the stand after assembly, the grease distribution run has to be performed, according to the section 2.4.4. The Fanuc CNC control station might be used as a tool for a full automatization of the time-consuming process of spindle run-in. The spindle rotational speed is supposed to be controlled by the CNC system; at the same time the bearings temperature could be monitored by installed temperature sensors. The signal from the temperature sensors could be assessed, and the rotation will be automatically stopped once the set temperature limit value is exceeded, preventing the excessive bearing heating. After the spindle is cooled down, the procedure can be automatically resumed..

3.7.5 Vibration testing

The vibration measurement procedure has to be adapted to SBS-5500 device (Figure 72). The device is able to measure the vibrations up to 1666 Hz, which is satisfactory for the vibration character assessment of a new spindle. It is recommended that the standard cylindrical magnetic sensors are replaced with the prismatic ones for better vibration signal quality.

The measured vibration signal is supposed to be exported from the device using a Putty software and the measurement output can be displayed as an Excel plot. Then the RMS value can be calculated and assessed. The resonances at the characteristic frequency ranges have to be controlled along with the other peak amplitude values

Figure 72. SB-5000 vibration analyzer [40]

3.7.6 Bearing sound patterns

Establishing a bearing sound patterns database containing different bearing patterns samples is also a useful tool for spindle bearing quality assessment. The database шы upposed to contain patterns which represent various bearing issues. Then, if a spindle produces a characteristic sound pattern, it can be recorded by the SKF sound measurement stethoscope (Figure 73), proceeded in the Audacity software and compared to the typical defects samples, or to the sample of „normal performance" proceeded in the Audacity software and compared to the typical defects samples, or to the sample of „normal performance", and the condition assessment could be performed.

Figure 73. SKF sound measurement stethoscope [41]

3.7.7 Temperatures monitoring

The temperature sensors have to be installed on both bearing planes of the spindle assembly to monitor the bearings temperature. The CNC control system can be programmed to stop the spindle run, if a limit temperature value is exceeded either during the grease distribution run, or a test run. It provides the reliable testing procedure, minimizing the risk of bearing damage.

3.7.8 Static stiffness measurement

It is practical to know the exact spindle static stiffness values both in radial and axial directions. The proposed stand could then be used for static stiffness control measurement. It has to be performed using a dynamometer and a dial indicator. The dependency between the deflection and the applied force has to be controlled. Then, it is important to have the patterns of a loose (compliable) spindle recorded to complete the bearing sound patterns database.

3.7.9 Quality assurance protocol

It has to be decided which of the above-mentioned stages have to be included in the final quality assurance procedure. Then, the output results of each of the stages could be entered into a digital spindle measurement protocol, which is issued and stored. The protocol

would become a helpful material for further spindle condition assessment for the possible service cases and can be used for condition monitoring.

4. **Conclusion and discussion**

This Master thesis was aimed to determine the quality-affecting parameters of an examined spindle assembly basing on the experimental vibration measurement, and to propose an appropriate quality control procedure. The research section of the work included the study of the vibration diagnostic methods and the appropriate equipment, the bearing-related problematics, such as bearing failure modes, and bearing assembly and control procedures along with the study of the assembly methods which are currently applied to Viking CNC spindles. The practical section of this work included the proposal of a test stand, vibration measurement equipment definition, and the description of the vibration measurement applied on the series of spindles, followed with the measurement results analysis and spindles condition assessment.

For the analysis purposes, the vibration signal was decomposed into several vibration categories, basing on the vibration character and its frequency range. The vibration amplitude values within each of these categories were cross-referenced with the spindles' actual dimensional and geometric parameters and the assumed correlations between the parameters and the degree of vibration excitement have been summarized and presented. The final assessment of the spindles' condition has been presented.

The performed experiment has shown that though the spindles do not give out excessive vibrations (the performance is generally satisfactory), the vibration character is sometimes uneven, peaks on vibration time history are typically present, and the uncommon bearings noise is present, which signalizes about not inconsiderable irregularities brought either by dimensional configurations, or assembly conditions. The vibration character typically comprises an excitement of the spindle rotational speed frequency and its harmonics, which have a large contribution to the overall spindle vibrations. The vibration amplitudes at these frequencies depend, i. a., on the looseness in the assembly: the correlations between the bearing seats dimensional parameters and the amplitudes have been figured out and presented. Typically, the amplitudes are larger for larger dimensional deviations and looser fits. The other significant vibration type is the excitement of wider frequency ranges. There are spindle behavior patterns where the same spindle shows both high and relatively low degree of excitement at these ranges. The excitement of these ranges is likely related to the bearings' fit parameters, potentially to the front bearings spacer rings parameters (but it is also needed to consider that the wide frequency range excitement partly

depends on the spindle spring placement on the test stand). Besides, it has been figured out that spindle spacer rings have a large height deviation, which exceeds the values recommended for the precise spindle bearings spacer rings. This parameter might be related to the several front bearings vibration ranges degree of excitement, so it is highly recommended to revise the bearing spacer rings manufacturing prescriptions regarding planarity and parallelism.

The bearing characteristic frequencies have been excited with very low amplitude which is expectable for new bearings. The magnitude of the amplitude value at these frequencies might be in a correlation between the bearings inner diameter circularity and the bearing fits. At higher rotational speeds, some of the spindles also tend to vibrate at high frequencies, and typically, at bearing characteristic frequencies' harmonics with rotational speed frequency sidebands. There has not been detected an explicit correlation between these frequencies excitement and the measured dimensional parameters, so it is supposed that these frequencies exitement has been influenced by assembly conditions.

The following limitations of the proposed methods have to be pointed out: the proposed study is focused mainly on revealing problems associated with the bearing proper fits and assembly. The conclusions and the following quality assurance procedure is based on the spindle vibration and measurement with the maximum rotational speed of 6000 RPM, and it covers the spindle vibrations behaviour only in unloaded state. This fact has to be taken into account, as under load the effects of bearing preload induced by the front bearing nut and the spacer rings, especially the front nut tightening moment, can be significantly different. Then, only the effect of selected dimensional and geometrical parameters has been studied, so it is possible that some other vibration-affecting dimensional and geometrical factors have not been taken into account.

The main contribution of this paper is to bring the systematic approach to the spindle vibration ploblematics and to propose a comprehensive informative material about quality-affecting factors regarding company's spindles namely, along with the spindle test stend conception proposal and establishing the environment for test and measurement purposes. The presented measurement results followed by the vibration analysis are intended to extend the company's spindle-related problematics overview. It is recommended, that in the future the spindle quality control and assurance procedure is completed with the static stiffness measurement and the geometrical accuracy of axis of rotation measurement; then, the

knowledge base could be extended by the spindle placement resonant frequency measurement results, temperature behavior study results, behavior under load study results, potentially with the confirmation of the proposed correlation hypotheses.

References

[1]   NORTON, M. a D. KARCZUB. *Fundamentals of Noise and Vibration Analysis for Engineers*. 2. edition. New York: Cambridge University Press.

[2]   BILOŠ, Jan a Alena BILOŠOVÁ. *Aplikovaný mechanik jako součást týmu konstruktérů a vývojářů: část Vibrační diagnostika*. První vzdání. Ostrava: Vysoká škola báňská – Technická univerzita Ostrava, 2012. ISBN 978-80-248-2755-1.

[3]   All about Vibration Measuring Systems - IMV CORPORATION. *IMV Corporation* [online]. IMV Corporation [cit. 2020-11-09]. Dostupné z: https://www.imv-tec.eu/pr/vibration_measuring/chapter03/

[4]   LECINSKI, Pawel. Bearing Problems – Fault Frequency and Artificial Intelligence-Based Methods. *Reliability Connect* [online]. [cit. 2021-03-04]. Dostupné z: https://www.reliabilityconnect.com/bearing-problems-fault-frequency-and-artificial-intelligence-based-methods/

[5]   KONSTANTIN-HANSEN, Hans. *APPLICATION NOTE: Envelope Analysis for Diagnostics of Local Faults in Rolling Element Bearings* [online]. [cit. 2021-03-18]. Dostupné z: https://www.bksv.com/media/doc/bo0501.pdf

[6]   FERNANDEZ, Alfonso. *Demodulation or envelope analysis* [online]. [cit. 2021-03-06]. Dostupné z: https://power-mi.com/content/demodulation-or-envelope-analysis

[7]   LIN, Ciao-Shin. *Fault Detection of Rolling Element Bearings*. ProQuest Information and Learning Company, 2005. Dissertation. University of Washington.

[8]   XU, Ming. *SPIKE ENERGY MEASUREMENT AND CASE HISTORIES*. Ohio: Rockwell Automation, Integrated Condition Monitoring, Westerville.

[9]   GAGNON, Frank. *Spike Energy Diagnostics (and Similar Techniques): History, Usefulness & Future Outlook*. Vibra-K Consultants Ltd., 2006.

[10]   Shock Pulse goes Spectrum. *Maintenance World* [online]. [cit. 2021-03-13]. Dostupné z: http://www.maintenanceworld.com/wp-content/uploads/2013/07/shockpulse.pdf

[11]   GOLUMB, Scott. Shock Pulse Analyzing Case Study. *Machinery Lubrication* [online]. Noria Corporation, **2003**(11) [cit. 2021-03-13]. Dostupné z: https://www.machinerylubrication.com/Read/554/shock-pulse-analyzing

[12]   LEE, Greg. What is Shock Pulse Method?. *Reliabilityweb: A Culture of Reliability* [online]. [cit. 2021-03-13]. Dostupné z: https://reliabilityweb.com/articles/entry/what_is_shock_pulse_method

[13] ADAMS, Maurice L. *Bearings: basic concepts and design applications*. Boca Raton: CRC Press, Taylor & Francis Group, 2018. ISBN 9781138049086.

[14] *Bearing damage classification - ISO15243:2004: SKF e-learning course* [online]. In: . [cit. 2021-02-17]. Dostupné z: https://www.skf.com/id/services/training/elearning/brg-damage

[15] INTERNATIONAL ORGANIZATION FOR STANDARDIZATION (2003). *Mechanical vibration — Rotor balancing (ISO 21940-1:2019)*. 2019.

[16] INTERNATIONAL ORGANIZATION FOR STANDARDIZATION (2009). *Mechanical vibration — Evaluation of machine vibration by measurements on non-rotating parts (ISO 10816-3:2009)*. 2009.

[17] *Vibrometr Fluke 805 | Fluke* [online]. Fluke Corporation, 2020 [cit. 2020-11-19]. Dostupné z: https://www.fluke.com/cs-cz/produkt/mechanicka-udrzba/analyza-vibraci/fluke-805

[18] *A4900 Vibrio M – Vibration Meter, Analyzer and Data Collector in One | Adash* [online]. Adash, 2020 [cit. 2020-11-19]. Dostupné z: https://adash.com/portable-vibration-devices/a4900-vibrio-vibration-meter

[19] *SKF Microlog analyzer AX series | SKF* [online]. [cit. 2020-11-19]. Dostupné z: https://www.skf.com/id/products/condition-monitoring-systems/portable-systems/cmxa-ax

[20] *FAG Detector II – the "mobile" among data collectors: Technical Product Information*. Germany: Weppert Print & Media GmbH, 2005.

[21] *SKF QuickCollect sensor | SKF* [online]. [cit. 2020-11-19]. Dostupné z: https://www.skf.com/id/products/condition-monitoring-systems/basic-condition-monitoring-products/vibration-measurement/quickcollect-sensor

[22] *VIBSCANNER 2 | High-speed vibration measurement tool | PRUFTECHNIK* [online]. Fluke Deutschland GmbH, 2020 [cit. 2020-11-19]. Dostupné z: https://www.pruftechnik.com/com/Products-and-Services/Condition-Monitoring-Systems/Vibration-Analysis-and-Balancing/Vibration-Analyzer/VIBSCANNER-2/

[23] *VIBXPERT II | Vibration analysis system & balancing tool | PRUFTECHNIK* [online]. Fluke Deutschland GmbH, 2020 [cit. 2020-11-19]. Dostupné z: https://www.pruftechnik.com/com/Products-and-Services/Condition-Monitoring-Systems/Vibration-Analysis-and-Balancing/Vibration-Analyzer/VIBXPERT-II/

[24] *Fluke 810 | Vibration Tester | PRUFTECHNIK* [online]. Fluke Deutschland GmbH, 2020 [cit. 2020-11-19]. Dostupné z: https://www.pruftechnik.com/com/Products-and-Services/Condition-Monitoring-Systems/Vibration-Analysis-and-Balancing/Vibration-Analyzer/Fluke-810-Vibration-Tester/

[25] *SmartBalancer - Schenck v České republice* [online]. [cit. 2020-11-19]. Dostupné z: https://www.schenck-rotec.cz/products/product-catalog/product-details/cs-smartbalancer.html?p=79

[26] *FAG Detector III – The Solution for Monitoring and Balancing*. Germany: mandelkow, 2014.

[27] *VIBGUARD IIoT | Online Condition Monitoring System | PRUFTECHNIK* [online]. Fluke Deutschland GmbH, 2020 [cit. 2020-11-19]. Dostupné z: https://www.pruftechnik.com/com/Products-and-Services/Condition-Monitoring-Systems/Online-Condition-Monitoring/Online-Condition-Monitoring-Systems/VIBGUARD-IIoT/

[28] *VIBCODE - Vibrodiagnostika - Snímače - konektory - kabely* [online]. [cit. 2020-11-19]. Dostupné z: http://www.lamikappa.cz/vibcode/

[29] *Analysis and reporting manager | SKF | SKF* [online]. [cit. 2020-11-19]. Dostupné z: https://www.skf.com/id/products/condition-monitoring-systems/software/analysis-reporting-manager

[30] *OMNITREND Center | Condition Monitoring Software | PRUFTECHNIK* [online]. Fluke Deutschland GmbH, 2020 [cit. 2020-11-20]. Dostupné z: https://www.pruftechnik.com/com/Products-and-Services/Condition-Monitoring-Systems/Online-Condition-Monitoring/Software/OMNITREND-Center/

[31] *DDS Software – Powerfull Tool for Data Storing and Data Evaluation | Adash* [online]. Adash, 2020 [cit. 2020-11-20]. Dostupné z: https://adash.com/cs/software/digital-diagnostics-system

[32] *VIBROPORT 80 & VIBROTEST 80 - SCHENCK USA* [online]. [cit. 2020-11-20]. Dostupné z: https://www.schenck-usa.com/products/product-finder/product-detail-page/vibroport-80-vibrotest-80.html

[33] SCHAEFFLER KG. *Condition monitoring using FAG products Technical Product Information*. Germany: Weppert, 2008.

[34] *Super-precision bearings*. SKF Group, 2016.

[35] HU, Gaofeng, Dawei ZHANGA, Weiguo GAOA, Ye CHENA, Teng LIUB a Yanling TIANAC. Study on variable pressure/position preload spindle-bearing system by using piezoelectric actuators under close-loop control. *International Journal of Machine Tools and Manufacture* [online]. 2018, (125), 68-88 [cit. 2021-03-17]. Dostupné z: https://doi.org/10.1016/j.ijmachtools.2017.11.004

[36] *FAG Super Precision Bearings* [online]. Herzogenaurach: Schaeffler KG, 2008 [cit. 2021-03-17]. Dostupné z:

FACULTY
OF MECHANICAL
ENGINEERING
CTU IN PRAGUE

DEPARTMENT OF
PRODUCTION MACHINES
AND EQUIPMENT

https://www.schaeffler.com/remotemedien/media/_shared_media/08_media_library/
01_publications/schaeffler_2/brochure/downloads_1/ac_41130_7_de_en.pdf

[37]   KBK, KBE3C Coupling. In: *Motion Solutions* [online]. [cit. 2021-07-15]. Dostupné
       z: http://www.motionsolutions.com/store/pc/viewPrd.asp?idproduct=1298

[38]   *NI-9234 NATIONAL INSTRUMENTS C Series Sound and Vibration Input Module -
       $1,211.00 | PicClick* [online]. In: . [cit. 2021-06-25]. Dostupné z:
       https://picclick.com/NI-9234-National-Instruments-C-Series-Sound-and-Vibration-
       152937875796.html#&gid=1&pid=1

[39]   *(1) (PDF) Vibration analysis techniques for gearbox diagnostic: A review* [online].
       In: . [cit. 2021-06-25]. Dostupné z:
       https://www.researchgate.net/publication/302931893_Vibration_analysis_techniques
       _for_gearbox_diagnostic_A_review/figures?lo=1

[40]   *SB-5500 Controller for grinding wheel balancers* [online]. In: . [cit. 2021-06-25].
       Dostupné z: http://www.schmitt.co.uk/Balancers/SB-5500.html

[41]   *Electronic stethoscope TMST 3 | SKF* [online]. In: . [cit. 2021-06-25]. Dostupné z:
       https://www.skf.com/group/products/condition-monitoring-systems/basic-condition-
       monitoring-products/sound-measurement/stethoscope

List of tables

List of figures

List of used software

MATLAB 2017b

Microsoft Excel

List of Appendices

Text Appendices:

Appendix 1   Failure submodes chains of causation

Appendix 2   Vibration measurement devices overview

Appendix 3   Spindle assembly mounting procedure

Appendix 4   Waterfall plots

Appendix 5   Selected frequency spectra

Electronic Appendices:

DP_1793.pdf

DP_1793_Assignment.pdf

DP_1793_Text_Appendices.pdf

Matlab_scripts.zip

Frequency_spectra.zip

Waterfall_plots.zip

Correlations.zip